

**DESIGN AND FPGA IMPLEMENTATION OF NON-
LINEAR INTELLIGENT CONTROL FOR SPECIAL
ELECTRIC DRIVES**

A THESIS

Submitted by

ARUN PRASAD K.M.

for the award of the degree

of

DOCTOR OF PHILOSOPHY



**DIVISION OF ELECTRICAL ENGINEERING
SCHOOL OF ENGINEERING
COCHIN UNIVERSITY OF SCIENCE AND TECHNOLOGY, KOCHI**

FEBRUARY 2019

THESIS CERTIFICATE

This is to certify that the thesis entitled “**DESIGN AND FPGA IMPLEMENTATION OF NON-LINEAR INTELLIGENT CONTROL FOR SPECIAL ELECTRIC DRIVES**” submitted by **ARUN PRASAD K.M.** to the Cochin University of Science and Technology, Kochi for the award of the degree of Doctor of Philosophy is a bonafide record of research work carried out by him under my supervision and guidance at the Division of Electrical Engineering, School of Engineering, Cochin University of Science and Technology. The contents of this thesis, in full or in parts, have not been submitted to any other University or Institute for the award of any degree or diploma. All the relevant corrections and modifications suggested by the audience during the pre-synopsis seminar and recommended by the Doctoral committee have been incorporated in this thesis.

Kochi-682 022
Date:

Dr. Usha Nair
(Research Guide)
Professor,
Division of Electrical Engineering,
School of Engineering,
CUSAT, Kochi-22.

DECLARATION

I hereby declare that the work presented in the thesis entitled "**DESIGN AND FPGA IMPLEMENTATION OF NON-LINEAR INTELLIGENT CONTROL FOR SPECIAL ELECTRIC DRIVES** " is based on the original research work carried out by me under the supervision and guidance of **Dr. Usha Nair**, Professor, Division of Electrical Engineering, SOE, CUSAT for the award of degree of Doctor of Philosophy with Cochin University of Science and Technology. I further declare that the contents of this thesis in full or in parts have not been submitted to any other University or Institute for the award any degree or diploma.

Kochi-682 022

Date:

Arun Prasad K.M.

ACKNOWLEDEMENTS

I thank God almighty for blessing me with willpower and all qualities required for completion of my work as well as getting along with life. The investigations in this thesis have been carried out under the supervision of Dr. Usha Nair, Professor, Division of Electrical Engineering, School of Engineering (SOE), Cochin University of Science and Technology (CUSAT). I express my deep sense of gratitude for her excellent guidance, competent advice, keen observations and persistent encouragement as well as personal attention given to me during the entire course of work, without which the successful completion of this work would not have been possible. I am deeply indebted to her for all the above considerations. I extend my sincere and heartfelt gratitude to Dr. Unnikrishnan A., Principal, Rajagiri School of Engineering and Technology, Kochi, for his endless support, constant encouragement and valuable suggestion throughout this work.

I also express my heartfelt gratitude to Dr. C.A. Babu, Head of Department, Division of Electrical Engineering, SOE, CUSAT and member of Doctoral Committee for his valuable suggestions, constant support and motivation. I extend my sincere gratitude to Dr. Radhakrishna Panicker, Principal, School of Engineering, CUSAT and other former principals of the Department for allowing me to use the facilities of the Department.

I would like to express my sincere gratitude to Dr. Bindu M Krishna for her great support at every stage of my work. I express my gratitude to Mr. Mohammed Salih, Assistant Professor, Govt. Engineering College, Thrissur for his valuable support for the completion of this work. I am immensely thankful to Dr. Asha Elizabeth Daniel, Professor, Division of Electrical Engineering, SOE, CUSAT for the valuable

suggestions and advice during the period of this work. I take this opportunity to thank all the faculty members in Division of Electrical Engineering, SOE, CUSAT specially Dr. P.G.Latha, Associate Professor for their constant support at all stages of this research. I express my sincere gratitude to all nonteaching staff of CUSAT who have helped and supported me during the entire period of work.

I am grateful to my colleagues in Model Engineering College especially Dr. Bindu V. (HOD, Department of Electrical Engineering), Dr. Rajeevan A.K, Dr. Bindu C.J. and Mrs. Vidhya K. for their support and encouragement given to me during the course of work. I also express my sincere thanks to my former colleagues Mrs. Leena T Timothy and Mrs. Shaija P.J. for helping me with various points during my work.

I record my sincere and utmost gratitude to my parents Mr. P.K. Hari Narayanan and Mrs. K.M.Radha for the constant encouragement and support given to me throughout my life. I am indebted to my parents in law Mr. K.P.Radhakrishnan and Mrs. P. K. Vijayalakshmi for the support extended to me during the entire period of my work. I am thankful to all my relatives and well-wishers. Words cannot express how grateful I am to my wife Mrs. Veena Krishna who has given me motivation and help throughout my life especially in the course of this work. I am truly grateful to my loving daughter Devika Arun Menon for her patience and tolerance during the entire period of my work. I am deeply indebted to them for their love and affection.

I was benefitted from the advice, support, co-operation and encouragement extended by a number of individuals during the course of the research work. Heartfelt thanks to all of them.

Arun Prasad K.M.

ABSTRACT

Key words: Fuzzy Sliding Mode Control, Special Electric Machines, Field Programmable Gate Array, Brushless DC motor, Permanent Magnet Synchronous Motor, Switched Reluctance Motor.

An electric drive is a power conversion means that is utilized by most of the industrial automation systems and processes to convert electrical power to mechanical power for controlling the torque, speed or position of the load. A modern electric drive system consists of a motor, an electric converter and a controller integrated together to perform a mechanical manoeuvre for a given load. Electric motors used in servo control applications for solar tracking, antenna positioning, robotic arm movement, hybrid electric vehicles and aerospace vehicles are some of the examples of special electric machines. Recent developments in advanced manufacturing and automation in processing industry demands very fast and robust techniques of characterization and control of these electric drives.

Drives are generally controlled by conventional Proportional plus Integral (PI) controllers due to the advantages of its simple design, low cost, low maintenance and their effectiveness. However, it has been known that conventional PI controllers generally do not work well for non-linear systems, particularly for complex and approximated mathematical models. Also, this control technique is not capable enough in dealing with system uncertainties such as parameter variation and external disturbances. Sliding mode control (SMC) is one of the widely used strategies to deal with these disadvantages. The chattering effect in the conventional SMC is reduced

by suitably modifying its control law. A Fuzzy Sliding Mode Controller (FSMC) combines the intelligence of a fuzzy inference system with the conventional SMC for further improvement in its performance characteristics and accuracy.

In this work, an intelligent FSMC for the speed/position control of special electric drives such as DC servo motor, BrushlessDC (BLDC) motor, Switched Reluctance Motor (SRM) and Permanent Magnet Synchronous Motor (PMSM) incorporating their important nonlinearities is designed and its performance is compared with that of modified SMC, Fuzzy PI and PI controllers under no load as well as loaded condition to identify the most suitable technique. Simulation results show that when FSMC is applied for the speed control, the peak overshoot is completely eliminated and the rise time and settling time are drastically reduced compared with the other controllers. Hardware in loop (HIL) simulation of FSMC using Field Programmable Gate Arrays (FPGA) is carried out for BLDC motor and PMSM and the results are validated with the hardware implementation of the original drive system. Experimental results clearly indicate that FSMC is highly suitable for the speed control of these special electric drives when accuracy and precision are highly significant in the presence of parametric uncertainties and external disturbances.

CONTENTS

ACKNOWLEDEMENTS.....	i
ABSTRACT	iii
LIST OF TABLES.....	ix
LIST OF FIGURES	xi
LIST OF ABBREVIATIONS	xv
NOTATIONS	xvii

CHAPTER 1 INTRODUCTION ----- 1

1.1	Motivation of the Research-----	6
1.2	Objectives of the Research -----	7
1.3	Outline of the Thesis -----	7

CHAPTER 2 LITERATURE SURVEY----- 9

2.1	Modelling of Industrial Drives-----	9
2.2	Linear Control Techniques -----	12
2.3	Non- Linear Control Techniques -----	13
2.3.1	Sliding Mode Control (SMC)-----	13
2.3.2	Back stepping control -----	15
2.4	Soft computing techniques in control -----	16
2.4.1	Fuzzy Logic -----	17
2.4.2	Artificial Neural Network -----	18
2.4.3	Genetic Algorithm-----	18
2.5	Adaptive Control -----	19
2.6	Robust control -----	20
2.7	Sensor less control-----	20
2.8	Fuzzy Sliding Mode Control -----	22
2.9	Optimization of the controller gain-----	22
2.10	Hardware implementation of the controller -----	24

CHAPTER 3 MODELLING OF DC AND AC DRIVES ----- 27

3.1	DC Drives -----	29
3.1.1	DC Servo motor-----	29
3.1.2	Brushless DC Motor (BLDC)-----	34
3.1.3	Switched Reluctance Motor (SRM)-----	41

3.2	AC Drives -----	44
3.2.1	Permanent Magnet Synchronous Motor (PMSM)-----	45
CHAPTER	4 CONTROL TECHNIQUES FOR INDUSTRIAL DRIVES-----	50
4.1	Linear Control Methods -----	50
4.2	Nonlinear Control Methods -----	52
4.2.1	Sliding Mode Control (SMC)-----	54
4.2.2	Modified Chattering free SMC -----	58
4.2.3	Fuzzy Logic Control (FLC) -----	59
4.3	Intelligent Controllers Using Fuzzy Logic -----	61
4.3.1	Fuzzy PI Control-----	62
4.3.2	Fuzzy Sliding Mode Control (Fuzzy SMC)-----	62
CHAPTER	5 NON-LINEAR INTELLIGENT CONTROL OF DC DRIVES -----	65
5.1	Position Control of DC Servo Motor-----	65
5.1.1	Stability Analysis of the System-----	66
5.1.2	PI Controller-----	68
5.1.3	Fuzzy Logic Controller (FLC)-----	68
5.1.4	Fuzzy PI Controller-----	70
5.1.5	Modified Sliding Mode Controller (SMC)-----	71
5.1.6	Fuzzy SMC (FSMC) -----	72
5.1.7	Results and Discussions -----	73
5.2	Speed Control of DC Servo Motor -----	77
5.2.1	Stability Analysis of the System-----	78
5.2.2	PI Controller-----	79
5.2.3	Fuzzy PI Controller-----	80
5.2.4	Modified Sliding Mode Controller (SMC)-----	81
5.2.5	Fuzzy SMC (FSMC) -----	81
5.2.6	Results and Discussions -----	82
5.3	Speed Control of BLDC Motor -----	84
5.3.1	Stability Analysis of the System-----	85
5.3.2	Sensitivity analysis -----	87

5.3.3	PI Controller-----	89
5.3.4	Fuzzy PI Controller-----	89
5.3.5	Modified Sliding Mode Controller -----	91
5.3.6	Fuzzy SMC (FSMC) -----	91
5.3.7	Optimization of Controller Gain using Krill Herd Algorithm-----	92
5.3.8	Results and Discussions -----	97
5.4	Speed Control of Switched Reluctance Motor-----	101
5.4.1	Stability Analysis of the System-----	102
5.4.2	PI Controller-----	104
5.4.3	Fuzzy PI Controller-----	104
5.4.4	Modified Sliding Mode Controller (SMC)-----	105
5.4.5	Fuzzy SMC (FSMC) -----	105
5.4.6	Results and Discussions -----	107
CHAPTER	6 NON-LINEAR INTELLIGENT CONTROL OF AC DRIVES -----	113
6.1	Field Oriented Control of PMSM -----	113
6.2	Stability Analysis of the System-----	116
6.3	PI Controller-----	118
6.4	Fuzzy PI Controller-----	118
6.5	Modified Sliding Mode Controller (SMC)-----	119
6.6	Fuzzy SMC (FSMC) -----	119
6.6.1	Optimization of Controller Gain using Krill Herd Algorithm-----	121
6.7	Results & Discussion-----	122
CHAPTER	7 FPGA IMPLEMENTATION OF CONTROL ALGORITHM IN INDUSTRIAL DRIVES -----	128
7.1	Implementation of MATLAB and Simulink Algorithms on FPGAs-----	130
7.2	Implementation of Controller on FPGA -----	131
7.3	Hardware in the loop Simulation -----	132
7.3.1	Hardware in the loop (HIL) Simulation for the speed control of PMSM -----	133

7.3.2	Hardware in the loop Simulation for the speed control of BLDC -----	137
7.4	Hardware implementation of FSMC of BLDC -----	141
7.5	Result and Discussion-----	142
CHAPTER 8	CONCLUSIONS AND FUTURE DIRECTIONS -	147
8.1	Conclusions -----	147
8.2	Research Contributions -----	152
8.3	Future Directions -----	153
	REFERENCES -----	154
	LIST OF PAPERS SUBMITTED ON THE BASIS OF THIS THESIS --	170
	CURRICULUM VITAE	

LIST OF TABLES

Table	Title	Page No
Table 2.1	Evolution of Control Techniques -----	26
Table 3.1	Advantages and Disadvantages of DC Servo Motor -----	29
Table 3.2	Switching Sequence of BLDC Motor -----	37
Table 3.3	Advantages and Disadvantages of BLDC Motor -----	38
Table 3.4	Advantages and Disadvantages of SRM-----	43
Table 3.5	Advantages and Disadvantages of PMSM -----	46
Table 4.1	Zeigler- Nichols Parameters for QDR Response -----	52
Table 5.1	Parameters of DC Servo Motor -----	66
Table 5.2	Fuzzy Rules for FLC -----	69
Table 5.3	Fuzzy Rules for Fuzzy PI-----	71
Table 5.4	Fuzzy Rules for FSMC-----	73
Table 5.5	Comparison of Modified SMC and PI controllers-----	75
Table 5.6	Performance comparison for the position control of DC servo motor using various controllers -----	77
Table 5.7	Fuzzy Rules for Fuzzy PI Controller -----	81
Table 5.8	Fuzzy Rules for FSMC-----	82
Table 5.9	Performance comparison for the speed control of DC servo motor using various controllers -----	84
Table 5.10	BLDC motor parameters-----	85
Table 5.11	Variation of speed with voltage-----	87
Table 5.12	Sensitivity with change in voltage-----	88
Table 5.13	Fuzzy Rules for Fuzzy PI Controller-----	90
Table 5.14	Fuzzy Rules for FSMC-----	92
Table 5.15	Parameter values initialized in KH algorithm-----	95
Table 5.16	Optimized values of controller gain-----	97
Table 5.17	Performance comparison with various controllers -----	101
Table 5.18	Parameters of SRM-----	102
Table 5.19	Fuzzy Rules for Fuzzy PI Controller-----	105
Table 5.20	Fuzzy Rules for FSMC-----	106

Table 5.21	Performance comparison with various controllers -----	110
Table 6.1	PMSM parameters -----	116
Table 6.2	Fuzzy Rules for Fuzzy PI Controller -----	119
Table 6.3	Fuzzy Rules for FSMC -----	120
Table 6.4	Details of parameter values initialized in KH algorithm -----	121
Table 6.5	Optimized values of the controller gain -----	122
Table 6.6	Performance comparison with different controllers -----	125
Table 7.1	Comparison of HIL Simulation and Simulation (PMSM) -----	136
Table 7.2	Comparison of HIL Simulation and Simulation (BLDC) -----	141
Table 7.3	Comparison of Hardware with Simulation Results -----	146

LIST OF FIGURES

Figure	Title	Page
Fig. 3.1	Functional blocks of a drive system-----	27
Fig. 3.2	Structure of a DC servo motor-----	31
Fig. 3.3	Motor torque with saturation-----	33
Fig. 3.4(a)	Structure of BLDC motor -----	35
Fig. 3.4(b)	Cross section of BLDC motor -----	35
Fig. 3.5	Circuit diagram of BLDC drive system -----	36
Fig. 3.6	Ideal back EMFs, current and position sensor signals -----	37
Fig. 3.7	Structure of 3 phase 6/4 SRM-----	42
Fig. 3.8	Cross section of surface PMSM -----	45
Fig. 3.9	Equivalent circuit of PMSM -----	47
Fig. 4.1	Open loop representation of a second order system -----	55
Fig. 4.2	Block diagram of closed loop system -----	56
Fig. 4.3	Phase- plane diagram of closed loop system for small s_1 -----	56
Fig. 4.4	Phase- plane diagram of closed loop system for large s_1 -----	57
Fig. 4.5	Block diagram of a Fuzzy logic controller -----	61
Fig. 4.6	Block diagram of a Fuzzy SMC -----	64
Fig. 5.1	Block diagram of the position control of DC servo motor -----	65
Fig. 5.2	Input membership functions for e and \dot{e} -----	69
Fig. 5.3	Output membership function-----	69
Fig. 5.4	Surface view of fuzzy system-----	70
Fig. 5.5	Input membership functions for e and \dot{e} -----	70
Fig. 5.6	Output membership functions -----	71
Fig. 5.7	Input membership functions for e and \dot{e} -----	72
Fig. 5.8	Output membership functions -----	73
Fig. 5.9	Step response with PI and conventional SMC in cyclic loaded condition-----	74
Fig. 5.10	Step response with PI and modified SMC at no-load-----	74
Fig. 5.11	Step response with PI and modified SMC in cyclic loaded-----	74
Fig. 5.12	Step response with FLC and PI controller at constant load -----	76

Fig. 5.13	Step response with Fuzzy SMC, Fuzzy PI and PI controller at constant load -----	77
Fig. 5.14	Block diagram of the speed control of DC Motor-----	78
Fig. 5.15	Input membership functions for e and \dot{e} -----	80
Fig. 5.16	Output membership functions -----	80
Fig. 5.17	Input membership functions for e and \dot{e} -----	82
Fig. 5.18	Output membership functions -----	82
Fig. 5.19	Step response with Fuzzy SMC, Fuzzy PI and PI controller for the speed control-----	83
Fig. 5.20	Block diagram of BLDC speed control-----	84
Fig. 5.21	Variation of speed with voltage -----	88
Fig. 5.22	Variation of sensitivity with time -----	89
Fig. 5.23	Input membership functions for e and \dot{e} -----	90
Fig. 5.24	Output membership functions -----	90
Fig. 5.25	Input membership functions for e and \dot{e} -----	92
Fig. 5.26	Output membership functions -----	92
Fig. 5.27	Flow chart of KH algorithm-----	96
Fig. 5.28	Step response of BLDC motor with Fuzzy SMC, SMC, Fuzzy PI and PI controllers -----	99
Fig. 5.29	Current in the three phases of BLDC motor -----	99
Fig. 5.30	Back EMF in the three phases of BLDC motor -----	100
Fig. 5.31	Variation of speed and current with FSMC -----	100
Fig. 5.32	Block diagram of SRM speed control -----	101
Fig. 5.33	Input membership functions for e and \dot{e} -----	104
Fig. 5.34	Output membership functions -----	104
Fig. 5.35	Input membership functions for e and \dot{e} -----	106
Fig. 5.36	Output membership functions -----	106
Fig. 5.37	Step response of SRM with Fuzzy SMC and other controllers---	109
Fig. 5.38	Response while loading with Fuzzy SMC and other controllers -	109
Fig. 5.39(a)	Comparison of rise time of selected drives with FSMC, Modified SMC, Fuzzy PI and PI controllers-----	110

Fig. 5.39(b)	Comparison of peak overshoot of selected drives with FSMC, Modified SMC, Fuzzy PI and PI controllers-----	111
Fig. 5.39(c)	Comparison of settling time of selected drives with FSMC, Modified SMC, Fuzzy PI and PI controllers-----	111
Fig. 5.39(d)	Comparison of steady state error of selected drives with FSMC, Modified SMC, Fuzzy PI and PI controllers -----	112
Fig. 6.1	Block diagram of the vector control of PMSM -----	115
Fig. 6.2	Input membership functions for e and \dot{e} -----	118
Fig. 6.3	Output membership functions -----	119
Fig. 6.4	Input membership functions for e and \dot{e} -----	120
Fig. 6.5	Output membership functions -----	120
Fig. 6.6	Step response of PMSM with various controllers -----	124
Fig. 6.7	Speed variation of PMSM under loaded condition-----	124
Fig. 6.8	Speed and Current variation of PMSM with FSMC -----	125
Fig. 6.9	Comparison of performance indices of PMSM using FSMC, Modified SMC, Fuzzy PI and PI controllers-----	126
Fig. 7.1	Xilinx System generator window-----	129
Fig. 7.2	Arrangement for the hardware in loop simulation -----	132
Fig. 7.3	Block diagram of FPGA implementation of Speed Control of PMSM using FSMC-----	134
Fig. 7.4	Step response of PMSM with FSMC using HIL simulation and simulation -----	135
Fig. 7.5	Step response of PMSM with SMC using HIL simulation and simulation -----	135
Fig. 7.6	Step response of PMSM with PI controller using HIL simulation and hardware simulation -----	136
Fig. 7.7	Block diagram of hardware implementation-----	139
Fig. 7.8	Step response of BLDC motor with FSMC using HIL simulation and simulation -----	139
Fig. 7.9	Step response of BLDC motor with SMC using HIL simulation and simulation -----	140
Fig. 7.10	Step response of BLDC motor with PI controller using HIL simulation and simulation -----	140
Fig. 7.11	Circuit diagram of 3 phase inverter -----	143

Fig. 7.12	Driver cum isolation circuit -----	144
Fig. 7.13	The Hardware setup for the speed control of BLDC motor using FSMC -----	144
Fig. 7.14	Step Response of Actual Hardware, HIL simulation and Simulation -----	145
Fig. 7.15	Speed variation while loading with actual Hardware, HIL simulation and Simulation-----	145

LIST OF ABBREVIATIONS

ACO	-	Ant Colony Optimization
ANFIS	-	Adaptive Neuro-Fuzzy Inference System
ANN	-	Artificial Neural Network
ASIC	-	Application Specific Integrated Chips
BLDC	-	Brushless DC Motor
DSP	-	Digital Signal Processor
EKF	-	Extended Kalman Filter
ELO	-	Extended Luenburger Observer
EV	-	Electric Vehicle
FIS	-	Fuzzy Inference System
FLC	-	Fuzzy Logic Controller
FPGA	-	Field Programmable Gate Arrays
FSMC	-	Fuzzy Sliding Mode Control
GA	-	Genetic Algorithm
HDL	-	Hardware Description Language
HEV	-	Hybrid Electric Vehicle
HIL	-	Hardware in the Loop
KH	-	Krill Herd
LQG	-	Linear Quadratic Gaussian
LQR	-	Linear Quadratic Regulator
MRAS	-	Model Reference Adaptive System
NB	-	Negative Big
NS	-	Negative Small

PB	-	Positive Big
PI	-	Proportional plus Integral
PID	-	Proportional plus Integral plus Derivative
PMSM	-	Permanent Magnet Synchronous Motor
PS	-	Positive Small
PSO	-	Particle Swarm Optimization
QDR	-	Quarter Decay Response
SMC	-	Sliding Mode Control
SRM	-	Switched Reluctance Motor
VHDL	-	Very High Speed Integrated Chip Hardware Description Language
VSC	-	Variable Structure Control
Z	-	Zero

NOTATIONS

B	Friction coefficient in N-m/rad/s
$e(t)$	Error signal
e_a, e_b, e_c	Back EMF of BLDC in 3phases in V
E_b	DC motor back emf in V
f_a, f_b, f_c	Trapezoidal functions
i	Stator current of SRM in A
i_a, i_b, i_c	Input currents in 3 phases of BLDC motor in A
I_a	Armature current of DC motor in A
i_d, i_q	Direct and quadrature components of stator current of PMSM in A
J	Moment of inertia of the rotor in Kg-m ²
K	Gain constant of FSMC
K_b	Back emf constant in V/rad/s
K_d	Differential gain
K_i	Integral gain
K_p	Proportional gain
K_t	Toque constant in N-m/A
L	Stator inductance of SRM/PMSM in H
L_a	Armature self-inductance of DC/BLDC motor in H
L_d, L_q	Direct and quadrature components of stator inductance of PMSM in H
M	Armature mutual inductance of BLDC motor in H
p	differential operator
R	Stator resistance of SRM/PMSM in ohm
R_a	Armature resistance in ohm
s	Seconds

s	Sliding surface
sat	Saturation function
sgn	Signum function
T	time
T	Torque developed by DC motor in N-m
T_e	Electro-magnetic torque in N-m
T_l	Load torque in N-m
u	Control signal
V	Stator voltage of SRM/PMSM in V
V_a	Armature voltage of DC motor in V
V_a, V_b, V_c	Terminal phase voltage of BLDC motor in V
v_d, v_q	Direct and quadrature components of stator voltage of PMSM in V
Θ	Angular position in rad
λ_1, λ_2	Constants of sliding surface
Φ	Flux per pole in Wb
Φ	Thickness of the boundary layer
Ψ or λ_p	Flux linkage in Wb
ψ_d, ψ_q	Direct and quadrature components of stator flux linkage of PMSM in Wb
ψ_f	Flux linkage due to permanent magnet in PMSM
ω	Angular velocity in rad/sec

CHAPTER 1

INTRODUCTION

An electric drive is a power conversion means utilized by most of the industrial automation systems and processes to convert electrical power to mechanical power, and to control the torque, speed or position of the load. A modern electric drive system consists of a motor, an electric converter and a controller integrated together to perform a mechanical manoeuvre for a given load (Barrero and Duran, 2016). Electric motors that are used in servo control applications for solar tracking, antenna positioning, robotic arm movement, hybrid electric vehicles and aerospace vehicles are some of the examples of special electric machines. Recent developments in advanced manufacturing and automation in industries demand very fast and robust techniques of characterization and control mechanisms of these electric drives. Ultra precision and high speed machining are two major challenges with great scientific relevance to meet the requirement of industrial automation (Rind *et al.*, 2017). Speed control of electric machines has become very fast and efficient with the evolution of power electronic switches and various power converters that help to convert and control electrical power from ac to dc, dc to dc, dc to ac as well as ac to ac. DC Servo motors, Brush Less DC Motor (BLDC), Permanent Magnet Synchronous Motor (PMSM) are some of the widely used special electric motors for various industrial applications, viz. DC servo motor in traction, BLDC, PMSM and Switched Reluctance Motor (SRM) motors in aerospace and electric vehicles (Bose, 2009). The basic criterion in selecting an electric motor for a particular application depends on the power demand as well as characteristic performance during its steady state and dynamic operations under no load as well as loaded conditions.

Characteristics of mechanical load, environmental factors and cost are also extremely important factors that decide the selection of motor for its specific application. For example, in applications like traction and elevators where high starting torque is required, a DC series motor is a better choice than an induction motor where as in petrochemical industries these motors are unsuitable as it produces sparking between the brushes and commutator segments. Similarly PMSM find more promising applications in Electric Vehicle (EV) / Hybrid Electric Vehicle (HEV) due to its higher efficiency and lower rotor inertia even though they are more expensive than induction motors (Rahman *et al.*, 2006).

Drives are generally controlled by conventional Proportional – Integral – Derivative (PID) controllers due to the advantages of its simple design, low cost, low maintenance and their effectiveness. It is necessary to know the mathematical model of the drive system or to setup some experiments for the tuning of PID parameters for its control. However, it has been known that conventional PID controllers generally do not work well for non-linear systems, particularly for complex and approximated mathematical models (Pundaleek *et al.*, 2010). Also, this control technique is not capable enough in dealing with system uncertainties such as parameter variation and external disturbances. A controller without D mode is preferred when large disturbances and noise are present during the operation of the drive system. Subsequently alternate control mechanism suitable for handling non-linearity in the system, machine parameter variations and load variations are suggested. Recently developed control mechanisms like back stepping control (Cai *et al.*, 2017), adaptive control (Wai *et al.*, 2015), H- infinity control (Zhou and Hu, 2015) and Artificial Neural Network (ANN) based control (Ali *et al.*, 2014) can be used for the control and stabilization of systems with parameter uncertainty and disturbances. Even though these controllers perform better than the linear controllers,

their algorithms are quite complex and computationally expensive which necessitates a comparatively simple and effective controller for drive systems. Sliding Mode Control (SMC), Fuzzy Logic Control (FLC) and their combination are found to be a better solution from the point of view of design, implementation and economic considerations for the control of drives.

SMC is a widely used method to handle uncertain non-linear systems (Young *et al.*, 1999). The main advantage of using SMC is that it is robust against external disturbances and parameter variations (Decarlo *et al.*, 1998). The control strategy in SMC is designed such that the system states are directed and then constrained to lie on a specified sliding surface or within a neighbourhood of a suitable switching surface as long as the system trajectories stay on the surface. The closed-loop dynamics are completely governed by the equations that define the surface (Spurgeon and Edwards, 1998). Conventional SMC has been successfully implemented to control drive systems like DC motor (Dumanay *et al.*, 2016) and BLDC motor (Chen *et al.*, 2017) for the control of position as well as speed. However for this SMC, the sliding surface uses a discontinuous switching function resulting in chattering, a phenomenon of high frequency oscillations in the output due to the high frequency switching of the control action. The effect of chattering can be significantly reduced by boundary layer solution (Lee and Utkin, 2007) in which, a boundary layer is introduced around the sliding surface, which is achieved by replacing the discontinuous switching function with a continuous form mostly by a saturation function. Performance of a chatter free SMC using a continuous function with the gain made variable to adapt to the changes in load as well as system parameters will definitely improve its performance. Fuzzy logic is an effective method that can be used for varying parameters under certain rules.

Fuzzy Logic Controllers (FLC) that uses fuzzy set theory (Zadeh, 1965) expresses the feedback control laws using heuristic knowledge, when parameters of the control plants are unknown and is an effective tool to handle imprecise and uncertain decision-making problems. FLC has been successfully applied to various industrial control applications, such as speed control of DC motor (Montiel *et al.*, 2007), balancing of Ball and Beam system (Emhemed, 2013), vector control of Induction motors (Uddin *et al.*, 2002) etc. By combining the intelligence of Fuzzy logic with the SMC, a considerable improvement in the controller output and thereby significant enhancement in the system performance can be achieved (Baround *et al.*, 2018). FSMC is a combination of modified SMC and Fuzzy Inference system and it has been successfully implemented in industrial applications like closed-loop vector control for a grid-connected Wave Energy Conversion System (WECS) driven Self-Excited Induction Generator (SEIG) (Elgammal, 2014), erection system with un-modelled dynamics (Feng *et al.*, 2017) and uncertain MIMO nonlinear systems (Roopaei *et al.*, 2009)

BLDC motor is widely used in robotic arm movement where various linear as well as nonlinear techniques are applied for its accurate position control (Camorali *et al.*, 2006). In order to achieve such precise control without overshoot and with fast settling, a robust nonlinear intelligent controller is to be developed. Another key area in which accurate speed control is essential is in electric vehicle where BLDC motor and SRM are widely used. These motors are inherently nonlinear due to the presence of variation in reluctance and magnetic saturation which results in coupled and nonlinear dynamic system. Accurate speed control of the vehicle with continuously varying load due to road condition can be accomplished with the use of a nonlinear intelligent control method (Monteiro *et al.*, 2015).

For the realization of any designed controller, both Application Specific Integrated Chip (ASIC) and Field Programmable Gate Array (FPGA) provide a good solution. An FPGA is a large-scale integrated circuit, for which the hardware configuration can be changed by programming using Hardware Description Languages (HDL) like VHDL (Very High Speed Integrated Chip HDL) and Verilog. Digital Signal Processor (DSP) like ASIC is having predetermined, unchangeable hardware function and hence computation of any complex controller like Fuzzy SMC becomes a challenge using this. For the implementation of digital systems, FPGA is preferred over ASIC due to the fast computational ability, configurable hardware construction, low power consumption, embedded processor and shorter design cycle (Kung and Tsai, 2007; Chou *et al.*, 2013). FPGA is successfully used for the implementation of aircraft control (Hartley *et al.*, 2014), power generation control of hybrid power system (Nagraj and Panigrahi, 2015) and in various similar servo applications.

Performance of a controller is normally evaluated using simulation software like MATLAB based Simulink, Pspice or Psim. In the present research work the design and simulation of the modified sliding mode controller, fuzzy controller and fuzzy sliding mode controller for various DC and AC drives are carried out and their performance is compared with that of Fuzzy PI and conventional PI controllers. Hardware in the loop simulation (HIL) and actual hardware of the fuzzy sliding mode controller using FPGA are also implemented. The performance of this actual controller is compared with that of the simulation results for the validation purpose.

1.1 MOTIVATION FOR THE RESEARCH

Industrial drive systems are generally controlled by conventional Proportional – Integral (PI) controllers. The main problem associated with the conventional linear PI controllers is its inverse relationship between the speed of response and the peak overshoot. The peak overshoot can be reduced only at the cost of speed of response or the settling time of the system. Other linear controllers like Linear Quadratic Regulator (LQR) and Linear Quadratic Gaussian (LQG) also exhibit the same problem and this point towards the need of an alternate simple and economic technique suitable to achieve better steady state as well as transient performance indices.

Non-linear and adaptive control methods have been applied to the speed and position control of drive systems to overcome the problems associated with linear control techniques. Back stepping control, Adaptive control, ANN control, FLC, SMC are some of them. Of these, back stepping control lacks robustness and its practical implementation is laborious due to its complex algorithm. Adaptive control gives better performance when an accurate model is available. ANN is also a modern intelligent control technique used mainly in robotic applications (Chaoui *et al.* 2009), speech recognition (Kamble, 2016), pattern recognition (Basu *et al.* 2010) and many more. Due to its limitation of training using algorithms, this method can lead to variations in the output of the drive systems with very fast dynamic response and sudden load variations. Fuzzy control is a better solution for intelligent control that depends on heuristic rules even though it lacks a perfect mathematical model. On the other hand it is found that parameter variation and external disturbances are dealt with SMC and it is effectively used to eliminate the peak overshoot along with

improvement in the speed of response (Spurgeon and Edwards, 1998). The problem associated with chattering in conventional SMC is reduced by modifying the control law. The performance of modified SMC is further improved by intelligently varying the controller parameters within an optimized range using a fuzzy inference system (FIS).

1.2 OBJECTIVES OF THE RESEARCH

The main objective of this work is to design, develop and implement non-linear controllers of DC & AC drives suitable for the industrial applications with the following properties.

- Robust against machine parameter variation and external disturbances like sudden load variation
- Having high speed of response with reduced overshoot and steady state error
- Less Complex and easy to design and implement
- Economical

A conventional DC motor, SRM, BLDC motor and PMSM are considered for the performance evaluation of various controllers. Hardware implementation of the most suitable controller using FPGA on a BLDC motor, for the verification of design and corresponding validation of results, is also the objective of this research work.

1.3 OUTLINE OF THE THESIS

The proposed thesis is organized in 8 chapters. The first chapter introduces the problem and defines the aim of the thesis. Chapter 2 contains review of background literature on various developments in linear and non-linear control techniques

especially for DC and AC drive systems. Chapter 3 explains various DC and AC drives and their characteristics that make them applicable in different industrial environment. This chapter includes the mathematical modelling of conventional DC motor, BLDC motor, SRM and PMSM. Various linear and non-linear control strategies used in drive systems are discussed in chapter 4. Chapter 5 presents the design of controllers for position/speed control of DC servo motor, BLDC motor and SRM. Design and performance analysis of FSMC, chatter free SMC, Fuzzy controller, Fuzzy PI controller and conventional PI controller for these motors are carried out in this chapter. Design of various controllers for AC motor is discussed in chapter 6. FSMC, chatter free SMC, fuzzy PI controller and conventional PI controller are designed for the field oriented control of a PMSM and their performance comparison and analysis are carried out in this chapter.

The hardware implementation of the FSMC using FPGA is explained in chapter 7. HIL Simulation of FSMC for PMSM and BLDC motor are carried out using Xilinx Virtex 4 FPGA board and the results are analysed. The hardware implementation of FSMC for the BLDC motor using FPGA is carried out and the results are validated in this chapter. Chapter 8 concludes with a summary of the work done along with suggestions for the future research.

CHAPTER 2

LITERATURE SURVEY

A brief review of existing modern industrial drives, linear control strategies, necessity of non-linear controllers and advanced non-linear control techniques are discussed here.

2.1 MODELLING OF INDUSTRIAL DRIVES

An electric drive is an electromechanical device for converting electrical energy into mechanical energy to impart motion to different machines and mechanisms for various kinds of industrial applications. It is the workhorse in a variable-speed drive system and is generally classified as dc and ac machines. Traditionally, ac motors, particularly induction motors are used in constant-speed applications whereas DC motors are widely used in variable-speed applications. A modern electric drive system has a power source that supplies the energy, a converter which provides adjustable voltage/current and/or frequency and a controller to ensure the stability as well as the system performance (El-Sharkawi, 2000). The adjustable speed drive constitutes a multivariable control system and therefore, in principle, the general theory of multivariable control system is applicable. Here, the voltages and the frequency are the control inputs and the outputs may be speed, position, torque, air gap flux, stator current or a combination of these (Leonhard, 1984; Dong *et al.*, 2018).

Mathematical model of a system is a set of equations to describe the behaviour of it and is used for the simulation and analysis. Naresh K. Sinha et al. describes three different mathematical models of an armature-controlled dc servo motor: (i) a precise nonlinear

model, (ii) a piecewise linear model, and (iii) a second-order linear model. Experimental results are presented by comparing the various models, and a range of applications for each is suggested (Sinha *et al.*, 2018). A mathematical model of DC servo motor used for the position control of a robotic arm is found in literature (Benksik, 2004). The non-linear model incorporating the saturation effect of the core of a DC motor for its speed control is found in (Mahajan and Deshpande, 2013). Also non-linear modelling and identification of a DC motor rotating in two directions together with real time experiments is demonstrated in (Kara and Eker, 2003).

A brushless DC (BLDC) motor model is explained by (Pillai and Krishnan, 1989b) in which the motor has a trapezoidal back EMF, and rectangular stator currents to produce a constant electric torque. State space model of BLDC motor for the Simulink simulation of its speed control is described by (Muruganatham and Palani, 2010). Mathematical model of an inverter fed BLDC motor with PI control is described by (Purnalal and Sunil Kumar, 2015). A BLDC motor with improved magnetic material having high B-H product that is suitable for high power applications is modelled by (Luk and Lee, 1994). A simplified model for simulation and experimental analysis of BLDC motor suitable for sensor less operation is explained by (Kaliappan and Chellamuthu, 2012). Here the technique of zero crossing of back EMF is used to estimate the rotor position for the sensor less operation instead of measuring it using Hall Effect sensors.

Iqbal Husain and Syed A. Hossain explain the modelling and control of switched reluctance motor (SRM) including possible nonlinearities (Husain and Hossain, 2005). A novel model of SRM with C-core is explained by (Mao and Tsai, 2005).

This motor has the advantages of low-cost production that possesses high slot space for ease of coil winding which can be used for high power applications. A simplified model of IGBT inverter driven three phase 6/4 SRM used for variable speed pumping is described by (Parker, 2004). A simple model of SRM with nonlinear magnetization characteristics is used for computer-aided designs is described (Roux and Morcos, 2002).

(Pillai and Krishnan, 1989a) describes the dynamic d-q model for the vector control of Permanent Magnet Synchronous Motor (PMSM). As the vector control transforms the PMSM to an equivalent separately excited dc machine, the transfer function between the electric torque and current is linear. Model for the direct torque control (DTC) of PMSM is explained by (L. Zhong *et al.*, 1997) and the simulation results show that the torque response is much faster than the one with current control. A PMSM is modelled and the motor parameters are optimized using genetic algorithm for the performance improvement is carried out in (Shahat and Shewy, 2010). This model can be used in various applications such as automotive, mechatronics, green energy applications, and machine drives. A flux-weakening control for a current-regulated surface mounted PMSM to obtain an extended speed range is demonstrated in (sudhoff *et al.*, 1995).

Mathematical modelling and speed/position control of various special electric motors are also given by (Krishnan, 2001). A detailed survey of various existing linear as well as non-linear control techniques is carried for the purpose of design and implementation of an effective control strategy for the industrial drives.

2.2 LINEAR CONTROL TECHNIQUES

Proportional-integral-derivative (PID) controller is very widely used in many control applications due to its simplicity and effectiveness (Ang *et al.*, 2005). It is extensively used in drive control applications such as speed control of DC motor (singh *et al.*, 2013), BLDC motor (Kumar *et al.*, 2014), SRM (Nanda *et al.*, 2016) and PMSM (Chakravarthi and Karpagavalli, 2016). Even though the use of PID control has a long history in the field of control engineering, the three controller gain parameters, proportional gain K_P , integral gain K_I , and derivative gain K_D , are usually fixed and are obtained using the tuning process. The disadvantage of PID controller is its poor capability in dealing with system uncertainty, i.e. parameter variations and external disturbances. A very important step in the use of these controllers is the tuning process which becomes complex due to its iterative procedure. Tuning a PID algorithm generally aims to match some preconceived 'ideal' response profile for the closed loop system. Many algorithms have been developed to guarantee the best performance of the PID controller of which Ziegler-Nichols tuning method is the most popular one (Wang *et al.*, 1997; Lin and Jan, 2002; Yu and Hwang, 2004).

Another substitute to PID controller is the Linear Quadratic Regulator (LQR) for which all the system states must be measurable, and its design methodology is explained in detail by (Katsuhiko Ogata, 2002). If the system state variables are not measurable, the alternative to LQR is the Linear Quadratic Gaussian (LQG) controller in which all the state variables are estimated using a Kalman estimator and the measuring noise is assumed to be Gaussian. Michael Athans, in his paper (Athans, 1971) has demonstrated the design philosophy of LQG controller based on

deterministic perturbation control, stochastic state estimation and linearized stochastic control. The LQR and LQG design is also explained by (Stephani *et al.*, 1998) and Balazs Kulcsar in his paper discusses the fundamental aspects of LQR/LQG control theory with an example of aircraft, controlled by a flight controller (Kulcsar, 2000). The LQG controller design for balancing an Inverted Pendulum Mobile Robot is described by (Eide *et al.*, 2011).

2.3 NON- LINEAR CONTROL TECHNIQUES

Many dynamic systems behave as almost linear, under certain operating conditions and therefore linear control theory is widely applicable in reality. But quite often, when operating a system on its limits, different kinds of nonlinearities make them self-known and may degrade the stability and performance properties to such an extent that they are no longer acceptable. These nonlinearities must then be taken into account while designing and implementing the controller for real time applications. Different popularly used novel non-linear control techniques found in literature are sliding mode control (SMC), back stepping control, gain scheduling and feedback linearization of which SMC and back stepping are the most popular and are discussed below. For analysing the stability of non-linear systems Lyapunov Stability criterion and phase portrait methods are generally used (Slotine, 1991).

2.3.1 Sliding Mode Control (SMC)

SMC is a variable structure control (VSC) method which is explained by (Utkin, 1977; Dracunov and Utkin, 1992). It is a nonlinear control method that alters the dynamics of a nonlinear system by application of a discontinuous control signal which forces the

system to "slide" along a cross-section of the system's normal behaviour. The state-feedback control law is not a continuous function of time. Instead, it can switch from one continuous structure to another based on the current position in the state space. The most distinguished feature of VSC is that it is completely insensitive to parametric uncertainty and external disturbances (Hung *et al.*, 1993; Manjunath, 1995). The term "variable structure control" arises because the controller structure around the plant is intentionally changed by some external influence to obtain a desired plant behaviour or response. The multiple control structures are designed so that trajectories always move towards an adjacent region with a different control structure, and hence the ultimate trajectory will not exist entirely within one control structure, instead, it will *slide* along the boundaries of the control structures. The motion of the system as it slides along these boundaries is called a *sliding mode* and the geometrical locus consisting of the boundaries is called the *sliding surface*. The important feature of it is the relative simplicity of design, control of independent motion (as long as sliding conditions are maintained), invariance to process dynamics characteristics and external perturbations. This means the system is insensitive to any variation or perturbation of the plant parameters (Decarlo *et al.*, 1988).

The main drawback of SMC is the phenomenon of chattering which produces high frequency oscillations in the output due to the high frequency switching in the input. V.I.Utkin *et al.* presented a guide to sliding mode control for practicing control engineers. It offers an accurate assessment of the so-called chattering phenomenon catalogues implementable sliding mode control design solutions and provides a frame of reference for future sliding mode control research (Young *et al.*, 1999). There are many methods found in the literature to overcome the phenomenon of chattering and

one of the best solutions is to introduce a boundary layer around the switching surface (Slotine and Sastry, 1983). The applications of sliding mode controller for electric drives are also presented by (Utkin, 1993). A novel DC drive control scheme based on the VSC theory has been proposed in (Damiano *et al.*, 2004; Sarwer *et al.*, 2004). A sliding mode controller is designed and implemented for the speed estimation and control of permanent magnet synchronous motor (Corradini *et al.*, 2012) and a chattering free SMC is realized for an electromechanical actuator with backlash nonlinearity (Ma *et al.*, 2017). A second order SMC algorithm, that reduces the effect of chattering, is used to control a robust dc-drive which demands only rough information about the actual motor parameters, is proposed by (Damiano *et al.*, 2004). The design of a PI-Sliding Mode controller for the speed control of an induction motor used for electric vehicle is explained and the results are compared with that of conventional SMC and PI controller by (Ltifi *et al.*, 2014). Speed control of an electromechanical system using back stepping integral sliding mode controller (BSISMC) is implemented and its performance in the presence of uncertainties and disturbances is compared with that of conventional SMC and the results indicate robust performance with good tracking ability (coban, 2018).

2.3.2 Back stepping control

Back stepping is a novel non-linear design technique for non-linear systems where the useful nonlinearities are not cancelled in the design process. It is a Lyapunov method based versatile nonlinear control design approach that is particularly well suited for addressing the problem of multivariable control problem of complex nonlinear systems developed by (Kokotovic *et al.*, 1995) for a special class of dynamical

systems. This technique focuses on breaking down the complex nonlinear systems into smaller subsystems for the design of Lyapunov functions for the control. The virtual control for these subsystems is obtained by integrating the individual controllers into an actual controller by stepping back through the sub system and re-assembling it from its component subsystems (Joseph and Geetha, 2007). Because of this recursive structure, the designer can start the design process at the known-stable system and "back out" new controllers that progressively stabilize each outer subsystem. The process terminates when the final external control is reached and hence is known as back stepping control.

Back stepping control is applied for the stabilization of permanent magnet synchronous motor (Merzoug, 2010) and linear induction motor (Hasirci *et al.*, 2009; Bousserhane *et al.*, 2009). A model reference adaptive estimator with back stepping control is used for the control of induction motor (Mehazzem *et al.*, 2009), brushless DC motor (Lin *et al.*, 2009a) and interior permanent magnet (IPM) synchronous motor (Lin *et al.*, 2009b; Lin *et al.*, 2011a). Adaptive back stepping with PI sliding mode position control for synchronous reluctance motor drives is found in (Lin *et al.*, 2011b). A comparison between chaos synchronization using active control and back stepping control is also found in (Vincent, 2008).

2.4 SOFT COMPUTING TECHNIQUES IN CONTROL

Soft-Computing is a collection of techniques spanning many fields that fall under various categories in Computational Intelligence and Fuzzy Logic, Neural Networks and Evolutionary Computation are three main branches of it. Soft computing deals with imprecision, uncertainty, partial truth and approximation to achieve practicability, robustness and low solution cost.

2.4.1 Fuzzy Logic

Fuzzy logic is an approach to computing based on "degrees of truth" rather than the usual "true or false" (1 or 0) Boolean logic on which the modern computer is based. The idea of fuzzy logic was first advanced by Dr. Lotfi A. Zadeh of the University of California at Berkeley in the 1960s (Zadeh, 1965). Fuzzy logic not only includes 0 and 1 as extreme cases of truth (or "the state of matters" or "fact") but also the various states of truth in between. For example, the result of a comparison between two things could be not "tall" or "short" but "0.38 of tallness". Fuzzy logic seems closer to the way our brains work. Fuzzy theory is extensively used for the control of dynamic plant and process control applications (Mamdani, 1974; Jang *et al.*, 1997).

Fuzzy logic is used along with conventional controllers to encounter actuator saturation has been reported earlier in the literature (Gharieb and Nagib, 2001), in which 'I' term of PID controller is nullified in order to prevent integrator windup. A comparison of fuzzy controller with a PID controller for the control of a DC motor is explained in (Sousa and Bose, 1994) and the design of a fuzzy PID controller is proposed in (Upalanchiwar and Sakhare, 2014). Sliding mode speed control and fuzzy torque control of IPM synchronous motor (Abianeh, 2011), fuzzy gain scheduling of PID controller (Vijamaa, 2002; Zhao *et al.*, 1993) are also found in literature. Fuzzy logic control when used for the speed control of BLDC motor gives better adaptability compared to conventional PI controller and offers improved transient as well as steady state performance (Usman and Rajpurohit, 2014). The SRM drive with the angle position closed-loop speed control based on fuzzy logic shows good dynamic performance and high efficiency (Chen *et al.*, 2002).

2.4.2 Artificial Neural Net work

Neural network controllers have emerged as a tool for difficult control problems of unknown nonlinear systems and are used for modelling and control of physical systems due to their ability to handle complex input-output mapping without detailed analytical models (Haykins, 1999). The application of Neural Network for the speed control of DC motor (Minkova *et al.*, 1998; Nouri *et al.*, 2008] and gain scheduling (Tan *et al.*, 1997) are found in literature. A wavelet-neural network can also be used along with sliding mode controller (El-Sousy, 2011) for the PMSM drives for its speed control. Recently much research has been done on the applications of fuzzy neural network (FNN) systems, which have the advantages of both fuzzy systems and neural networks, in the control fields to deal with nonlinearities and uncertainties of the control systems (Cirstea *et al.*, 2002). Moreover, the FNN's are universal approximators which can approximate any dynamics to a pre-specified accuracy by the learning process. Back stepping FNN controller combines the advantages of the back stepping control with robust characteristics and FNN with on-line learning ability for the accurate speed control of PMSM (Lin and Lin, 2009). Optimum position control of a BLDC motor is achieved using PID controller and the estimation of the mechanical parameters at various load setting as well as PID parameters are carried out using ANN (Ganesh *et al.*, 2012).

2.4.3 Genetic Algorithm

Genetic Algorithm (GA) is a soft computing technique used for optimization of controller parameters, based on natural selection, a process that drives the biological evolution (Chaiyaratana and Zalzala, 1997). The use of genetic algorithm for the

tuning of a PID controller is proposed in (Lin *et al.*, 2003) for the speed control of linear model BLDC motor and a GA tuned PI controller is used for the vector control of PMSM (Kuntol and Seok-kwon, 2013) and induction motor (Dey *et al.*, 2009).

2.5 ADAPTIVE CONTROL

Adaptive Control is used for system with parameter variation and uncertainties and this controller can modify the systems behaviour in response to changes in the dynamics of the process and character of the disturbances. For example, when an aircraft flies, its mass will slowly decrease as a result of fuel consumption and the control law has to adapt itself to such changing conditions. The adaptive control systems are mainly classified in to three categories namely Gain scheduling, Model Reference Adaptive Control (MRAC) and Self tuning regulators (STR) (Astrom and Wittenmark, 1997). Gain scheduling is an approach to control of non-linear systems that uses a family of linear controllers, each of which provides satisfactory control for a different operating point of the system (Lawrence and Rugh, 1995). Model Reference Adaptive Systems (MRAS) may be regarded as an adaptive control technique in which the desired performance is expressed in terms of a reference model, which gives the response to the command signal. MRAC technique is found to be used for the speed control of a BLDC motor (Bernat and Stepien, 2011) and the design of a Model Reference Adaptive Controller using modified MIT rule for a Second Order System is explained (Jain and Nigam, 2013). In Self tuning regulators, the process parameters are estimated in real time and the controller parameters are varied according to the process parameters and the algorithm and applications of STR is explained by (Astrom *et al.*, 1977). The use of STR for the tracking control of a DC servo motor is explained in (Khamis, 2013).

2.6 ROBUST CONTROL

Robust control originates with the need to cope with systems that has modelling uncertainty and these methods aim to achieve robust performance in the presence of bounded modelling errors. Most popular robust control techniques are H-infinity control and μ - synthesis. A robust H-infinity optimal speed control scheme for a DC motor with parameters variations and disturbance torque using a linear matrix inequality (LMI) approach is presented in (Lu *et al.*, 2008) and an H-infinity controller design for permanent-magnet DC motor is proposed in (Brezina and Brezina, 2011). A μ synthesis controller design method for a DC-motor-based active suspension is described by (Zhang *et al.*, 2012).

2.7 SENSOR LESS CONTROL

Sensor less control is used in drive system where the measurement of speed/ position using sensors is difficult and in such cases, several rotor speed and position estimation techniques have been applied. The back-EMF based rotor speed estimation method works satisfactorily at higher speeds. However, the speed estimation becomes very difficult at lower speeds, due to the small values and distorted EMF signal. State observer methods based on Extended Kalman Filter (EKF) (Bolognani *et al.*, 2003), Extended Luenburger Observer (ELO) (Li and Zhu, 2008), and Sliding Mode Observer (Li and Elbuluk, 2001) are used for the speed estimation of PMSM. Most of these methods suffer from complex computation, sensitivity to parameter variation and need of accurate initial conditions. The EKF has the advantage of estimating the parameters and speed simultaneously by considering them as state. However, it is

computationally extensive and requires a high sampling frequency so that a simple discrete-time equivalent model can be used. The sliding mode observer is simple and offers a limited robustness against the parameter variation. However, sliding mode being a discontinuous control with variable switching characteristics has chattering problems and it may affect the control accuracy. Recently, some more advanced adaptive estimation techniques based on Artificial Neural Network (ANN) (Batzel and Lee, 2000; Liu and Wang, 2006) and Fuzzy Logic Control (FLC) (Adam and Gulez, 2008) have also been reported for the speed estimation of PMSM. However, the estimation accuracy depends on number of neurons and number of fuzzy membership functions used for rule base and requires off-line tuning. One of the recent speed estimation techniques is Model Reference Adaptive System (MRAS) which is based on the adaptive control (Liang and Li, 2003). MRAS method uses two models one independent of rotor speed (Reference Model) and the other dependant on rotor speed (Adjustable Model), both having same output. The error of these actual and estimated outputs is fed to the adaptation mechanism that outputs the estimated rotor speed. This estimated value of speed is used to tune the adjustable model till error is zero where the estimated speed is equal to the actual speed. MRAS method suffers from parameter dependence and pure integrator related problems in reference model. To overcome this problem, an alternative MRAS structure along with Adaptive Neuro-Fuzzy Inference System (ANFIS) is used in PMSM motor (Jain *et al.*, 2011) which is again facing the problem of computational complexity. From the literature it is found that some of the speed/ position estimation techniques have several limitations while some others are computationally complex. Also it is required to use sensors to measure the other state variables such as voltage and current in order

to estimate the speed/ position. Due to these disadvantages it is better to use the speed /position sensors in applications where their use is not limited due to the environmental conditions.

2.8 FUZZY SLIDING MODE CONTROL

By combining the intelligence of Fuzzy logic with SMC, a considerable improvement in the controller performance can be achieved. This method has been successfully implemented for the air flow control of a fuel cell (Baround *et al.*, 2018), closed-loop vector control for a grid-connected Wave Energy Conversion System (WECS) driven Self-Excited Induction Generator (SEIG) (Elgammal, 2014), erection system with unmodelled dynamics (Feng *et al.*, 2017), and to handle uncertain MIMO nonlinear systems (Roopaei *et al.*, 2009). A two dimensional fuzzy sliding mode control of a field-sensed magnetic suspension system is given in (Li and Chiou, 2014) and FSMC with low pass filter in order to reduce chattering is given in (Balamurugan *et al.*, 2017).

2.9 OPTIMIZATION OF THE CONTROLLER GAIN

Optimization can be defined as the act of achieving the best possible solution to problem under given circumstances. In recent years, meta-heuristic algorithms have been widely used for solving optimization tasks and are proven to be efficient when compared to the other conventional methods based on the Linear and Non-Linear programming. The main advantage of these algorithms is the avoidance of local minima and the other benefits are simplicity, flexibility and derivation free structure (yang, 2010). Some of the popular meta-heuristic algorithms are as follows. Genetic algorithm (GA) is one of the evolutionary search algorithms, which was proposed by

Holland in 1967 based on Darwinian evolution of survival of the fittest that uses crossover and mutation as two operators (Holland, 1967). Simulated annealing is another example which is inspired by annealing process of melts, proposed in 1983 (Kirkpatrick *et.al.*, 1983). Particle Swarm Optimization (PSO) proposed by Kennedy and Eberhart in 1995 in which the particles sharing the information of the best position they ever found to find the global optimal (Eberhart and Kennedy, 1995). Ant Colony Optimization (ACO) proposed by Dorigo *et al.* in 1996 inspired by the behaviour of ants in nature in finding the nearest path between their nest and the food source (Dorigo *et al.*, 1996). Differential evolution is proposed by Storn and Price in 1997 (Storn and Price, 1997) and Bees Algorithm proposed by Pharm *et al* in 2005 (Pharm *et al.*, 2005) is a swarm-based optimization algorithm that mimics the food foraging behaviour of honey bees. Optimizing the parameters of a PID controller using meta-heuristic methods like Genetic Algorithm (GA), particle swarm optimization (PSO) and the method of cross entropy (CE) for process control application is described in (Mora, *et al.*, 2016). An efficient algorithm based on Ant colony optimization (ACO) applied for the parameter optimization of PID controller for DC motor speed control which can preferably conquer the shortcomings of traditional optimization methods and efficiently improve the global convergence speed is described in (Ibrahim *et al.*, 2014). PSO is applied for the parameter optimization of an H- infinity controller for the control of a pneumatic servo actuator (Ali *et al.*, 2010).

One of the recent bio-based swarm intelligence algorithms, called Krill Herd (KH), proposed by Gandomi and Alavi in 2012 by idealizing the swarm behaviour of krill (Gandomi and Alavi, 2012; Wang *et al.*, 2014). For the krill movement, the objective function used in KH is determined by the least distances from food and the highest

herd density. By idealizing the swarm behaviour of krill, KH is a meta-heuristic optimization approach for solving optimization problems. In KH, the position of Krill is mainly affected by three actions, namely movement affected by other krill, foraging action and physical diffusion. Comparing with other algorithms, one of the advantages of the KH algorithm is that it requires only few control variables to regulate. An optimal PID controller is designed for the frequency oscillation damping of a wind-diesel hybrid system using Krill Herd (KH) algorithm by Shayanfar et al. in (Shayanfar *et al.*, 2015). In the present study, it is aimed to optimize the gain of Fuzzy SMC controller based on Krill Herd Algorithm to control the speed with optimum performance. The controller gain is optimized by using an objective function based on improvements of parameters such as rise time, maximum overshoot, settling time and minimum steady state error.

2.10 HARDWARE IMPLEMENTATION OF THE CONTROLLER

For the real time application of any controller its realization using a suitable processor is essential. When, the model incorporating various system nonlinearities in the presence of modelling error, disturbances and noise, an embedded processor capable of fast computational ability and high switching speed, is required for its implementation. Application Specific Integrated Chip (ASIC) like digital signal processor (DSP) and field programmable gate array (FPGA) are the popularly used processors for the realization of complex control algorithms. Implementation of a PI controller for the speed control of an induction motor drive using DSP processor is explained in (Mohznty and Muthu, 2011). However DSP operates in the KHz range and becomes unsuitable when used for embedded applications with higher switching frequency (Li, *et al.*, 2011). Moreover, DSP has the limitation of fixed hardware

configuration that makes it application specific and hence FPGA with programmable hardwired feature, fast computation ability, shorter design cycle, embedding processor, low power consumption and higher density is preferred for the implementation of the digital controllers (Kung and Tsai, 2007; Chou *et al.*, 2013). A review of the state of art of FPGA design methodologies with a focus on industrial control system applications is suggested in (Monmasson and Cirstea, 2007). Design and implementation of PID controller based on FPGA for low voltage synchronous DC to DC buck converter is described in (Chnader *et al.*, 2010). The effectiveness of a FPGA based lag-lead compensator for the position control of a CNC machine is explained in (Osornio-Rios, 2017). FPGA implementation of SMC is found in many literatures, viz. Voltage control of a DC-DC Single-Ended Primary Inductor Converter (SEPIC) (Li, *et al.*, 2011) and the position control of a robot manipulator (Piltan *et al.*, 2015; Piltan *et al.*, 2011). Also an FPGA based adaptive back stepping sliding-mode controller is proposed to control the mover position of a linear induction motor (Lin *et al.*, 2007). The implementation of fuzzy logic controller for the speed control of electric vehicle with DC motor using FPGA is given in (Poorani *et al.*, 2005) and an improved adaptive fuzzy logic speed controller for a DC motor, based on FPGA implementation is proposed in (Ramadan *et al.*, 2013). Moreover the design of the Fuzzy-PI controller for omnidirectional robot navigation system and its hardware implementation using FPGA is explained by (Masmoudi *et al.*, 2016).

Here we aim to analyse the suitability of Fuzzy SMC for the speed control of selected industrial drives under real time conditions of parameter variation and external disturbances. For this purpose modelling of DC servo motor, BLDC motor, SRM and PMSM are designed incorporating their important nonlinearities.

The development of various control techniques used for different drive system as given in literature are summarised in table 2.1

Table 2.1 Evolution of Control Techniques

Linear Control Techniques	Nonlinear Control Techniques	Robust Control Techniques	Intelligent Control Using soft computing	Adaptive Control
PID (1922) LQR/ LQG (1972)	SMC (1977) Back stepping (1990)	H infinity (1978) Mu synthesis (1995)	Fuzzy Logic(1965) ANN (1954) Genetic Algorithm (1970)	STR(1978) MRAC (1978)

CHAPTER 3

MODELLING OF DC AND AC DRIVES

An electric drive is a power conversion means utilized by most of the industrial automation system and process to convert electrical power to mechanical power. Speed, position and torque control are the major functions of an electric drive in industrial applications.

A modern electric drive system has five main functional blocks, a power source, a converter, a motor, a controller and a mechanical load as shown in fig 3.1. The power source provides the energy required for the drive system. The converter interfaces the motor with the power source and provides the motor with adjustable voltage/current and/or frequency. The controller supervises the operation of the entire system to enhance overall system performance and stability (El-Sharkawi, 2000).

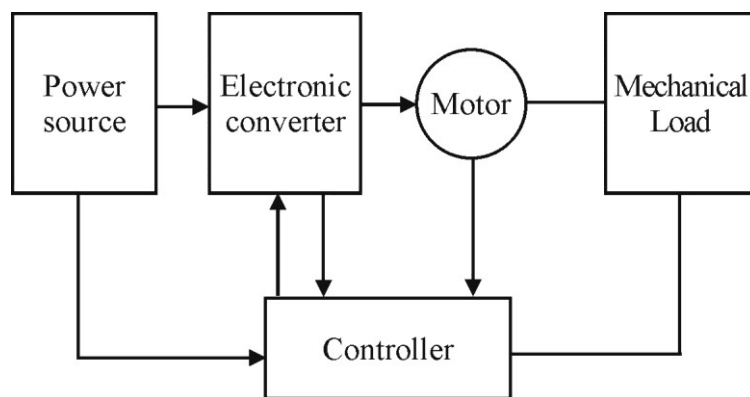


Fig 3.1 Functional blocks of a drive system

The electric motor is the electro-mechanical energy conversion device which acts as the work horse of the drive system whose speed/position and torque is to be controlled in such a way that it matches with the application requirement. In order to

achieve the desired performance of the motor, an electronic converter along with a suitable controller is employed. The most basic function of the controller is to monitor the system variables, compare them with some desired values and readjust the converter output until the system achieves the desired performance and this feature is used in speed or position control applications in electric drives. The controller is also used to enhance the stability of the system. For the design of a controller, a suitable mathematical model represented by a set of equations that describe the behaviour of the system and provides the complete specification of the real drive is required.

Drives are broadly classified into two categories, namely DC and AC according to the nature of the power source used. Traditionally DC drives are used for variable speed applications where as AC drives are used for constant speed applications.

Conventional DC motors, Brushless DC Motor (BLDC), Permanent Magnet Synchronous Motor (PMSM) are very widely used for various industrial applications, viz. conventional DC motor in traction, BLDC, PMSM and Switched Reluctance Motor (SRM) motors in aerospace and electric vehicles (Rind *et al.*, 2017). The basic criterion in selecting an electric motor for a particular application depends on the power demand as well as characteristic performance during its steady state and dynamic operations under no load as well as loaded conditions. Characteristics of mechanical load, environmental factors and cost are also extremely important factors that decide the selection of motor for its specific application. For example, in applications like traction and elevators where high starting torque is required, a DC series motor is a better choice than an induction motor where as in petrochemical

industries these motors are unsuitable as it produces sparking between the brushes and commutator segments. Similarly PMSM find more promising applications in Electric Vehicle (EV) or Hybrid Electric Vehicle due to its higher efficiency and lower rotor inertia even though they are more expensive than induction motors (Rahman *et al.*, 2006).

3.1 DC DRIVES

DC drives are the electro-mechanical power converters that use DC power as the source of energy. Commonly available DC motors are conventional DC motor, BLDC motor and Switched Reluctance Motor (SRM). In the present chapter the mathematical modelling incorporating their important nonlinearities are carried out.

Table 3.1 Advantages and Disadvantages of DC motor

Advantages	Disadvantages
1. Very precise speed and position control	1. Sparking in commutator results in reduced brush and commutator life
2. Wide range of speed and torque	2. High maintenance cost
3. More powerful than permanent magnet motors	3. Require more current than permanent magnet motors

3.1.1 DC Servo motor

DC motor plays a significant role in modern industry due to their simple, effective and wide range of provision for speed and position control (Tripathi *et al.*, 2013). Numerous applications that demand good speed control with high accuracy and fast dynamic responses are in various fields' viz. rolling mills, pulp and paper mills,

cranes, hoists, elevators, machine tools, transit system and locomotive drives (Leonard, 1984). Various advantages and disadvantage of a conventional DC servo motors are given in table 3.1.

Mathematical Modelling of a DC Servo Motor

The general approach in mathematical modelling of a DC motor is to neglect the nonlinear effects due to the magnetic saturation and friction and build a linear transfer function representation for the input–output relationship of the motor and the load it drives. Some of the electromechanical systems driven by DC motor exhibits nonlinear behaviour, because of the motor saturation, friction and quantization noise in the measurement sensors. In the presence of these non-linear behaviours, it is difficult to use a linear controller as the nonlinear effects need not predict and vary according to the plant load as expected. Under such circumstances, the modelling of the machine and their linear control strategies often fails to work in the real world system.

The electric circuit of the armature and the free body diagram of the rotor are shown in fig. 3.2. Depending on the application, the speed/position of a DC motor is controlled by varying the input voltage or field current. The desired speed is tracked according to the shaft position of the motor and is determined by a reference signal using a suitable controller. This controller is selected so that the error between the system output and reference signal corresponding to the desired position and/or speed eventually tends to its minimum value, ideally zero.

Here the variation of input voltage is used as the control parameter for the position control of the motor. A constant dc voltage is selected as a reference signal to obtain the desired position of the motor. However, the method works successfully for any reference signal, particularly for any stepwise time-continuous function, that may be a periodic signal to get a desired shaft position, with desired angle between 0 and 360 degrees from a virtual horizontal line.

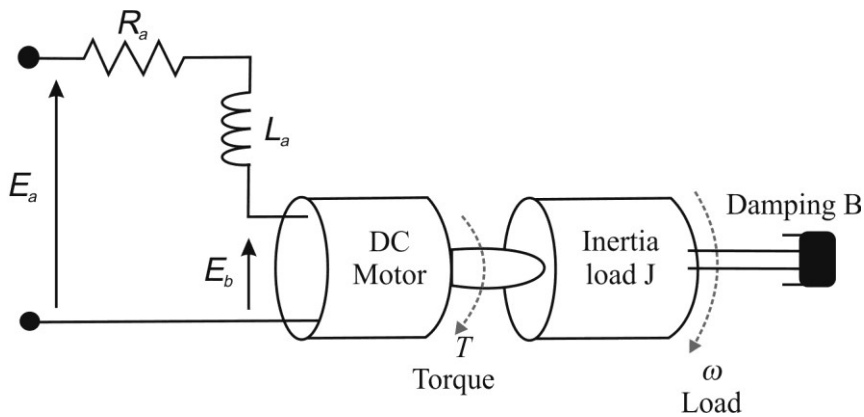


Fig.3.2 Structure of a DC Motor

The dynamics of a linearized DC servo motor is given in equations (3.1) to (3.5)

$$V_a = R_a I_a + L_a \frac{dI_a}{dt} + E_b \quad (3.1)$$

$$T = J \frac{d\omega}{dt} + B\omega - T_L \quad (3.2)$$

$$T = K_\phi \Phi I_a = K_t I_a \quad (3.3)$$

$$E_b = K_b \omega \quad (3.4)$$

$$\omega = \frac{d\theta}{dt} \quad (3.5)$$

Where R_a is armature resistance [Ω], L_a is armature self-inductance [H], V_a is the armature voltage [V], I_a is the armature current [A], E_b is the motor back emf [V], T is the torque developed [N-m], T_L is the load torque[N-m], J is the moment of inertia of the rotor[$\text{kg}\cdot\text{m}^2$], B is the friction coefficient[N-m/rad/s], Φ is the flux per pole [wb], K_t is the torque constant[N-m/A], K_b is the back emf constant[V/rad/s], ω is the angular velocity[rad/sec] and θ is the angular position[rad].

From the above equations, the state variable model of DC motor at no-load ($T_L=0$) and loaded condition are given by eqs. (3.6) and (3.7) respectively

$$\begin{bmatrix} \dot{I}_a \\ \dot{\omega} \\ \dot{\theta} \end{bmatrix} = \begin{bmatrix} -\frac{R_a}{L_a} & -\frac{K_b}{L_b} & 0 \\ \frac{K_t}{J} & -\frac{B}{J} & 0 \\ 0 & 1 & 0 \end{bmatrix} \begin{bmatrix} I_a \\ \omega \\ \theta \end{bmatrix} + \begin{bmatrix} \frac{1}{L_a} \\ 0 \\ 0 \end{bmatrix} V_a \quad (3.6)$$

$$\begin{bmatrix} \dot{I}_a \\ \dot{\omega} \\ \dot{\theta} \end{bmatrix} = \begin{bmatrix} -\frac{R_a}{L_a} & -\frac{K_b}{L_b} & 0 \\ \frac{K_t}{J} & -\frac{B}{J} & 0 \\ 0 & 1 & 0 \end{bmatrix} \begin{bmatrix} I_a \\ \omega \\ \theta \end{bmatrix} + \begin{bmatrix} \frac{1}{L_a} & 0 \\ 0 & -\frac{1}{J} \\ 0 & 0 \end{bmatrix} V_a \quad (3.7)$$

The corresponding output equation is

$$Y = \begin{bmatrix} 0 & 0 & 1 \end{bmatrix} \begin{bmatrix} I_a \\ \omega \\ \theta \end{bmatrix} \quad (3.8)$$

Where Y is the position of the motor

Even though the machine normally operates in the linear range of its characteristics where the saturation effect is neglected, under certain conditions like high starting current and overloaded states this becomes very significant and adversely affect the accuracy of the output. Without considering the effect of magnetic saturation, electrical torque represented by eq. (3.3) will be lower than the expected value due to the armature reaction that distorts the flux in the air-gap resulting in a nonlinear torque function. Another significant nonlinearity present in the DC motor is the Coulomb friction. Stiction (or starting friction) is the amount of force required to start the relative motion and is greater than the amount required to sustain it. However the effect of Coulomb friction is significant only at extremely low speeds and hence magnetic saturation is considered as more predominant nonlinearity in an electric motor. The block diagram of the system considering the effect of magnetic saturation is shown in fig 3.3.

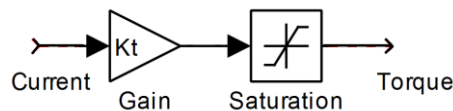


Fig.3.3 Motor torque with saturation

Considering the effect of magnetic saturation, eq. (3.3) is modified as

$$T = sat(K_t I_a) \quad (3.9)$$

The complete state model incorporating the nonlinearity due to magnetic saturation under loaded condition is

$$\begin{bmatrix} \dot{i}_a \\ \dot{\omega} \\ \dot{\theta} \end{bmatrix} = \begin{bmatrix} -\frac{R_a}{L_a} & -\frac{K_b}{L_b} & 0 \\ \frac{K_t}{J} & -\frac{B}{J} & 0 \\ 0 & 1 & 0 \end{bmatrix} \begin{bmatrix} sat(I_a) \\ \omega \\ \theta \end{bmatrix} + \begin{bmatrix} \frac{1}{L_a} & 0 \\ 0 & -\frac{1}{J} \\ 0 & 0 \end{bmatrix} \begin{bmatrix} V_a \\ T_L \end{bmatrix} \quad (3.10)$$

3.1.2 Brushless DC Motor (BLDC)

BLDC Motors are popularly used in many applications such as automotive, computers, aerospace, medical, industrial automation equipment and instrumentation (Mathew and Caroline, 2013). They have several advantages over brushed DC motor such as lower maintenance due to the elimination of the mechanical commutator and high power density which makes them ideal for high torque to weight ratio applications (Luk and Lee, 1994).

Modern brushless motors are very similar to ac motors. A permanent Magnet AC motor with a trapezoidal back EMF is referred to as BLDC motor and those with sinusoidal back EMF is referred as permanent magnet synchronous motor (PMSM). The brushes and commutator are eliminated in BLDC motor and it has a rotor with permanent magnets and a stator with windings that are connected to an electronic commutator which energizes the windings with particular sequence of switching pulses.

The structure of a typical three-phase brushless dc motor is illustrated in fig.3.4 (a) and (b). The stator windings are similar to those in a poly phase ac motor, and the rotor is composed of one or more permanent magnets. Brushless DC motors are different from AC synchronous motors where, the former incorporates some means for detection of rotor position (or magnetic poles) to produce signals to control the

electronic switches (Puranalal and Kumar, 2015) whereas in AC synchronous motor, there are no position sensors and the rotor poles are magnetically locked with the stator poles to continue the rotation. The BLDC motor operates either with sensors or without any position sensors. When it operates with sensor, three Hall Effect sensors are employed for sensing the rotor position whereas in sensor less operation the rotor position is estimated from the back EMF. The Hall Effect sensor is a transducer that varies its output voltage in response to the magnetic field.

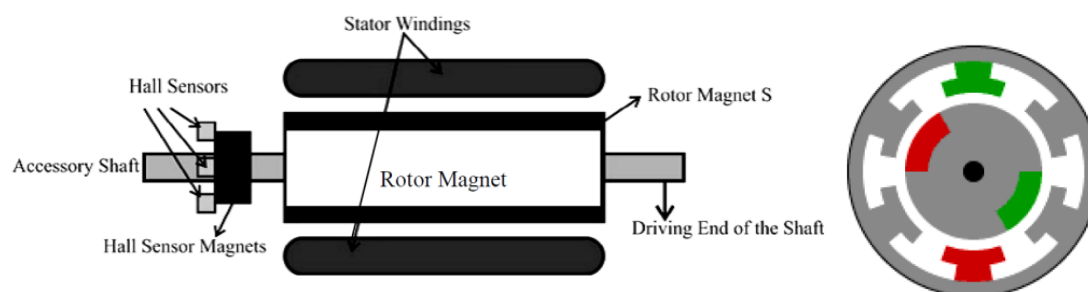


Fig 3.4 (a) Structure of BLDC motor Fig 3.4(b) Cross section of BLDC motor.

Principle of Operation

The stator windings are energized in a predefined sequence in such a way that they lead the rotor magnets and switches so that the rotor aligns with the stator and by this continuous operation the motor rotates. The motor runs in the opposite direction by reversing the sequence. The sequence defines the direction of the current flow in the coils that determines the orientation of the magnetic field generated by the coil. The equivalent circuit of the stator of BLDC motor is similar to that of an AC motor with star connection. The stator is fed from a DC source through an electronic converter which acts as the electronic commutator. The circuit diagram of a three phase BLDC motor is shown in fig 3.5

Three phase BLDC motor is operated by switching on two phases at a time. The signals from the Hall Effect position sensors produce a three digit number which changes at every 60 electrical degrees. These switching signals and the ideal back EMF and current waveforms are shown in fig 3.6. Table 3.2 shows the switching sequence, current direction and the position sensor signals. The voltage is applied to each of the three stator winding for a duration of 120° electrical in each cycle with a current limit to hold the stator current within the motor capabilities, which results in trapezoidal or quasi-rectangle shaped currents in the stator windings. Because the phase currents are excited in synchronism with the constant value of the back EMF, constant torque is generated. The electromagnetic torque of the BLDC motor is proportional to the product of phase values of back EMF and current. The back EMF in each phase is trapezoidal in shape and is displaced by 120 electrical degrees with respect to each other in 3 phase machine and a quasi-rectangle current pulse is injected into each phase so that current coincides with the back EMF waveform and hence the motor develops an almost constant torque.

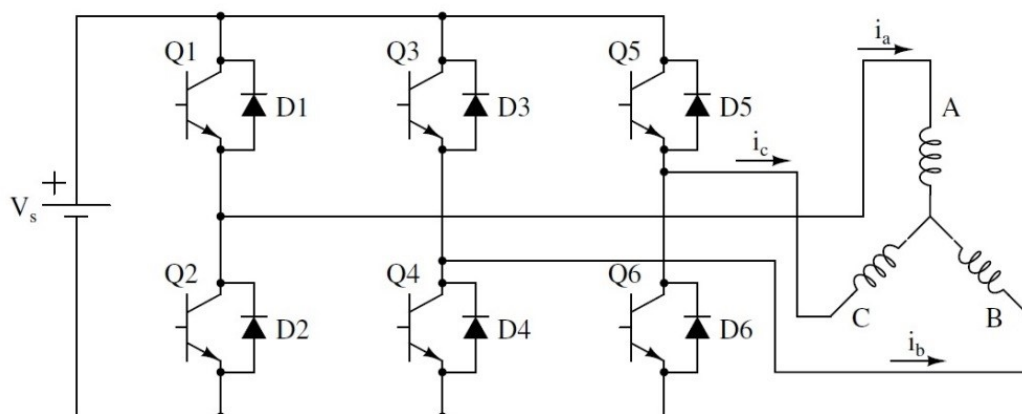


Fig 3.5 Circuit diagram of BLDC drive system

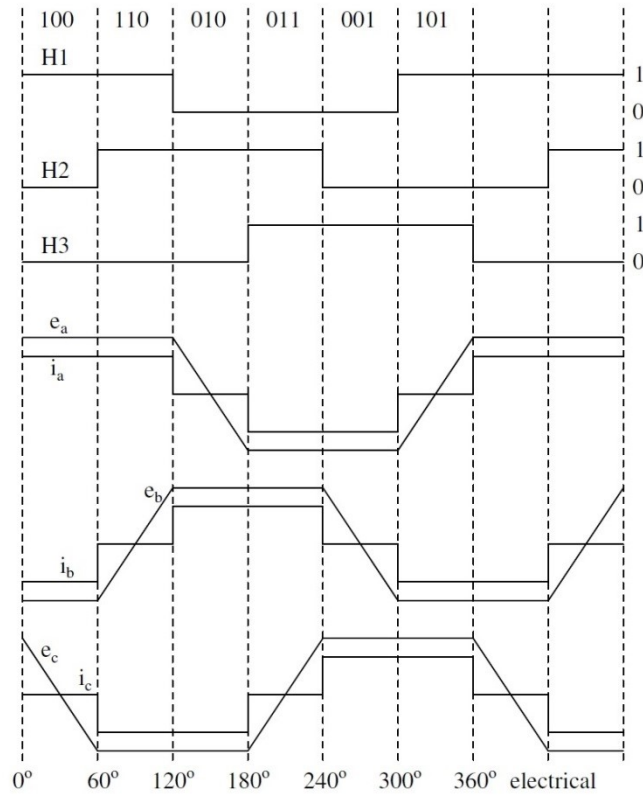


Fig.3.6 Ideal back EMFs, Phase currents and Position sensor signals

Table 3.2 Switching sequence

Switching interval	Seq. number	Pos. sensors			Switch closed		Phase Current		
		H1	H2	H3			A	B	C
0° – 60°	0	1	0	0	Q1	Q4	+	-	off
60° – 120°	1	1	1	0	Q1	Q6	+	off	-
120° – 180°	2	0	1	0	Q3	Q6	off	+	-
180° – 240°	3	0	1	1	Q3	Q2	-	+	off
240° – 300°	4	0	0	1	Q5	Q2	-	off	+
300° – 360°	5	1	0	1	Q5	Q4	off	-	+

The main advantages and disadvantage of conventional BLDC motors are listed in table 3.3(Dong *et al.* 2018).

Table 3.3 Advantages and Disadvantages of BLDC motor

Advantages	Disadvantages
1. No sparks during operation which allows using the motor in hazardous areas.	1. Torque produced is less due to the use of permanent magnets.
2. No noise from commutating sparks	2. Higher cost.
3. Low maintenance cost, long life as there are no brushes to be replaced.	3. Require complex electronic speed controllers to run.
4. Smaller motor size.	4. Temperature limit on rotor due to the magnets.
5. Speed torque linearity, capability of controlling the speed by changing the applied DC voltage	5. Harmonic content in back EMF results in torque ripple.
6. No friction at commutator.	

Mathematical Modelling

BLDC Motor has three stator windings a, b, c and permanent magnets in the rotor. The rotor is cylindrical in nature and hence the air gap is uniform. Since both the magnet and the stainless steel retaining sleeves have high resistivity, the rotor induced currents are neglected, and the presence of damper windings is not considered for modelling. Stator has 3 phases with distributed winding structure and is star connected. The dynamic equation of phase a, phase b and phase c are as given in equations (3.11), (3.12) and (3.13) respectively.

$$V_a = R_a i_a + L_a \frac{di_a}{dt} + M \frac{di_b}{dt} + M \frac{di_c}{dt} + e_a \quad (3.11)$$

$$V_b = R_a i_b + L_a \frac{di_b}{dt} + M \frac{di_a}{dt} + M \frac{di_c}{dt} + e_b \quad (3.12)$$

$$V_c = R_a i_c + L_a \frac{di_c}{dt} + M \frac{di_b}{dt} + M \frac{di_a}{dt} + e_c \quad (3.13)$$

Where L_a is armature self-inductance [H], M is armature mutual inductance [H], R_a is armature resistance [Ω], V_a , V_b and V_c are terminal phase voltages [V], i_a , i_b and i_c are motor input current [A], e_a , e_b and e_c are motor back -EMF [V]. The rotor does not have windings and hence it is not represented by any equation. The stator equations can be represented in matrix form

$$\begin{bmatrix} V_a \\ V_b \\ V_c \end{bmatrix} = \begin{bmatrix} R_a & 0 & 0 \\ 0 & R_a & 0 \\ 0 & 0 & R_a \end{bmatrix} \begin{bmatrix} i_a \\ i_b \\ i_c \end{bmatrix} + \begin{bmatrix} L_a & M & M \\ M & L_a & M \\ M & M & L_a \end{bmatrix} p \begin{bmatrix} i_a \\ i_b \\ i_c \end{bmatrix} + \begin{bmatrix} e_a \\ e_b \\ e_c \end{bmatrix} \quad (3.14)$$

where p is the differential operator.

But $i_a + i_b + i_c = 0$ therefore $Mi_b + Mi_c = -Mi_a$ and hence

$$\begin{bmatrix} V_a \\ V_b \\ V_c \end{bmatrix} = \begin{bmatrix} R_a & 0 & 0 \\ 0 & R_a & 0 \\ 0 & 0 & R_a \end{bmatrix} \begin{bmatrix} i_a \\ i_b \\ i_c \end{bmatrix} + \begin{bmatrix} L_a - M & 0 & 0 \\ 0 & L_a - M & 0 \\ 0 & 0 & L_a - M \end{bmatrix} p \begin{bmatrix} i_a \\ i_b \\ i_c \end{bmatrix} + \begin{bmatrix} e_a \\ e_b \\ e_c \end{bmatrix} \quad (3.15)$$

Hence the matrix form of the equation is

$$p \begin{bmatrix} i_a \\ i_b \\ i_c \end{bmatrix} = \begin{bmatrix} 1/L_a - M & 0 & 0 \\ 0 & 1/L_a - M & 0 \\ 0 & 0 & 1/L_a - M \end{bmatrix} \begin{bmatrix} V_a \\ V_b \\ V_c \end{bmatrix} - \begin{bmatrix} R_a & 0 & 0 \\ 0 & R_a & 0 \\ 0 & 0 & R_a \end{bmatrix} \begin{bmatrix} i_a \\ i_b \\ i_c \end{bmatrix} - \begin{bmatrix} e_a \\ e_b \\ e_c \end{bmatrix} \quad (3.16)$$

The electro-magnetic torque is given by

$$T_e = P_m / \omega = (e_a i_a + e_b i_b + e_c i_c) / \omega \quad (3.17)$$

The equation of motion is given by

$$T_e = Jp\omega + B\omega + T_l \quad (3.18)$$

Rewriting the equation as

$$p\omega = (T_e - T_l - B\omega) / J \quad (3.19)$$

Combining equations (3.16) and (3.19) state space form of BLDC motor is

$$\dot{x} = Ax + Bu \quad (3.20)$$

Where $x = [i_a \quad i_b \quad i_c \quad \omega \quad \theta]^T$

$$A = \begin{bmatrix} -R_a/L_1 & 0 & 0 & (\lambda_p/L_1)f_a(\theta) & 0 \\ 0 & -R_a/L_1 & 0 & (\lambda_p/L_1)f_b(\theta) & 0 \\ 0 & 0 & -R_a/L_1 & (\lambda_p/L_1)f_c(\theta) & 0 \\ (\lambda_p/J)f_a(\theta) & (\lambda_p/J)f_b(\theta) & (\lambda_p/J)f_c(\theta) & -B/J & 0 \\ 0 & 0 & 0 & P/2 & 0 \end{bmatrix}$$

$$B = \begin{bmatrix} 1/L_1 & 0 & 0 & 0 \\ 0 & 1/L_1 & 0 & 0 \\ 0 & 0 & 1/L_1 & 0 \\ 0 & 0 & 0 & 1/J \\ 0 & 0 & 0 & 0 \end{bmatrix}$$

Where $L_1 = L_a - M$

$$u = [V_a \quad V_b \quad V_c \quad T_l]^T$$

λ_p is the flux linkage and

f_a, f_b, f_c are trapezoidal functions

The corresponding output equation is

$$Y = \begin{bmatrix} 0 & 0 & 0 & 1 & 0 \end{bmatrix} \begin{bmatrix} i_a \\ i_b \\ i_c \\ \omega \\ \theta \end{bmatrix} \quad (3.21)$$

Where Y is the speed of the motor

3.1.3 Switched Reluctance Motor (SRM)

SRM is an electric motor which runs by reluctance torque and is used for industrial applications where very high speed of about 50,000 rpm is required. Simplicity, ruggedness, and low cost of a SRM make it a viable candidate for various general-purpose adjustable-speed and servo-type applications in electric vehicles, aerospace applications and in hazardous environments like mines and petrochemical industries (Mao and Tsai, 2005).

An SRM is a singly excited, doubly-salient machine in which the electromagnetic torque is developed due to variable reluctance principle. Both stator and rotor has salient poles but only stator carries winding similar to the field winding of dc motor, and the rotor has no attached coils or magnets (Parker, 2004). The projecting magnetic poles of salient pole rotor are made of soft magnetic material. Figure 3.7 illustrates the 6/4 SRM drive which consists 6 stator poles and 4 rotor poles.

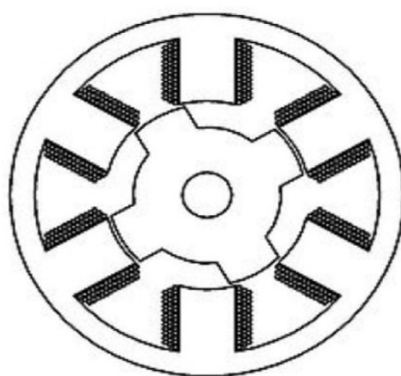


Fig.3.7 Structure of 3 phase 6/4 SRM

Principle of Operation

When the excitation is given to the stator windings, a force is developed by magnetic reluctance of the rotor that bid to align the rotor pole with the adjacent stator pole. In order to preserve the sequence of rotation, the windings of stator pole switches in a sequential manner with the help of an electronic control system or an electronic commutator, so that the magnetic field of the rotor pole that lead by the stator pole pulls towards it. The rotor pole is said to be “fully unaligned position” when the rotor pole is equidistant from the two adjacent stator pole. At this position the rotor has maximum magnetic reluctance where as in fully aligned position the rotor poles with the stator poles have minimum reluctance. Various advantages and disadvantage of SRM are given in table 3.4. (Roux and Morcos, 2002)

Table 3.4 Advantages and Disadvantages of SRM

Advantages	Disadvantages
1. No permanent magnets	1. Lower torque capability and are
2. Can be employed in high- temperature and harsh operating environments.	generally noisy
3. Low cost and less maintenance	2. High torque ripple
4. Rigid construction and brushless	3. Require complex electronic speed controllers to run.

Mathematical Modelling

The equation governing an SRM is given by equations (3.22) to (3.26) (Parker, 2004)

$$V = Ri + \frac{d\psi}{dt} \quad (3.22)$$

$$\psi = Li = N\phi \quad (3.23)$$

$$V = L \frac{di}{dt} + i \left(\frac{dL}{d\theta} \right) \left(\frac{d\theta}{dt} \right) \quad (3.24)$$

$$V = L \frac{di}{dt} + i\omega \frac{dL}{d\theta} \quad (3.25)$$

$$T = \frac{1}{2} i^2 \frac{dL}{d\theta} \quad (3.26)$$

Where V is the stator voltage [V], R is the stator resistance [ohm], i is the stator current [A], L is the stator inductance, Ψ is the flux linkage, θ is the Angular displacement, ω is the angular velocity and T is the Torque.

The above equations show that the developed torque depends only on current magnitude and phase inductance per rotor angle ($dL/d\theta$) direction but is independent of current direction. An SRM has pronounced nonlinear characteristics in its torque production due to the coupling effect of the state variables as given in equation (3.25). State variable model of the SRM is given by

$$p \begin{bmatrix} i \\ \omega \\ \theta \end{bmatrix} = \begin{bmatrix} -\frac{R}{L} & i \frac{dL}{d\theta} & 0 \\ 0 & -\frac{B}{J} & 0 \\ 0 & 1 & 0 \end{bmatrix} \begin{bmatrix} i \\ \omega \\ \theta \end{bmatrix} + \begin{bmatrix} \frac{1}{L} & 0 \\ 0 & -\frac{1}{J} \\ 0 & 0 \end{bmatrix} \begin{bmatrix} V \\ T_L \end{bmatrix} \quad (3.27)$$

Where p is the differential operator and the corresponding output equation is

$$Y = \begin{bmatrix} 0 & 1 & 0 \end{bmatrix} \begin{bmatrix} i \\ \omega \\ \theta \end{bmatrix} \quad (3.28)$$

Where Y is the speed of the motor

3.2 AC DRIVES

AC drives are the electro-mechanical power converters that use AC power as the source of energy. The commonly available AC motors are Induction motor, Synchronous motor and Permanent Magnet Synchronous Motor (PMSM). PMSM is known for having high efficiency, low torque ripple, superior dynamic performance, high power density, high torque to weight ratio and ease for maintenance than the other AC motors. Due to the above advantages these drives are often the best choice for applications where the output with very precise, accurate and fast response is required. Here the mathematical modelling of a PMSM motors is explained.

3.2.1 Permanent Magnet Synchronous Motor (PMSM)

With the recent development of permanent magnetic materials and control technology, PMSM is widely used for many industrial applications like CNC machine tools, industrial robots and electric vehicles (Shahat and Shewy, 2010). This machine uses permanent magnets to produce the air gap magnetic field rather than using electromagnets. These are similar to Brushless DC motors, which has a wound stator and permanent magnet rotor that provide sinusoidal flux distribution in the air gap, making the back EMF sinusoidal. Due to the presence of permanent magnets in the rotor it has high power efficiency and reduced motor size. Depending on how magnets are attached to the rotor, PMSM motors are classified into two types: surface PMSM in which all magnet pieces are mounted on the surface and interior PMSM in which magnets are buried inside the rotor. Interior PMSM is used only for the high speed applications due to their high cost and low power density whereas surface PMSM are more popular due to the ease of construction and higher power density. The cross section of a surface PMSM is shown in fig. 3.8

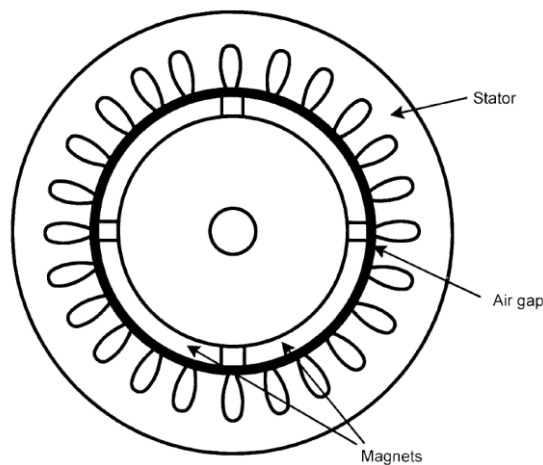


Fig.3.8 Cross section of surface PMSM

Principle of operation

The working of a PMSM is similar to that of a conventional synchronous motor: the difference is that the former uses permanent magnets in the rotor whereas the later uses electromagnets. The stator carries windings connected to an AC supply to produce a rotating magnetic field and at synchronous speed the rotor poles lock to this magnetic field. The stator windings are usually fed by a variable frequency inverter in order to achieve the desired speed. The main advantages and disadvantages of PMSM are given in table 3.5.

Table 3.5 Advantages and Disadvantages of PMSM

Advantages	Disadvantages
1. High efficiency	1. More expensive
2. Small size	2. Require electronic controller.
3. Rigidity	3. Presence of torque ripple
4. High speed operation	
5. Efficient heat dissipation	

Mathematical Modelling

Dynamic model developed on a synchronously rotating reference frame describes the behaviour of the motor for the vector control. The stator variables are transformed into a synchronously rotating d-q frame. The stator of the PMSM is similar to that of the wound rotor synchronous motor. The back emf produced by a permanent magnet is similar to that produced by an excited coil. A PMSM can be mathematically represented by the following equation in the d-q axis synchronously rotating rotor reference frame for assumed sinusoidal stator excitation (Pillay and Krishnan, 1989a).

$$v_q = Ri_q + p\psi_q + \omega\psi_d \quad (3.29)$$

$$v_d = Ri_d + p\psi_d - \omega\psi_q \quad (3.30)$$

where: v_d and v_q are direct and quadrature components of stator voltage, i_d and i_q are direct and quadrature components of stator current, ψ_d and ψ_q are direct and quadrature components of flux linkage, R is stator resistance, p is differential operator, ω is rotor electrical angular speed. The d - q flux linkage equations are

$$\psi_q = L_q i_q \quad (3.31)$$

$$\psi_d = L_d i_d + \psi_f \quad (3.32)$$

Where L_d and L_q are the direct and quadrature axis inductances and ψ_f is the flux linkage due to permanent magnet. Fig. 3.9 shows the dynamic equivalent circuit of a PMSM based on equations (3.31) and (3.32).

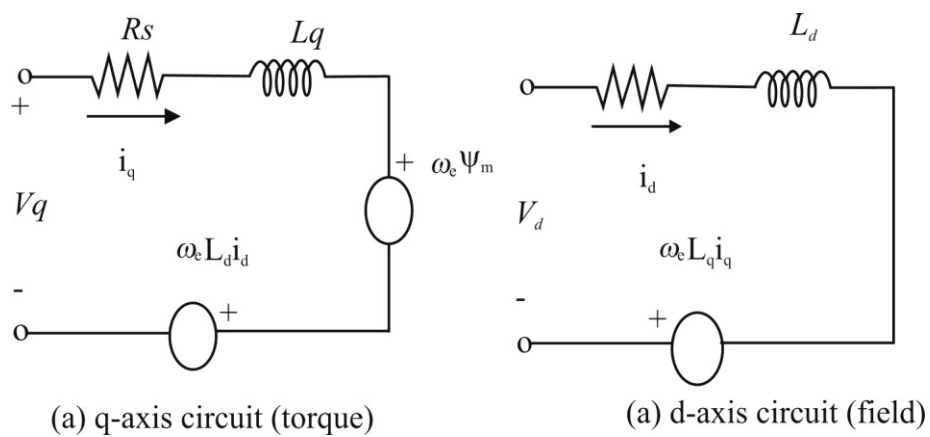


Fig. 3.9 Equivalent Circuit of a PM Synchronous Motor

The electromagnetic torque of motor is

$$T_e = \frac{3P}{2} [\psi_f i_q + (L_d - L_q) i_d i_q] \quad (3.33)$$

$$T_e = J_m p \omega_r + B_m \omega_r + T_l \quad (3.34)$$

T_e : the developed electric torque,

T_l : the load torque,

B : the rotor damping coefficient,

J : the inertia constant

For surface PMSM, $L_d = L_q$

The state variable model of surface PMSM is

$$\dot{x} = Ax + Bu \quad (3.35)$$

Where $x = [i_d \quad i_q \quad \omega \quad \theta]$

$$A = \begin{bmatrix} -\frac{R}{L} & \omega_r L & 0 & 0 \\ -\omega_r L & -\frac{R}{L} & -\frac{\psi_f}{L} & 0 \\ 0 & \frac{3\psi_f P}{2J} & -\frac{B}{J} & 0 \\ 0 & 0 & 1 & 0 \end{bmatrix} \quad B = \begin{bmatrix} \frac{1}{L} & 0 \\ 0 & \frac{1}{L} \\ 0 & 0 \\ 0 & 0 \end{bmatrix}$$

$$u = [v_d \quad v_q]^T$$

The corresponding output equation is

$$Y = \begin{bmatrix} 0 & 0 & 1 & 0 \end{bmatrix} \begin{bmatrix} i_d \\ i_q \\ \omega \\ \theta \end{bmatrix} \quad (3.36)$$

Where Y is the speed of the motor

CHAPTER 4

CONTROL TECHNIQUES FOR INDUSTRIAL DRIVES

The position/speed of an electric drive is precisely controlled using a power converter and an embedded digital control unit that consist of control hardware, sensors, processors and control algorithms. Selection of the controller and sensor is decided by the type of the machine for which it is applied as well as the field of application. A controller regulates the desired variables of the system such as speed, position, current and torque using the feedback control loop. The control techniques are widely classified into linear and non-linear methods according to the dynamics of the controller as well as the plant.

4.1 LINEAR CONTROL METHOD – PID CONTROLLER

Proportional-Integral-Derivative (PID) controller is the most popularly used linear control algorithm due to its simplicity and effectiveness and ease of implementation (Bassi *et al.*, 2011). The other popularly used linear control techniques are Linear Quadratic Regulator (LQR) and Linear Quadratic Gaussian (LQG) algorithm. The PID controller is a very popular choice in many control applications such as drives, aerospace and process control as it has the capacity to produce satisfactory outputs for linearized models.

The time domain representation of PID controller is given in equation (4.1)

$$u(t) = K_p e(t) + K_d \frac{de(t)}{dt} + K_i \int e(t) dt \quad (4.1)$$

Where $e(t)$ is the error (difference between reference input and output), $u(t)$ is the control variable, K_p is the proportional gain, K_d is the differential gain and K_i is the integral gain. Each of these coefficients makes changes in the characteristics of the response of the system. A control without D mode is used when large disturbances and noise are present during operation of the process. PI controllers are widely used to control drive systems as they are subjected to large disturbances during their operations and these are the most commonly used controllers in industry today.

The Control law of a PI controller is

$$u(t) = K_p \left[e(t) + \frac{1}{T_i} \int e(t) dt \right] \quad (4.2)$$

A very important step in the use of this controller is the tuning process where the best values of the gains of K_p , K_i and K_d are selected (Willis, 1999). The proportional gain is tuned first, then the integral and then the derivative gains to stabilize the system and reduce the overshoot. The tuning process is to be continued iteratively till the desired transient and steady state performance is reached. Even though various algorithms viz. Cohen Coon method, genetic algorithm etc. are available for tuning of the PID controller, Ziegler-Nichols method is easier and guarantees good performance (Bansal *et al.*, 2012). It is also the most popular method for tuning PID controller due to its simplicity and ease for implementation. Due to these advantages Ziegler-Nichols tuning method is used in our system. PID controller parameters K_p , K_i and K_d are selected for the Ziegler-Nichols Quarter Decay Response (QDR) according to the table 4.1. QDR is the response in which the overshoot amplitude reduces to one fourth of the previous value in each cycle.

Table 4.1. Zeigler-Nichols parameters for QDR response

Control Action	K_p	K_i	K_d
P	$K_u/2$		
PI	$K_u/2.2$	$1.2 K_p/P_u$	
PID	$K_u/1.7$	$2 K_p /P_u$	$K_p P_u/8$

The main drawback of PID controller is its poor capability of dealing with system uncertainty such as system parameter variations and external disturbances. Due to these limitations of PID controllers, robust controllers have gained much more attention to overcome the deficiency.

4.2 NONLINEAR CONTROL METHODS

Nonlinear control theory covers a wider class of systems that do not obey the superposition principle and applies to more real-world systems as all systems are practically non-linear due to the presence of common nonlinearities such as saturation, friction, hysteresis, dead zone etc.

PMSM model (Pillay and Krishnan, 1989a) and SRM model (Parker, 2004) are inherently nonlinear due to the coupling effect of their state variables, variation in reluctance and magnetic saturation. BLDC motor model (Pillay and Krishnan, 1989b) is also nonlinear due to the presence of trapezoidal function in the system matrix. These nonlinearities are not taken into account while designing and implementing the conventional linear controller. However, simple nonlinear controller can reasonably compensate the nonlinearities present in the system for accurate control. Also, hard nonlinearities like, saturation do not permit linear approximation of real-world systems (Banos *et al.*,2001) After predicting these nonlinearities, nonlinear

approaches properly compensate these to achieve unmatched performance. Moreover, real drive systems often exhibit uncertainties in the model parameters primarily due to sudden or slow change in the values of these parameters. A nonlinear controller with robustness and adaptability can handle the consequences due to model uncertainties (Iqbal *et al.*, 2017).

Recently developed control mechanisms like sliding mode control (SMC) (Decarlo *et al.*, 1999), back stepping control (Zhou and Zhang, 2004) , adaptive control (Marino *et al.*, 1993), H- infinity control (Alma *et al.*, 2012), Fuzzy logic controller (FLC) (Guillemin, 1996) and Artificial Neural Network (Wlas *et al.*, 2004) etc. are used for the control and stabilization of systems with parameter uncertainty and disturbances. These control techniques find applications in various electric drives used in robotics, textile mills and machine tools where high precision control is required even though these are complex and expensive.

In recent years, with the development of modern control theory, many non-linear and adaptive control methods have been applied to the speed and position control of drive system. Back stepping control, Adaptive control, Artificial Neural network control, are some of them. Even though the above modern controllers perform better than the linear controllers, it is found that the practical implementations of these controllers are difficult due to the complexity of algorithm and economic viability

SMC and FLC are found to be better solutions from the point of view of practical implementation and economical aspects of control of drives. It is also found that machine parameter variation and disturbances due to load variation can be adequately addressed with sliding mode control.

4.2.1 Sliding Mode Control (SMC)

SMC is a nonlinear method that alters the dynamics of a system by application of a discontinuous control signal and forces the system to "slide" along a cross-section of its normal behaviour. It is a robust control technique and the design is based on Lyapunov's method. SMC, generally insensitive to external disturbances and changes in system parameters, uses a high speed switching control law to drive the state trajectories on to a specified and user chosen surface in the state space. The direction of a state trajectory depends only on the position of the state with respect to the sliding surface.

State-feedback control law of SMC uses a signum function that can switch from one continuous structure to another based on the current position in the state space. Hence it is a variable structure control (VSC) method which is explained by V.I.Utkin with control law as (Utkin, 1977)

$$u = -k \operatorname{sgn}(s) \quad (4.3)$$

where s is the switching surface, k is the gain of the controller and $\operatorname{sign}(\cdot)$ is the signum function representing the nonlinearity.

VSC has several subsystems and switching between these subsystems is done in order to bring the plant states to a user defined surface called sliding surface. Usually the switching among the subsystems is determined by a switching function. The term "variable structure control" arises because the "controller structure" around the plant is intentionally changed by some external influence to obtain a desired plant behaviour or response. The multiple control structures are designed so that

trajectories always slide along the boundaries of these structures. The motion of the system as it slides along these boundaries is called a sliding mode and the geometrical locus consisting of the boundaries is called the sliding surface.

Consider a plant with two accessible states and one control input as described by the following state equations.

$$\begin{bmatrix} \dot{x}_1 \\ \dot{x}_2 \end{bmatrix} = \begin{bmatrix} 0 & 1 \\ 0 & 0 \end{bmatrix} \begin{bmatrix} x_1 \\ x_2 \end{bmatrix} + \begin{bmatrix} 0 \\ 1 \end{bmatrix} u, \quad |u| \leq 1 \quad (4.4)$$

Open loop representation of a second order system is shown in Fig. 4.1. Let the switching surface be $\sigma(x_1, x_2) = s_1 x_1 + x_2 = 0$

Where x_1 and x_2 are the state variables and s_1 is the slope of the sliding surface then the control law is given by

$$u = \text{sgn}[\sigma(x_1, x_2)] \quad (4.5)$$

where $\text{sgn}(\sigma) = \begin{cases} +1 & \sigma > 0 \\ -1 & \sigma < 0 \end{cases}$

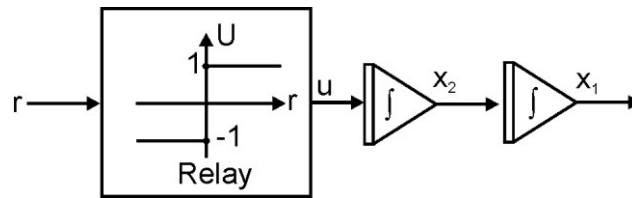


Fig 4.1 Open loop representation of a second order system

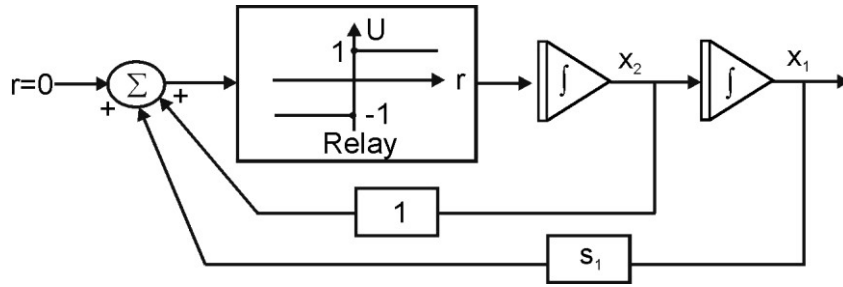


Fig 4.2 Block diagram of the closed loop system

Block diagram representation of the closed-loop system corresponding to equation (4.5) is shown in Fig. 4.2. The phase-plane plots of the system with the above control law for small and large value of $s_1 > 0$ and are illustrated in fig. 4.3 and fig. 4.4 respectively. Here upward motion in the trajectories is associated with $u = +1$ and downward motion is for $u = -1$. The relay element in the block diagram of Fig. 4.2 has a small delay when switching between the gains "+1" and "-1". The resulting system behaviour as this delay tends to zero and s_1 is small, then the switching line $\sigma = s_1 x_1 + x_2 = 0$ is described by the first order differential equation $s_1 x_1 + x_2 = 0$. It is clear that the behaviour of our system on $u = 0$ is dependent only on the slope s_1 of the switching surface.

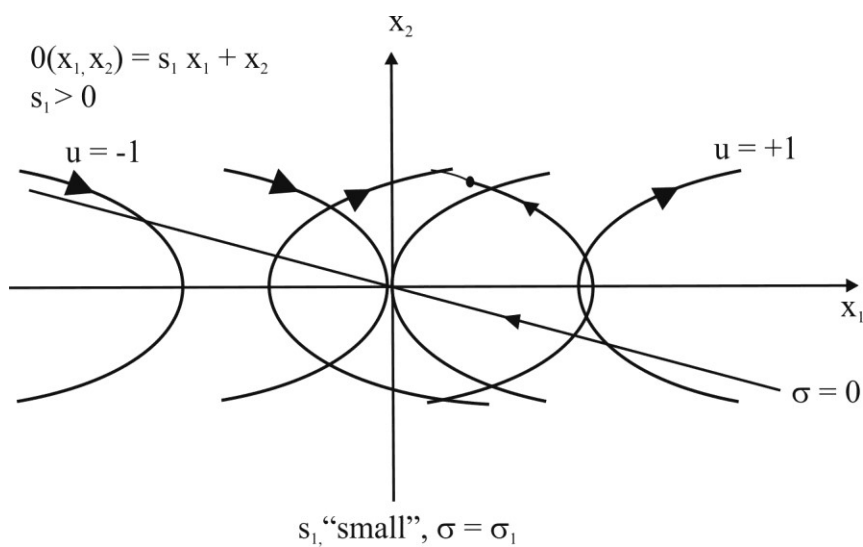


Fig 4.3 Phase-plane diagrams of the closed-loop system for small s_1

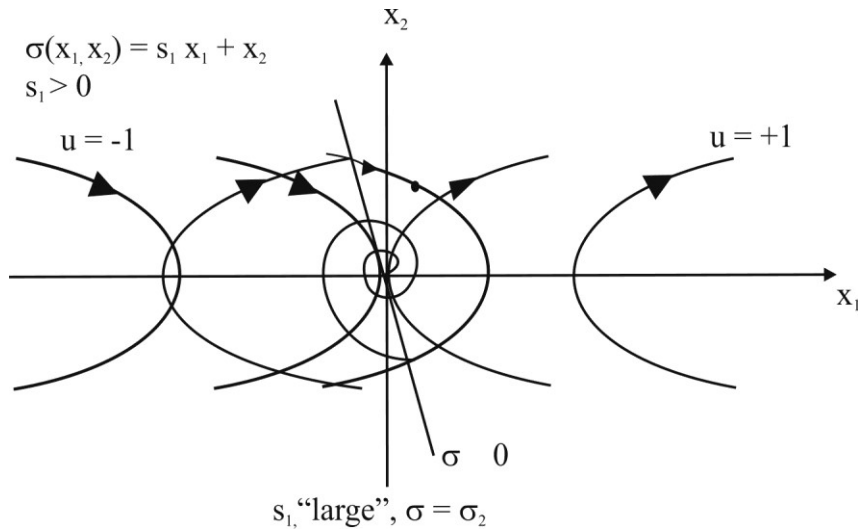


Fig.4.4 Phase-plane diagrams of the closed-loop system for large s_1

This means the system is insensitive to any variation or perturbation of the plant parameters contained in the A matrix. Fig 4.4 shows that the state trajectory switches to a new parabolic motion every time it intercepts the switching line $u = 0$ and the parabolic motions "spiral" into the origin (Decarlo *et al.*, 1988). So the most distinguished feature of VSC is its ability to result in very robust control systems that result in invariant control where it is completely insensitive to parametric uncertainty and external disturbances.

V.I.Utkin et al presented a guide to sliding mode control for practicing control engineers. It offers an accurate assessment of implementable sliding mode control design solutions and provides a frame of reference for future sliding mode control research (Young *et al.*, 1999). The application of SMC for electric drives is presented (Utkin, 1993) and the sliding mode control of a permanent magnet synchronous motor is proposed in (Zhang *et al.*, 2013). The main drawback in conventional SMC is chattering, a phenomenon of high frequency oscillation in the output that limits its applications in real time systems.

4.2.2 Modified Chattering free SMC (Modified SMC)

Use of signum function in the control law causes chattering due to the high frequency switching between the functions and this adversely affects the performance of the system significantly. One of the solutions to overcome this is to introduce a boundary layer around the switching surface even though this leads to a finite steady state error. The chattering in the sliding mode controller can effectively be reduced by modifying the control law as

$$u = -ksat(s/\phi) \quad (4.6)$$

where the constant factor ϕ defines the thickness of the boundary layer around the switching surface. $sat(s/\phi)$ is a saturation function defined by

$$sat(s/\phi) = \begin{cases} \frac{s}{\phi} & \text{if } \left| \frac{s}{\phi} \right| \leq 1 \\ \text{sgn}(s/\phi) & \text{if } \left| \frac{s}{\phi} \right| > 1 \end{cases} \quad (4.7)$$

The above control law guarantees the system trajectories move toward and stay on the sliding surface $s = 0$ from any initial condition, provided the following condition is satisfied:

$$s\dot{s} \leq -\eta|s| \quad (4.8)$$

where η is a positive constant that makes the system trajectories meet the sliding surface in a finite time. This controller is actually a continuous approximation of an

ideal relay control and the invariance of sliding mode control is eliminated here. The system robustness becomes a function of the width of the boundary layer and the control law of SMC of a plant of any order reduces the error and the derivative of error to zero. The switching surface of the SMC determines the transient response of the system if the sliding mode exists.

4.2.3 Fuzzy Logic Control (FLC)

Soft-Computing is a collection of techniques spanning many fields that fall under various categories in computational intelligence and has three main branches: Fuzzy Logic, Artificial Neural Networks (ANN) and Evolutionary Computation. Soft computing deals with imprecision, uncertainty, partial truth, and approximation to achieve practicability, robustness and low solution cost. ANN is widely used in the areas such as robotics, machine learning and speech recognition where high computational abilities are required and usually not preferred for the control of drive system that undergo sudden load variations. The evolutionary computing technique such as genetic algorithm is mainly for solving optimization problems and used in combination with conventional controllers for their parameter tuning to improve the performance of the system. On the other hand Fuzzy Logic is the most suitable and widely used method for industrial control applications such as drive control, due to its simplicity and ease of implementation. FLC has proven effective for complex nonlinear and imprecisely defined process for which standard model based control techniques are impractical (Guillemin, 1996).

Fuzzy logic is an approach to computing based on "degrees of truth" rather than the usual "true or false" (1 or 0) Boolean logic on which the modern computer is based. The idea of fuzzy logic was first introduced by Dr. Lotfi A. Zadeh of the University of California at Berkeley in 1960s (Zadeh, 1965). Lots of practical applications with FLC are performing better than the conventional controllers like PID controller (Montiel *et al.*, 2007). An FLC consist of a fuzzification unit, a decision making unit, and a de-fuzzification unit as shown in fig.4.5. The fuzzification unit converts the real inputs to corresponding fuzzy values by using appropriate input membership functions. The decision making unit performs the inference operation and generate the fuzzy output based on a number of logic statements called fuzzy rules in the form of IF-THEN statements. The number of fuzzy rules depends on the number of input membership functions. De-fuzzification unit converts the fuzzy output back into the crisp or real control output values using the output membership functions. There are several methods for de-fuzzification and the centroid method is most popular and widely used method (Guillemin, 1996) and is applied in this work.

One of the major challenges in the design of an FLC is the tuning of the membership functions and fuzzy rules. Even though various methods for tuning fuzzy controller are found in literature, it still lacks a standard method (Santos *et al.*, 1994). Here the universe of disclosure of input variables and output variable of the FIS are selected from the performance of PI controller. Triangular, trapezoidal and gaussian are the commonly used membership functions and combination of triangular and trapezoidal membership functions are used in this thesis as it is giving better results than the gaussian membership function (Prasad, K.M.A. *et al.*, 2015). Initially trapezoidal membership functions are used in both extremes and triangular membership functions

are used in the middle portion of the universe of discourse. During tuning the shapes are slightly modified to achieve the best performance. The fuzzy rules are selected according to the heuristic knowledge of the required variation in the controller output according to the variation of error signal and its rate of change. Fine tuning of the rule are done by trial and error to obtain improved results. Input- output nonlinearity in FIS depends on the surface view of the system which is the graphical relation between the inputs and output. Even with triangular membership function, nonlinear surface can be produced. However in this thesis a combination of triangular and trapezoidal membership functions are used which generate a nonlinear surface to address the nonlinearities in the system.

The main advantage of the fuzzy logic control is that it can be used as standalone controller as well as in combination with most of the linear as well as non-linear control techniques (Mahendiran *et al.*, 2011).

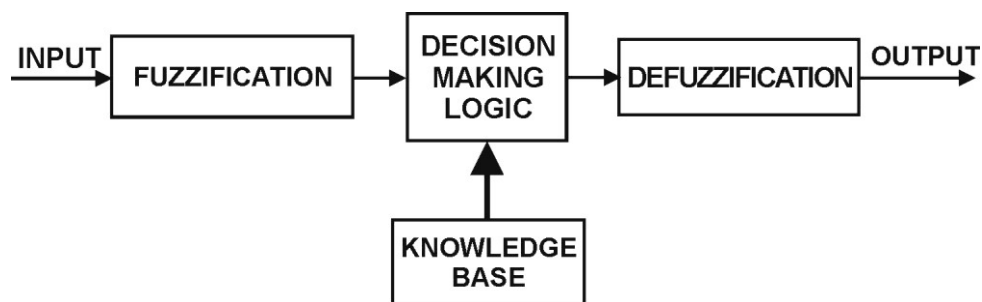


Fig 4.5 Block diagram of a Fuzzy Logic Controller

4.3 INTELLIGENT CONTROLLERS USING FUZZY LOGIC

The main drawback of a standalone FLC is that, it has no mathematical model and the hence analysis of the system becomes difficult. It is being used in combination with

various existing controllers like PI, LQR, LQG and back stepping controller that gives intelligence and adaptability to it. Fuzzy PI is one of the most widely used controllers of this category for drives.

4.3.1 Fuzzy PI Control

Conventional PI controller is stable, efficient, easy to implement and is highly reliable when used for a linear model. But most of the industrial processes are having different types of nonlinearities such as transport lag, saturation and backlash in addition to parameters variations and external disturbances. Conventional PI controllers cannot perform well under these conditions due to its fixed nature of the controller parameters K_p and K_i .

In adaptive-fuzzy PI controller the K_p and K_i are varied intelligently according to the variation of error signal and its rate of change (Hu, *et al.*, 1999). The inputs to the fuzzy inference system are the error (difference between the set value and the actual value) and its rate of change and the output is K_p and K_i . Individual set of rules are formed for each K_p and K_i by which the controller can adapt to changes in the system parameters.

4.3.2 Fuzzy Sliding Mode Control (FSMC)

Modified SMC and FLC have specific advantages of their own and have mode of operation in achieving control under uncertain and imprecise conditions. However there are highly demanding situation where the need for even more precise control schemes are found to be very essential. To address such demands in drive control, a suitable combination of modified SMC and FLC to achieve improved transient as well as steady state performance is proposed.

Conventional sliding mode controller has the problem of chattering and its effect can be reduced using a modified control law that uses a saturation function instead of the signum function in conventional SMC. For further improvement of the performance characteristics of the system, a Fuzzy SMC (FSMC) that integrates a fuzzy inference system with modified SMC is used. This also provides intelligence and adaptability of the modified SMC. FSMC has been successfully implemented in industrial applications like air flow control of a fuel cell (Baround *et al.*, 2018), closed-loop vector control for a grid-connected Wave Energy Conversion System (WECS) driven Self-Excited Induction Generator (SEIG) (Elgammal, 2014), erection system with un-modelled dynamics (Feng *et al.*, 2017) and uncertain MIMO nonlinear systems (Roopaei *et al.*, 2009). Hence FSMC can effectively be used for control of drive system due to its robustness and ease of hardware implementation.

In the proposed mode of combination of modified SMC and FLC, the value of the gain constant k in the control law of modified SMC given by equation (4.7) is suitably adjusted by the fuzzy inference system. With higher values of gain k , even though the speed of response of the system improves the effect of chattering also increases simultaneously. On the other hand with low values of gain k the speed of response and the effect of chattering decreases. Hence it is desirable to have high value of gain k during transient states to improve the speed of response and low value during steady states for reducing the chatter effect.

In the proposed Fuzzy SMC, the gain k in the modified control law of the chatter free SMC is varied according to the fuzzy rules decided by the variation in the error signal ' e ' and the rate of change of error signal ' \dot{e} '. The block diagram of the proposed intelligent Fuzzy SMC is given in fig. 4.6. Here the signals ' e ' and ' \dot{e} ' are taken as the input to the

fuzzy system and its output is the value of controller gain k of FSMC. The final control law u as given in equation (4.7) with adjustable gain is obtained by multiplying the output of FIS with saturation function of the control law used in modified SMC.

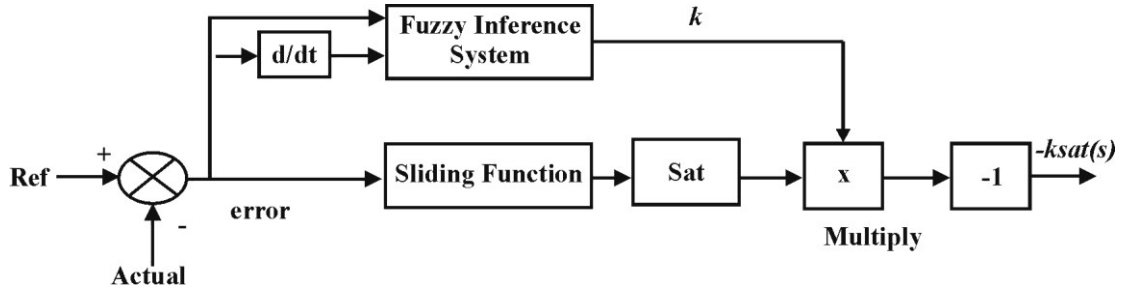


Fig 4.6 Block diagram of a FSMC

The control structure of this proposed FSMC differs from that of the existing one used in air flow control of a fuel cell (Baround *et al.*, 2018) is in the input variables of the FIS. Here we use the error signal ' e ' and its rate of change ' \dot{e} ' where as the latter uses the sliding function and its derivative as input to the FIS. Suitable variation of the controller gain with variation in error is achieved in the proposed controller using a faster algorithm which results in reduced complexity and easier implementation compared to the other one. Also the controller output using ' e ' and ' \dot{e} ' results in better output than the existing one.

CHAPTER 5

NON-LINEAR INTELLIGENT CONTROL OF DC DRIVES

Position and speed control of widely used special electric drives, viz. DC servo motor, BLDC motor and Switched Reluctance Motor using various nonlinear control techniques are discussed in this chapter. Fuzzy SMC, conventional SMC, Fuzzy PI and conventional PI control are designed and the simulation results are presented here.

5.1 POSITION CONTROL OF DC SERVO MOTOR

There has been significant effort in improving the performance of electric motors, during the last few years. DC motors are widely used in various industrial applications such as robotic manipulators and servo systems, due to their relatively simple control and reliable wide range of operating conditions. The position control of DC motors is suitable for applications such as antenna positioning, robotic arm and solar tracking (Mahendiran *et al.*, 2011).

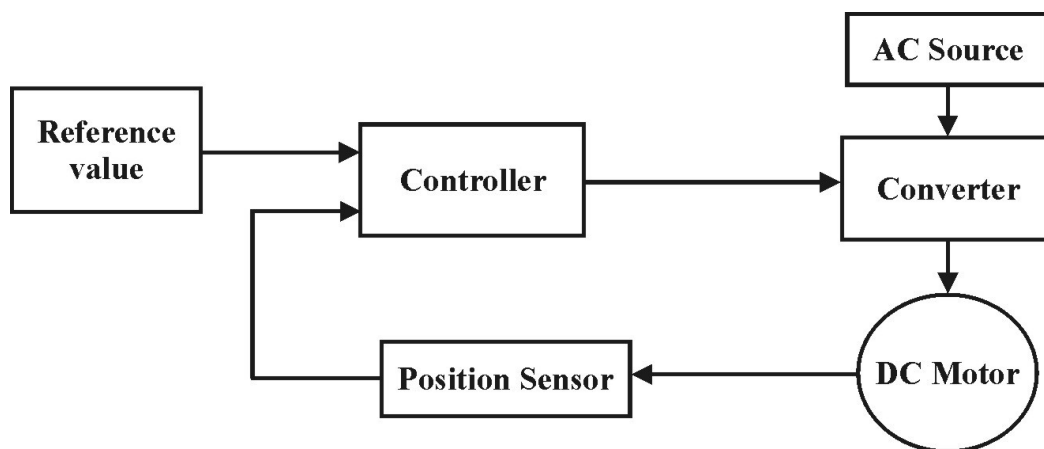


Fig. 5.1 Block diagram of the position control of DC Motor

DC motors are usually modelled as linear systems neglecting important nonlinearities like saturation of the core and suitable linear control approaches are implemented. In addition to this, controllers for nonlinear models of DC motor have also been developed for more precise and accurate system operation (Mahajan *et al.*, 2013). The block diagram representation of the position control of DC motor by varying armature voltage is shown in fig 5.1 where the DC input voltage to the armature is controlled according to the reference value and the actual rotor position.

A Fuzzy SMC, modified SMC, Fuzzy Logic controller, Fuzzy PI controller and conventional PI controllers are designed for a DC motor whose parameters are selected as shown in table 5.1.

Table 5.1 Parameters of DC servo motor

Motor Parameters	Value
Rated Power	1.5 kW
Rated current	7A
Rated speed	1500 rpm
Armature resistance R_a	0.05 ohms
Armature Inductance L_a	0.001 ohms
Moment of Inertia J	.001 Kg-m ²
Viscous friction coefficient	0.001
Back EMF Constant K_b	0.001 V/rad/s
Torque Constant K_t	0.008 N-m/A

5.1.1 Stability Analysis of the System

The stability of the system model given in equation 3.10 is ensured before considering the implementation various controllers. Stability analysis is carried out using Lyapunov stability theorem. The state variables of the DC motor model are armature current I_a , speed ω , and position θ . The positive definite Lyapunov function $V(x)$ to analyse the stability is chosen as

$$V(x) = x_1^2 + x_2^2 + x_3^2 \quad (5.1)$$

where $x_1 = I_a$, $x_2 = \omega$ and $x_3 = \theta$. Then the derivative of the Lyapunov function is given by

$$\dot{V}(x) = 2x_1\dot{x}_1 + 2x_2\dot{x}_2 + 2x_3\dot{x}_3 \quad (5.2)$$

By substituting the state variables and its derivatives in the above equation, it is found that $\dot{V}(x) = -2342$ which is negative definite and hence, the system is stable as per the Lyapunov stability criterion.

Controllability and observability are also verified by Kalman's test using controllability matrix Q_C and observability matrix Q_O respectively.

$$Q_c = [B \quad AB \quad A^2B] = \begin{bmatrix} 1000 & -5 \times 10^4 & 24.92 \times 10^5 \\ 0 & 8 \times 10^3 & 40.8 \times 10^4 \\ 0 & 0 & 8 \times 10^3 \end{bmatrix}$$

$$Q_o = [C^T \quad A^T C^T \quad A^{T^2} C^T] = \begin{bmatrix} 0 & 0 & 8 \\ 0 & 1 & -1 \\ 1 & 0 & 0 \end{bmatrix}$$

It is clear that $|Q_C| = 64 \times 10^9 \neq 0$ and $|Q_O| = -8 \neq 0$ and the rank of the matrices Q_C and Q_O are 3, which is equal to the dimension of the system and hence the system is completely state observable and controllable as per the Kalman's test.

The design and simulation of various control methods for the position control of DC servo motor are explained as follows.

5.1.2 PI Controller

A conventional PI controller is designed and simulated in order to compare the performance of fuzzy SMC, modified SMC, FLC and Fuzzy PI controller with it. The controller parameters are selected using Ziegler- Nichols tuning method for the Quarter Decay Response (QDR) as described in chapter 4. For the DC motor system the ultimate gain K_u and the time period P_u are obtained as $K_u = 3.8$, $P_u = 0.28\text{sec}$ using this method. From these the controller parameters are obtained as $K_p = 2.23$ and $K_i = 27.14$.

5.1.3 Fuzzy Logic Controller (FLC)

FLC is used independently for the control applications in security systems (Huang and Cheng, 2004), antilock braking systems (ABS) (Mirzaei *et al.*, 2005), speech enhancement (Thevaril and Kwan, 2005) and robot path planning (Wang and Liu, 2005). For the position control of DC servo motor, the error between the actual position and the measured position are taken as the first input and the rate of error as the second input. Five membership functions are assigned to the inputs and its output. The assigned membership functions are Negative Big (NB), Negative Small (NS), Zero (Z), Positive Small (PS), Positive Big (PB) and Medium (M). Triangular and trapezoidal membership functions are chosen for fuzzification and the universe of discourse for error and the error rate are taken as -40 to 40 and -10 to 10 respectively which gives the maximum variations in the normal operating region. For the output u , the universe of discourse is selected as -1 to 1 to get the best response. The input MFs are shown in fig. 5.2 (a) and (b) respectively and the corresponding output membership function is shown in fig.5.3.

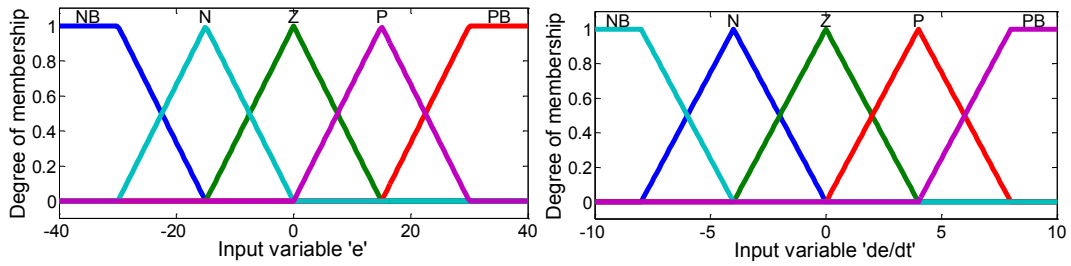


Fig.5.2 (a) Input membership functions e

Fig.5.2 (b) Input membership functions \dot{e}

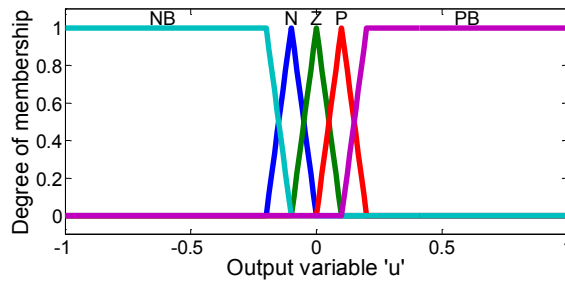


Fig.5.3 Output membership functions

The system has 25 numbers of rules as given in table 5.2. For example the first rule is if e and \dot{e} are NB then u is NB and similarly for other values of e and \dot{e} . Fig.5.4 shows the surface view of the fuzzy system which is a three dimensional graph between the two inputs and the output. This shows the dependency of output on the two inputs and from this it is clear that the variation of the output of the fuzzy controller with inputs is non-linear. The non-planar surface is due to the non-linearity incorporated in the controller whereas for a linear controller this surface will be plain.

Table 5.2 Fuzzy Rules

$e \backslash \dot{e}$	NB	N	Z	P	PB
NB	NB	NB	N	P	PB
N	NB	N	Z	P	PB
Z	NB	N	Z	P	PB
P	NB	N	Z	P	PB
PB	NB	N	P	PB	PB

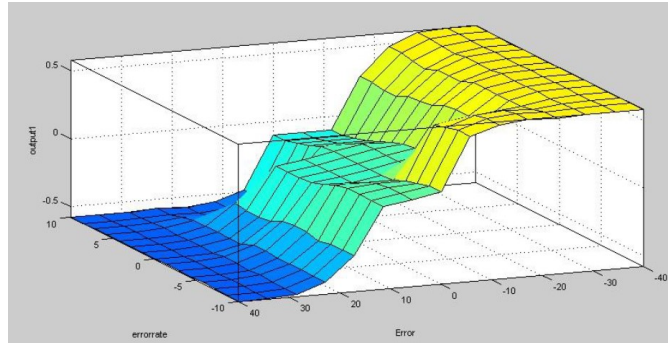


Fig 5.4 Surface view of the fuzzy system

5.1.4 Fuzzy PI Controller

The main problem associated with conventional PI controller is that the proportional constant K_p and integral time T_i are constants. The performance of the PI controller can be improved by varying K_p and T_i appropriately using a fuzzy inference system. In this work the gain of the controller K_p is varied according to the error and the rate of error. The inputs to the fuzzy system for the fuzzy PI controller are the error and the rate of change of error and the output is the gain K_p . The input and output membership functions are shown in fig 5.5 and 5.6 respectively. The universe of disclosure is taken according to the maximum range of variation of each variable and the corresponding fuzzy rules are given in table 5.3.

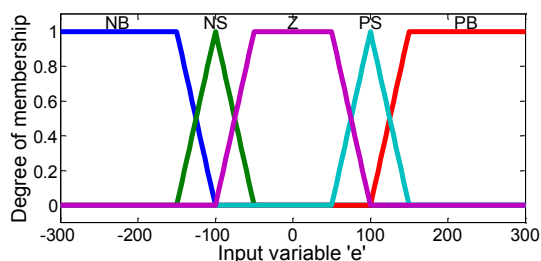


Fig 5.5 (a) Input membership function e

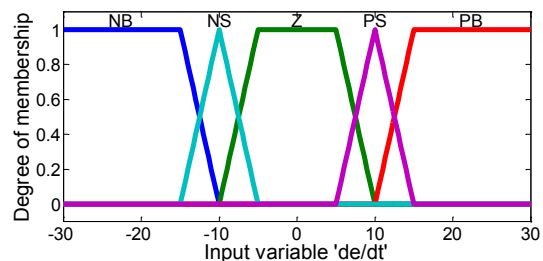


Fig 5.5(b) Input membership function \dot{e}

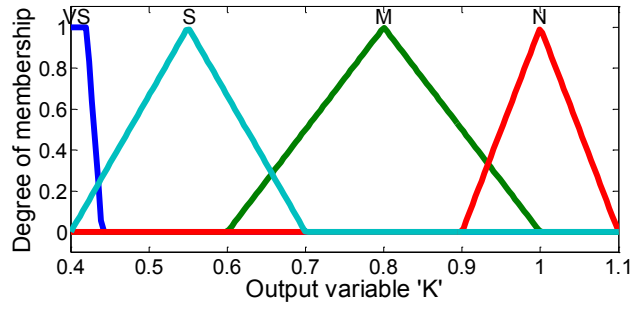


Fig. 5.6 Output membership function k

Table 5.3 Fuzzy Rules

\dot{e} \ E	NB	NS	Z	PS	PB
NB	VS	S	M	M	VS
NS	VS	S	N	M	VS
Z	VS	S	N	S	VS
PS	VS	M	N	S	VS
PB	VS	M	M	S	VS

5.1.5 Modified Sliding Mode Controller (Modified SMC)

The control law of modified SMC is $u = -ksat(s)$ as explained in section 4.3.2 of chapter 4 is designed for the position control of DC servo motor. The sliding surface is given by

$$s = \dot{e} + \lambda_1 e + \lambda_2 \int e dt$$

where $\lambda_1, \lambda_2 > 0$ are a strictly positive real constants. The value of λ_1, λ_2 and k are selected as 10, 0.1 and 2.1 respectively by proper tuning. Also the value of ϕ is taken as unity.

5.1.6 Fuzzy SMC (FSMC)

The performance of the sliding mode controller is improved further when the constant k in the control law is intelligently varied according to the variation in the error signal ' e ' and the rate of change of error signal \dot{e} using fuzzy logic. e and \dot{e} are the input and value of k is the output of the fuzzy system. The input membership function for e and \dot{e} are given in fig.5.7 (a) and (b) respectively. Triangular and trapezoidal membership functions are used and the universe of discourse is selected as -200 to 200 for e and -10 to 10 for \dot{e} respectively. The assigned input membership functions are Negative Big (NB), Negative Small (NS), Zero (Z), Positive Small (PS) and Positive Big (PB) for e and Negative (N), Zero (Z) and Positive (P) for \dot{e} . The corresponding output membership functions are given in fig.5.8 where triangular and trapezoidal functions are used for de-fuzzification and the universe of discourse is selected as 0.5 to 1.8. The assigned output membership functions are Small (S), Medium (M), Big (B). The fuzzy rules are given in in table 5.4.

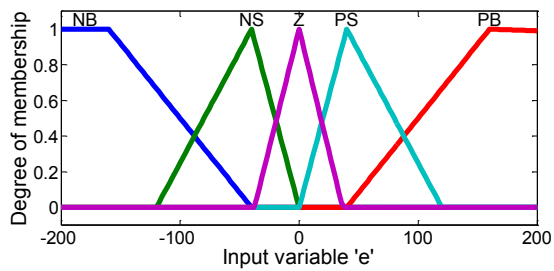


Fig. 5.7 (a) Input membership function e

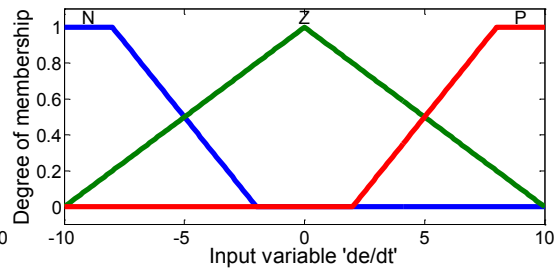


Fig. 5.7 (b) Input membership function \dot{e}

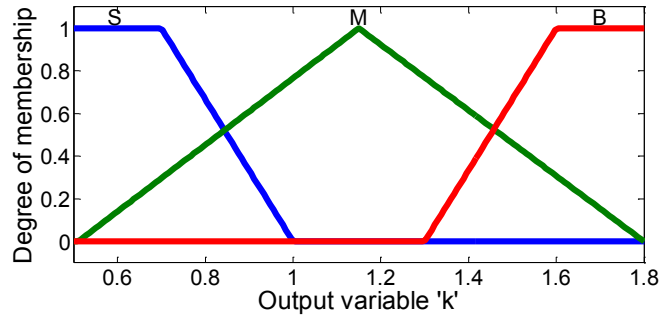


Fig. 5.8 Output membership function k

Table 5.4 Fuzzy Rules

e \dot{e}	<i>NB</i>	<i>NS</i>	<i>Z</i>	<i>PS</i>	<i>PB</i>
<i>N</i>	B	B	M	S	B
<i>Z</i>	B	M	S	M	B
<i>P</i>	B	S	M	B	B

5.1.7 Results and Discussions

When DC motors are used for applications such as antenna positioning and solar tracking that are subjected to cyclic disturbances due to wind. The performance of conventional SMC and PI controllers applied to DC servo motor under cyclic load variations is shown in fig 5.9. Here the overshoot is completely eliminated when conventional SMC is used for both no load as well as cyclic load conditions whereas the corresponding values are very high for PI controller under similar conditions. But the output with SMC is oscillating at high frequency due to the phenomenon of chattering. In order to eliminate the effect of chattering a modified chatter free SMC is employed and the step responses of the system with both modified SMC and PI controller at no-load and cyclic load are shown in fig. 5.10 and 5.11 respectively. From the figure it is clear that the high frequency switching effect is eliminated without affecting other performance indices when the control law of conventional SMC is modified. Corresponding performance comparison is given in table 5.5 and it

shows that the performance of the modified SMC is improved from that of the PI controller in terms of rise time, settling time, Peak overshoot and speed variation while loading.

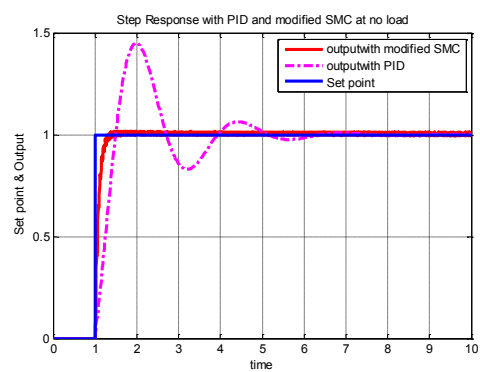
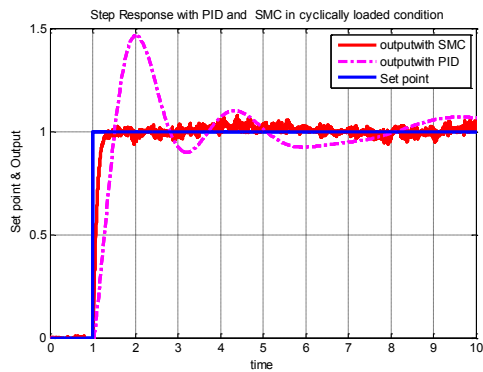


Fig.5.9 Step response with PI and conventional SMC in cyclically loaded condition

Fig.5.10 Step response with PI and modified SMC at no-load

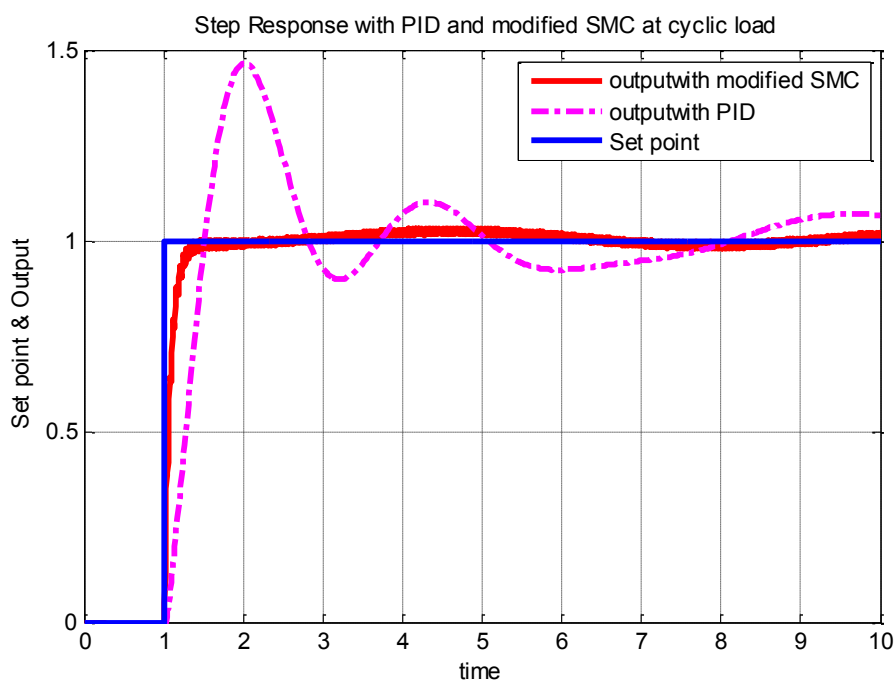


Fig.5.11. Step response with PI and modified SMC in cyclic loaded condition

Table 5.5 Comparison of Modified SMC and PI controllers

	Modified SMC	Modified SMC at cyclic load	PI	PI at cyclic load
Rise time (s)	0.4	0.43	0.6	0.63
Peak overshoot (%)	0	0	40	41
Settling time (s)	0.4	0.43	4	4
Steady state error (%)	0	0	0.05	0.05
Speed Variation due to load (%)	0	5	0	15

Now the system is simulated using the designed values of fuzzy parameters given in section 5.1.3 for a FLC. The input is given as a square wave pulse of 5s duration in order to get the performance during increasing and decreasing speed. Fig 5.12 shows the response of the system with FLC and PI for the square wave input at constant load and it is observed that the peak overshoot is completely eliminated with FLC whereas it is 40 per cent for PI controller. The settling time is reduced from 4s with PID to 1.2s with FLC though there is a small increase in rise time in the case of FLC. These improvements are due to the change in the gain of the controller according to the fuzzy rules in FIS. This small increase in rise time can be neglected when compared with other added advantages of reduction in settling time and elimination of overshoot.

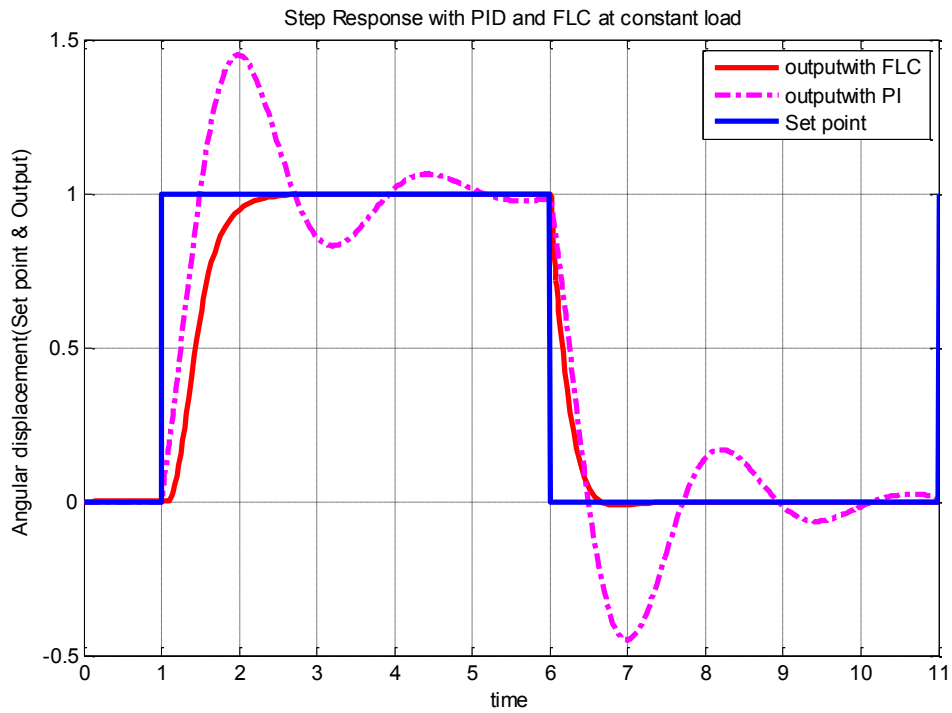


Fig.5.12 Step response with FLC and PI controller at constant load

The Fuzzy SMC is designed with modified control law and the fuzzy parameters given in section 5.1.6 and the step response of the system with Fuzzy SMC, Fuzzy PI and PI controllers are shown in fig 5.13. The performance comparisons with all these controllers are tabulated in table 5.6. It is found that the performance with Fuzzy SMC in terms of the rise time settling time, peak overshoot and speed variation while loading, is improved from that of modified SMC, FLC, Fuzzy PI and PI controllers.

From table 5.6 it is clear that the rise time and settling time are high when FLC is used independently. The main drawback of FLC is its absence of precise mathematical representation that can lead to difficulties in accurate tuning of the controller. Hence FLC alone is not considered for further speed/position control applications in this thesis.

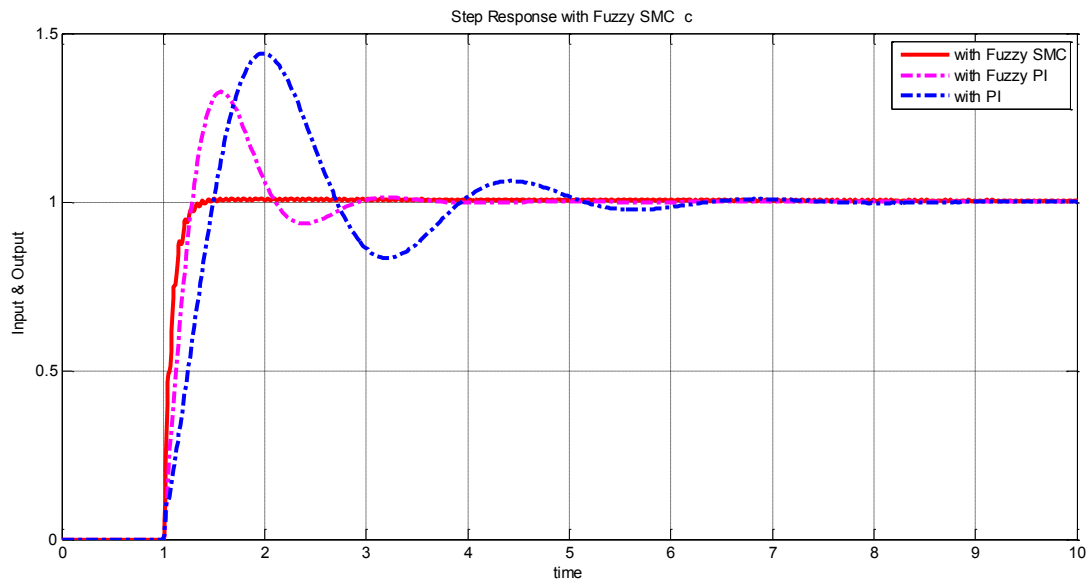


Fig.5.13 Step response with Fuzzy SMC, Fuzzy PI and PI controller at constant load

Table 5.6 Performance comparison for the position control of DC servo motor using various controllers

	FSMC	Modified SMC	Fuzzy Control	Fuzzy PI	PI
Rise time (s)	0.25	0.4	1.2	0.25	0.6
Peak overshoot (%)	0	0	0	28	40
Settling time (s)	0.25	0.4	1.2	1.8	4

5.2 SPEED CONTROL OF DC SERVO MOTOR

DC servo motor plays a significant role in modern industry where very accurate speed control is required. The purpose of a speed controller is to drive a motor at a demanded speed. There are numerous applications where speed control is required, as in rolling mills, cranes, hoists, elevators, machine tools, transit system and locomotive drives. These applications may demand high-speed control accuracy and good dynamic responses. Home appliances, washers, dryers and compressors are good

example for the application requiring accurate speed control. In conclusion, the simplicity of speed control made DC motors a driving device in equipment ranging from toys, home appliances and robotics to industrial applications.

The block diagram for the speed control of DC motor is shown in fig.5.14. Here the DC input voltage to the armature of DC motor is controlled according to the reference value and the actual rotor speed.

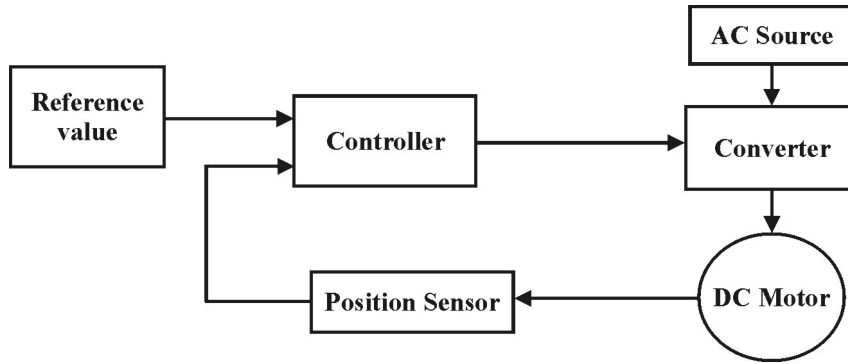


Fig. 5.14 Block diagram of the speed control of DC Motor

5.2.1 Stability Analysis of the System

Stability of the system model is ensured before considering the implementation of any controllers. The stability analysis is carried out using Lyapunov stability theorem. The state variables of the DC motor model are $x_1 = I_a$, and $x_2 = \omega$. The positive definite Lyapunov function, $V(x)$ for the stability analysis is chosen as

$$V(x) = x_1^2 + x_2^2 \quad (5.1)$$

Then the derivative of the Lyapunov function is given by

$$\dot{V}(x) = 2x_1\dot{x}_1 + 2x_2\dot{x}_2 \quad (5.2)$$

By substituting the state variables and its derivatives in equation (5.2) equation it is found that $\dot{V}(x) = -814$ which is negative definite and hence, the system is stable as stated by the Lyapunov stability criterion.

Controllability and observability tests are carried out on this model using Kalmans test using controllability matrix Q_C and observability matrix Q_O respectively.

$$Q_c = [B \quad AB] = \begin{bmatrix} 1000 & 50 \times 10^3 \\ 0 & 8 \times 10^3 \end{bmatrix}$$

$$Q_o = [C^T \quad A^T C^T] = \begin{bmatrix} 0 & 8 \\ 1 & -1 \end{bmatrix}$$

It is found that $|Q_C| = 8 \times 10^6 \neq 0$ and $|Q_O| = 8 \neq 0$ and rank of the matrix is 2, which is equal to the dimension of the system and the system is completely state controllable and observable as per the Kalman's test.

5.2.2 PI Controller

The PI controller parameters used for this speed control are selected using Ziegler-Nichols tuning method for the Quarter Decay Response as described in chapter 4. For the DC motor system the ultimate gain K_u and the time period is P_u are obtained as $K_u = 6.8$ and $P_u = 0.14$ s. From these the PI controller parameters are obtained as $K_p = 3.1$ and $K_i = 33.2$.

5.2.3 Fuzzy PI Controller

Conventional PI controller has constant values of proportional constant K_p and integral time T_i , and this limitation is overcome by suitably varying these gain values using a fuzzy inference system. In this work the gain of the controller K_p is varied according to the error and the rate of error. The inputs to the fuzzy system for the fuzzy PI controller are the error and the rate of change of error and the output is the gain K_p . The input and output membership functions are shown in fig 5.15(a) and (b) and 5.16 respectively. The universe of discourse is taken according to the maximum range variation of each variable and the fuzzy rules are given in table 5.8.

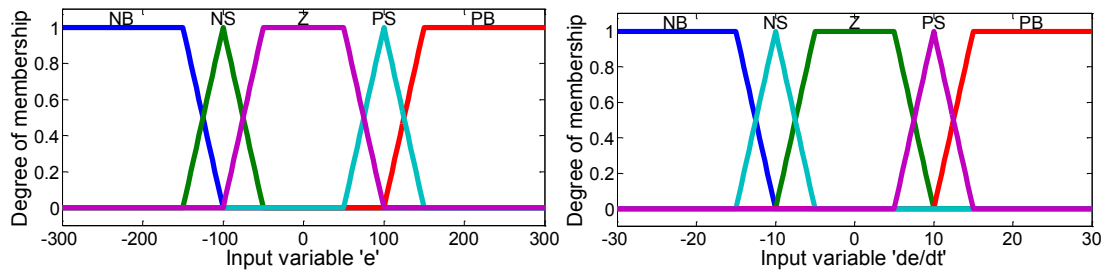


Fig 5.15 (a) Input membership function e Fig 5.15 (b) Input membership function \dot{e}

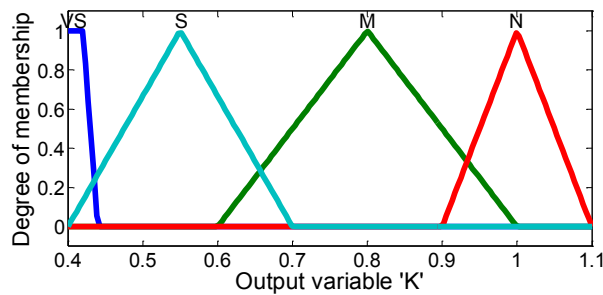


Fig. 5.16 Output membership function k

Table 5.7 Fuzzy Rules

\dot{e} \ E	NB	NS	Z	PS	PB
NB	VS	S	M	M	VS
NS	VS	S	N	M	VS
Z	VS	S	N	S	VS
PS	VS	M	N	S	VS
PB	VS	M	M	S	VS

5.2.4 Modified Sliding Mode Controller (modified SMC)

The modified SMC for the speed control of DC servo motor is designed. The control law of SMC is $u = -ksat(s)$ as explained in section 4.3.2. The sliding surface is given by $s = \dot{e} + \lambda_1 e + \lambda_2 \int e dt$ where $\lambda_1, \lambda_2 > 0$ are strictly positive real constant. The value of λ_1, λ_2 and k are selected as 8, 0.3 and 3.8 respectively by proper tuning. Also the value of ϕ is taken as unity.

5.2.5 Fuzzy SMC (FSMC)

The Fuzzy SMC for the speed control of DC servo motor is designed by selecting suitable membership functions and fuzzy rules. For designing the Fuzzy SMC, the error signal e and its rate of change \dot{e} are taken as the input to the fuzzy system and the value of k is the output of the fuzzy system. The input membership function for e and \dot{e} are given in fig.5.17 (a) and (b) respectively. Triangular and trapezoidal membership functions are used and the universe of disclosure is taken as -200 to 200 for e and -10 to 10 for \dot{e} respectively. The output membership functions are triangular and trapezoidal as shown in fig.5.18 are used for defuzzification with universe of disclosure taken as and 0.5 to 1.8. The fuzzy rules are given in in table 5.8 where NB, NS, Z, PS, PB has the same explanation as before.

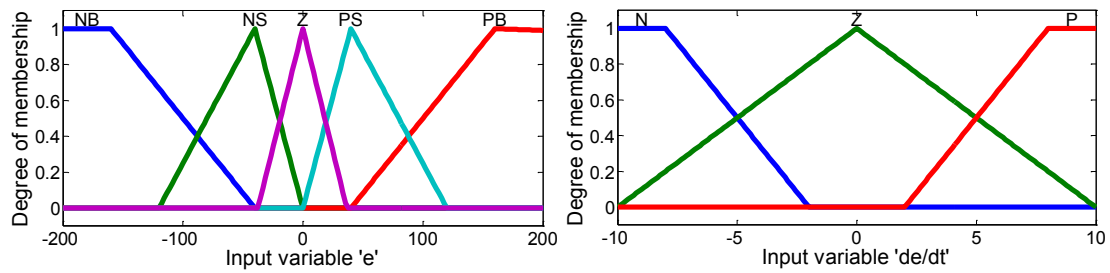


Fig.5.17 (a) Input membership function e Fig. 5.17 (b) Input membership function \dot{e}

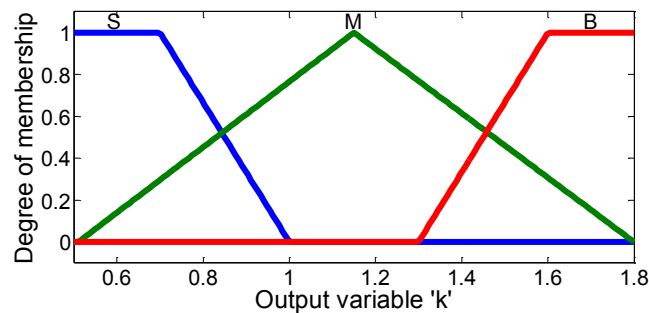


Fig. 5.18 Output membership function k

Table 5.8 Fuzzy Rules

$e \backslash \dot{e}$	NB	NS	Z	PS	PB
N	B	B	M	S	B
Z	B	M	S	M	B
P	B	S	M	B	B

5.2.6 Results and Discussions

The system shown in fig 5.14 is simulated using fuzzy sliding mode controller, chatter free SMC, Fuzzy PI and conventional PI controller. A load torque of 20 Nm is applied at 1.8 seconds after starting in each case. Fig.5.19 shows the step response of the system with fuzzy SMC, SMC, Fuzzy PI and Conventional PI controller respectively for a reference speed of 1500 rpm.

The performance comparison as obtained from graph is tabulated in table 5.9. It is observed that the rise time with proper tuning of PI controller is 90ms is reduced to 70ms by Fuzzy PI and it is further reduced to 50ms with FSMC. The rise time with chattering free SMC is observed to be quite high and is 150ms. The peak overshoot is completely eliminated with FSMC and modified SMC which is 6.67% with Fuzzy PI controller and 14% with PI controller. Moreover the settling time of 440ms with PI controller is reduced to 260ms with Fuzzy PI and further reduced to 150ms with modified chatter free SMC and finally to 50ms with FSMC. The steady state error is negligible with FSMC and modified SMC which is 0.1% and 0.15% respectively with Fuzzy PI and PI controllers. The motor is showing momentary variation in speed when load is applied suddenly at 1.8 s. The speed variation is 3% with PI controller, 2% with Fuzzy PI and 0.6% with chatter free SMC and finally with FSMC is only 0.4%. The rise time is reduced due to the fast action of sliding mode controller. The peak overshoot and settling time are reduced by suitably varying its controller gain using a properly tuned fuzzy inference system. Moreover the speed variation while loading is also reduced and this shows the robustness of FSMC for the speed control of DC servo motor.

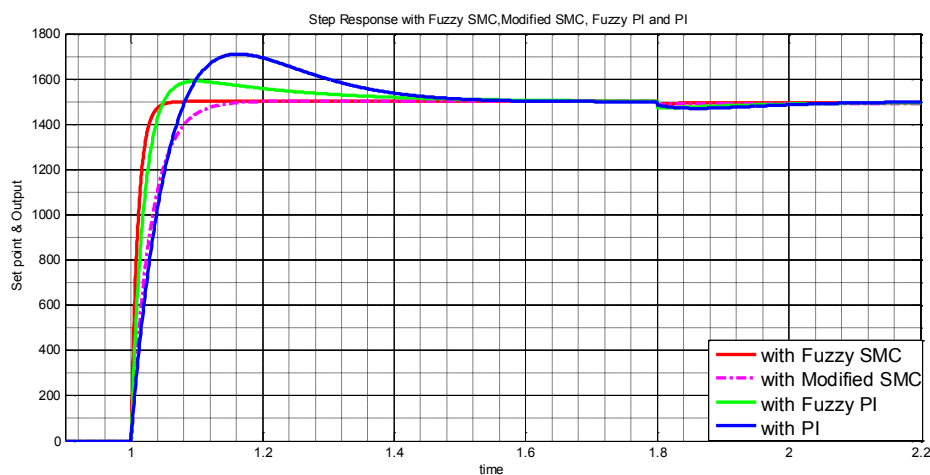


Fig.5.19 Step response with Fuzzy SMC, modified SMC, Fuzzy PI and PI controller for the speed control

Table 5.9 Performance comparison of the speed control of DC servo motor using various controllers

	FSMC	Modified SMC	Fuzzy PI	PI
Rise time (s)	0.05	0.15	0.07	0.09
Peak overshoot (%)	0	0	6.67	14
Settling time (s)	0.05	0.15	0.26	0.44
Steady state error (%)	0	0	0.1	0.15
Speed Variation while loading (%)	0.4	0.6	2	3

5.3 SPEED CONTROL OF BLDC MOTOR

The block diagram for the speed control scheme of a BLDC motor is shown in fig 5.20. The position of rotor is sensed by the Hall Effect sensors and the corresponding gate pulses generated by the pulse generator are used to drive the inverter. Error detector compares reference speed and actual speed to generate error signal which is given as the input to the controller. The signal from the controller is fed the converter or DC source which in turn controls the speed. Different controllers, viz. conventional PI, fuzzy PI, Fuzzy, chatter free SMC, Fuzzy SMC are designed for a 60W BLDC motor whose parameters are given in table 5.10

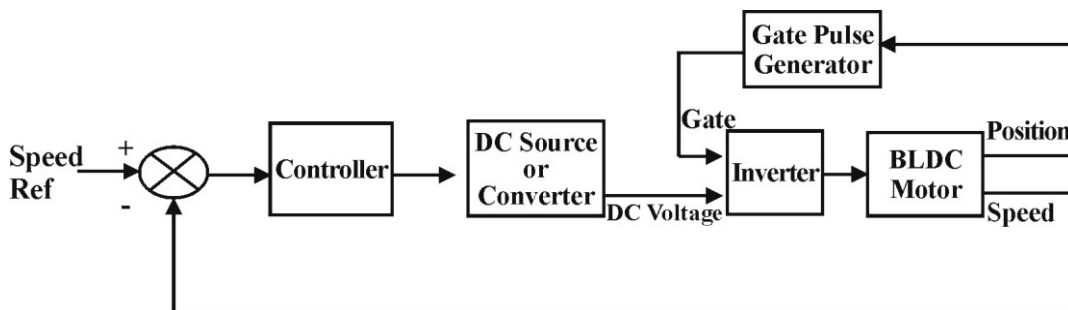


Fig 5.20 Block diagram of the speed control of BLDC motor

Table 5.10 BLDC motor parameters

Motor Parameters	Value
Rated speed	3000 rpm
Rated torque	0.16 N m
No of stator pole pairs	4
Stator Resistance (R)	2.875 ohm
Stator inductance (L)	0.0085H
Maximum flux linkage (ψ_m)	0.175 Wb
Voltage Constant	146.6
Torque constant	1.4 N-m/A
Moment of inertia (J)	0.0008 Kg-m ²
Viscous friction coefficient (B)	0.001 N-m-s/rad

5.3.1 Stability Analysis of the System

The stability of the system model is ensured using Lyapunov stability theorem. The state variables of the BLDC motor are the three stator currents I_a , I_b , I_c , speed ω and rotor position θ that is $x_1 = I_a$, $x_2 = I_b$, $x_3 = I_c$, $x_4 = \omega$ and $x_5 = \theta$. The positive definite Lyapunov function, $V(x)$ for the stability analysis is chosen as

$$V(x) = x_1^2 + x_2^2 + x_3^2 + x_4^2 + x_5^2 \quad (5.5)$$

Then the derivative of the Lyapunov function is given by

$$\dot{V}(x) = 2x_1\dot{x}_1 + 2x_2\dot{x}_2 + 2x_3\dot{x}_3 + 2x_4\dot{x}_4 + 2x_5\dot{x}_5 \quad (5.6)$$

By substituting the state variables and its derivatives in the above equation it is found that $\dot{V}(x) = -24.617 \times 10^5$ which is negative definite and hence, the system is stable as stated by the Lyapunov stability criterion.

Before designing the controller controllability and observability of the system are also verified using Kalman's test using controllability matrix Q_c and observability matrix Q_o respectively.

$$Q_c = [B \quad AB \quad A^2B \quad A^3B \quad A^4B]$$

$$= \begin{bmatrix} 1.176 \times 10^2 & 0.3978 \times 10^5 & 3.0747 \times 10^7 & -1.627 \times 10^{10} & 1.512 \times 10^{13} \\ 0 & 0 & 1.7293 \times 10^7 & -1.172 \times 10^{10} & 1.358 \times 10^{13} \\ 0 & 0 & 1.7293 \times 10^7 & -1.172 \times 10^{10} & 1.358 \times 10^5 \\ 0 & 1.47 \times 10^5 & -4.99 \times 10^7 & 8.1729 \times 10^{10} & -4.99 \times 10^{13} \\ 0 & 0 & 0.735 \times 10^7 & -0.249 \times 10^{10} & 0.409 \times 10^{13} \end{bmatrix}$$

$$Q_o = [C^T \quad A^T C^T \quad A^{T^2} C^T \quad A^{T^3} C^T \quad A^{T^4} C^T]$$

$$= \begin{bmatrix} 0 & 1.25 \times 10^3 & -4.24 \times 10^3 & 6.95 \times 10^8 & -4.23 \times 10^{11} \\ 0 & 1.25 \times 10^3 & -4.24 \times 10^3 & 6.95 \times 10^8 & -4.23 \times 10^{11} \\ 0 & 1.25 \times 10^3 & -4.24 \times 10^3 & 6.95 \times 10^8 & -4.23 \times 10^{11} \\ 1 & -1.3 & 4.41 \times 10^3 & -1.5 \times 10^8 & 2.45 \times 10^{11} \\ 0 & 0 & 0 & 0.85 \times 10^8 & 1.23 \times 10^{11} \end{bmatrix}$$

It is found that $|Q_c| = 1.0131 \times 10^{37} \neq 0$ and $|Q_o| = 1.9602 \times 10^{26} \neq 0$ and rank of the matrix is 5, which is equal to the dimension of the system and the system is completely state controllable and observable as per the Kalman's test.

5.3.2 Sensitivity analysis

Robustness and linearity are important properties of a system. The slight changes in the system parameters do not affect the performance of a robust system. Sensitivity analysis is defined as the study of how uncertainty in the output of a model can be attributed to different sources of uncertainty in the model. As the models are mathematical approximations of real system, sensitivity analysis is used to ensure non linearity and reliability of the system and determines how the input influences the output.

Table 5.11 Variation of speed with voltage

% of Rated voltage	Speed (RPM)
10	510
20	1005
30	1485
40	1975
50	2260
60	2390
70	2495
80	2710
90	2890
100	3000

To analyse the sensitivity of BLDC motor the speed variation with 10% increment in percentage of rated voltage is calculated and the results are tabulated in table 5.11. Fig 5.21 shows the variation of Speed with applied voltage. The sensitivity for every 20% increment in applied voltage is given in table 5.12

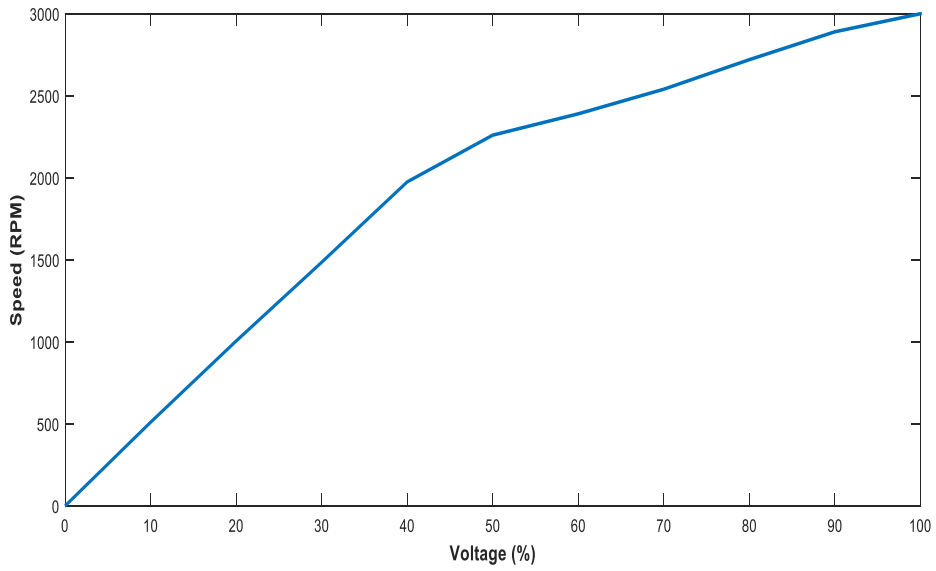


Fig 5.21 Variation of speed with voltage

Table 5.12 Sensitivity with change in voltage

% Voltage	Speed	Sensitivity
20	1005	48.5
40	1975	

% Voltage	Speed	Sensitivity
40	1975	20.75
60	2390	

% Voltage	Speed	Sensitivity
60	2390	16.5
80	2720	

% Voltage	Speed	Sensitivity
80	2720	14
100	3000	

From the above table 5.12 it is clear that the sensitivity is varying with voltage. Fig 5.22 shows the variation of sensitivity with respect time. From this it is observed that the sensitivity is varying continuously which confirm the nonlinear behaviour of the system.

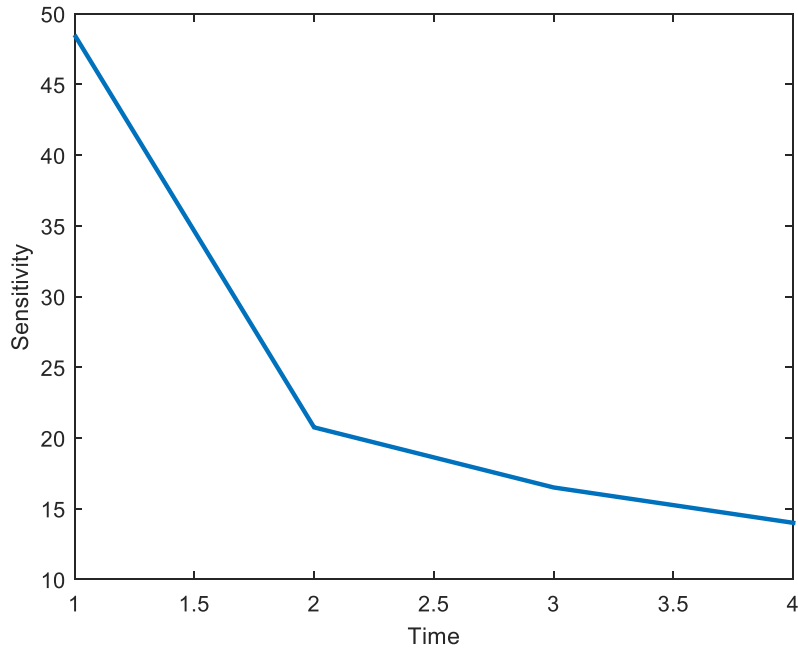


Fig 5.22 Variation of sensitivity with time

5.3.3 PI Controller

The controller constants K_p and K_i of the PI controller are tuned according to the Ziegler-Nichols quarter decay response and the values are obtained as $K_p = 2.1$ and $K_i = 26.6$.

5.3.4 Fuzzy PI Controller

The performance of the PI controller is improved by appropriately varying the gain K_p and integral time constant T_i using a fuzzy inference system. In this work the gain of the controller K_p is varied according to the error and the rate of error. The inputs to the fuzzy system for the controller are the error and the rate of change of error and the

output is the gain K_p . Input and output membership functions are shown in fig 5.23 (a) and (b) and 5.24 respectively. Triangular and trapezoidal membership functions are used and the universe of discourse is taken as -300 to 300 for e and -30 to 30 for \dot{e} respectively and the corresponding fuzzy rules are given in table 5.13 where NB, NS, Z, PS and PB has the same explanation as before.

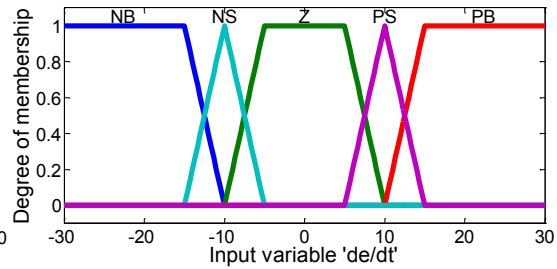
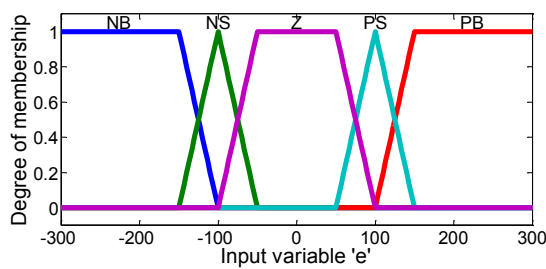


Fig 5.23 (a) Input membership function e

Fig 5.23(b) Input membership function \dot{e}

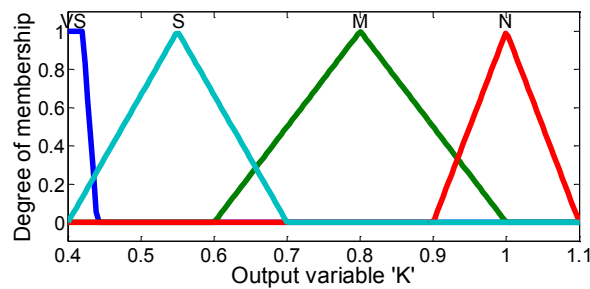


Fig. 5.24 Output membership function k

Table 5.13 Fuzzy Rules

$\dot{e} \backslash e$	NB	NS	Z	PS	PB
NB	VS	S	M	M	VS
NS	VS	S	N	M	VS
Z	VS	S	N	S	VS
PS	VS	M	N	S	VS
PB	VS	M	M	S	VS

5.3.5 Modified Sliding Mode Controller (SMC)

The modified SMC for the speed control of DC servo motor is designed. The control law of SMC is $u = -k_{sat}(s)$ as explained in section 4.3.2. The sliding surface is given

$$\text{by } s = \dot{e} + \lambda_1 e + \lambda_2 \int e dt$$

where $\lambda_1, \lambda_2 > 0$ are a strictly positive real constant. The value of λ_1, λ_2 and k are selected as 12, 0.6 and 13.8 respectively by proper tuning. Also the value of ϕ is taken as unity.

5.3.6 Fuzzy SMC (FSMC)

The performance of the sliding mode controller is improved with an adjustable gain k using a fuzzy system according to the variation in the error signal e and its rate of change \dot{e} . Error e and its derivative \dot{e} are taken as the input and the value of k is the output of the fuzzy system. The input membership function for e and \dot{e} are given in fig.5.25 (a) and (b) respectively. Triangular and trapezoidal membership functions are used and the universe of discourse is taken as -200 to 200 for e and -10 to 10 for \dot{e} respectively. Similarly output membership functions are also triangular and trapezoidal as shown in fig. 5.26 and are used for defuzzifications with the universe of discourse is taken as and 0.5 to 1.8. The corresponding fuzzy rules for the system are given in table 5.14 where NB, NS, Z, PS, PB has the same explanation as before.

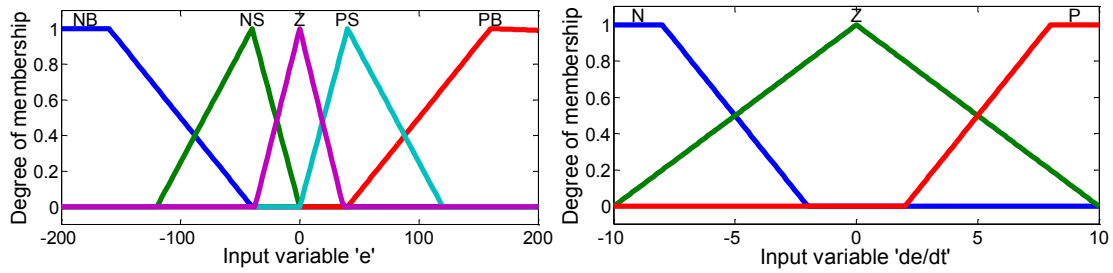


Fig. 5.25(a) Input membership function e Fig.5.25 (b) Input membership function \dot{e}

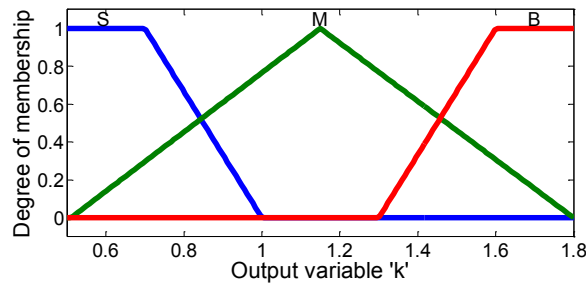


Fig. 5.26 Output membership function k

Table 5.14 Fuzzy Rules

$e \backslash \dot{e}$	NB	NS	Z	PS	PB
N	B	B	M	S	B
Z	B	M	S	M	B
P	B	S	M	B	B

5.3.7 Optimization of Controller Gain using Krill Herd Algorithm

The performance of the controller is greatly influenced by the selected value of the controller gain. Even though the rise time decreases by higher values of gain, other specifications like peak overshoot and settling time are adversely affected and the system stability reduces. Hence it is important to select an optimal controller gain that results in minimum rise time, peak overshoot, settling time and steady state error.

Krill Herd (KH) algorithm introduced by (Gandomi *et al.*, 2012) is applied for this purpose. This Algorithm is the simulation of krill's behaviour of motion and it has three main components that include induced motion, foraging motion and physical diffusion to find optimum point. When hunters attack krills, predation removes individual krills and this leads to diminish the krills density. Two main goals of herding them after reducing density are increasing krill density and reaching food that lead the krills to herd around the global optima. The objective function used in KH for krill movement is determined by the least distances from food and the highest herd density. The main advantage of this technique is that only few variables are required for optimisation. The position of krill consists of three main components viz. movement affected by other krill, foraging action, physical diffusion. The proposed KH algorithm is based on Lagrangian model, which states the objective function as combination of the highest density of the krill and the distance of food from the krill. In n-dimensional space, the fitness function of the algorithm for i^{th} krill individual is defined as:

$$\frac{dX_i}{dt} = N_i + F_i + D_i \quad (5.7)$$

where N_i is the motion induced by other krill individuals, F_i is the foraging motion and D_i is the physical diffusion of the i^{th} krill individual.

According to theoretical arguments, the krill individuals try to maintain a high density and move due to their mutual effects. The direction of motion induced is α_i and is estimated from the local swarm density, a target swarm density, and a repulsive swarm density. For a krill individual, this movement can be defined as:

$$N_i^{new} = N^{max} \alpha_i + \omega_n N_i^{old} \quad (5.8)$$

where N^{max} is the maximum induced speed, ω_n is the Inertia weight, N_i^{old} is previous motion induced. The direction α_i is the sum of local effect provided by the neighbouring krill individuals and target effect provided by the best krill individual. The foraging motion is the motion induced to a krill individual due to the presence of food and its previous locations. The foraging motion value for the i th krill individual is given by:

$$F_i = V_f \beta_f + \omega_f F_i^{old} \quad (5.9)$$

where V_f is foraging speed, ω_f is inertia weight of the foraging motion and is the last foraging motion value. The effect of food on the herding mechanism is defined depending on the food's location and β_f is the sum of effect due to the presence of food and the effect due to the current krill's best fitness value recorded. The random diffusion is based on a maximum diffusion speed and a random directional vector and is given by:

$$D_i = D^{max} \delta \quad (5.10)$$

Where D^{max} is the maximum diffusion speed and δ is the random directional vector and its arrays consist of random numbers. Here in, the position in KH from t to $t + \Delta t$ is formulated as follows:

$$X_i(t + \Delta t) = X_i(t) + \Delta t \frac{dX}{dt} \quad (5.11)$$

The flow chart of the KH algorithm is shown in fig.5.27. The aim of this algorithm is to arrive at a minimum distance of the krill individual from the food and achieve highest density of the krill swarm. In our case the objective of the optimization algorithm in FSMC is to design an optimal value for the gain to minimize rise time t_r , peak overshoot M_p , settling time t_s and steady state error ss . The constraints of the problem are to define the upper and lower limits for the gain k such that optimum performance without chatter effect is obtained.

The objective function used to optimize the controller gain is $f(x) = 0.5t_r + 0.5t_s + 3.5M_p + \frac{1}{2}ss^2$ subjected to $0 \leq k \leq 60$ and the KH parameters selected are given in table 5.15.

Table 5.15 Parameter values initialized in KH algorithm

KH Parameters	Value
Number of krills	30
Number of iterations	25
Foraging velocity	0.3
Inertia for foraging	0.4
Maximum diffusion	0.006
Maximum induced speed	0.2
Inertia for movement	0.1
Mutation	0.2

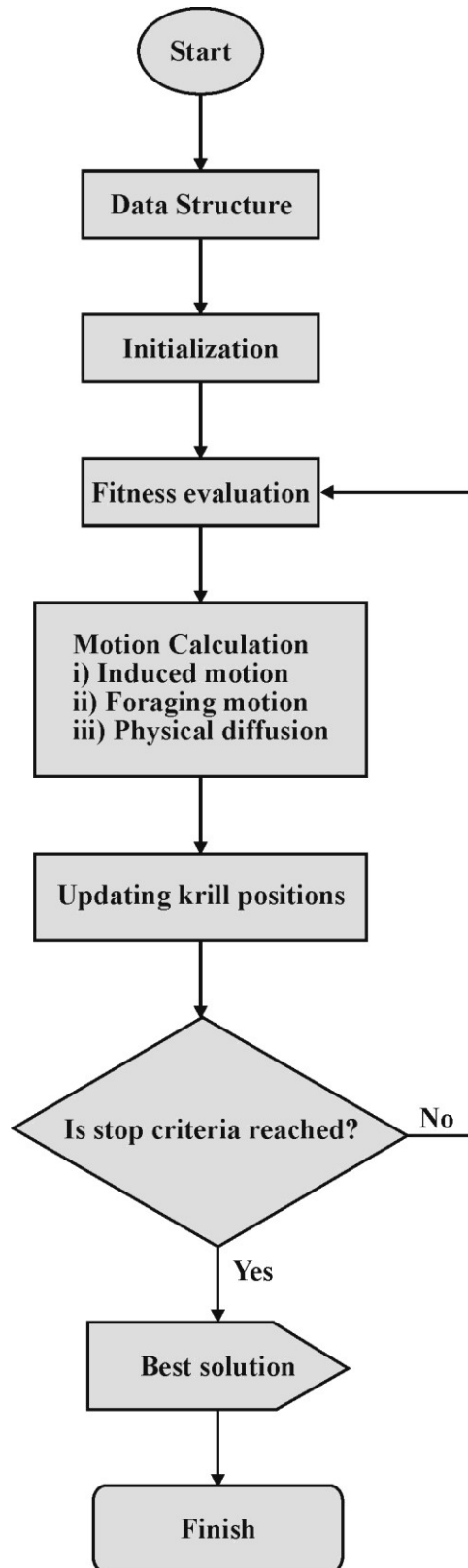


Fig. 5.27 Flow chart of KH algorithm

The controller gain obtained for various values of error are listed in table 5.16. From the above results it is clear that optimal performance of the controller can be achieved by appropriately varying the gain according to the value of error.

Table 5.16 Optimized values of the controller gain

Error	Optimized value of k
3000	18.75
2000	16.32
1000	15.13
500	13.85
50	12.12
10	11.28

5.3.8 Results and Discussions

Control system using FSMC, chattering free SMC, Fuzzy PI and PI controller with tuned values of parameters for a 60 W BLDC motor is simulated. The gain of FSMC is optimized to vary within the limits of 0 to 60 using KH algorithm. A load torque of 0.16 Nm is applied at 0.08 seconds after starting. Fig.5.28 shows the step response of the system using these four controllers for a reference speed of 3000 rpm. The performance comparison is given in table 5.17. It is observed that the rise time with proper tuning of PI controller is 25ms which is reduced to 20ms by Fuzzy PI and it is further reduced to 15ms with SMC and finally 8ms with optimized gain of FSMC. The peak overshoot is completely eliminated with FSMC and SMC, while it is 2.5% with Fuzzy PI and 3% with PI controller. The settling time of 46ms with PI

controller is reduced to 38ms with Fuzzy PI and further reduced to 15ms with modified SMC and finally to 8ms with FSMC. Moreover the steady state error is only 0.02% with FSMC which are 0.04%, 0.05% and 0.06% with chatter free SMC, Fuzzy PI and PI controllers respectively. The motor is showing momentary variation in speed when sudden load is applied. The speed variation is 5% with PI controller, 4% with Fuzzy PI and 3% with chatter free SMC and is completely eliminated when FSMC is used. The rise time is reduced due to the fast action of sliding mode controller. The peak overshoot and settling time are reduced by varying its controller gain appropriately using a fuzzy inference system. Moreover the speed variation while loading is eliminated and this shows the robustness of the FSMC. Fig. 5.29 shows the current waveform in the three phases of the motor. It is observed that the starting current is slightly higher with fuzzy SMC than that with other controllers, but this has negligible effect on the performance as the starting current lasts only for few milliseconds and there is only negligible variation under running condition. Fig. 5.30 shows the trapezoidal back EMF whose maximum value is almost the same with all the controllers. The results clearly indicate that the performance is greatly improved when FSMC with optimized gain is used, compared to other three controllers in terms of rise time, overshoot, settling time, fluctuation in speed with sudden load variation. However, the FSMC algorithm becomes more complex and hence suitable for applications where very precise speed control is necessary.

The variation of controlled variable (speed) vs. the manipulated variable (current) is shown in fig. 5.31. Rated load is applied at 0.08s and it is observed that in order to keep the controlled variable (speed) constant, the manipulated variable (current) is suitably adjusted by the controller according to the change in load.

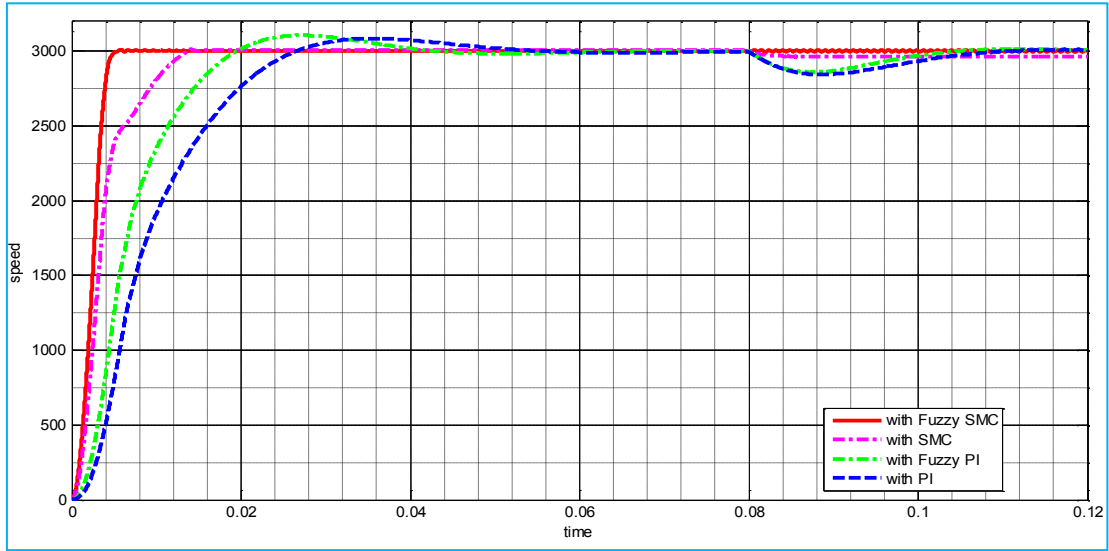


Fig 5.28 Step response of BLDC motor with Fuzzy SMC and other controllers

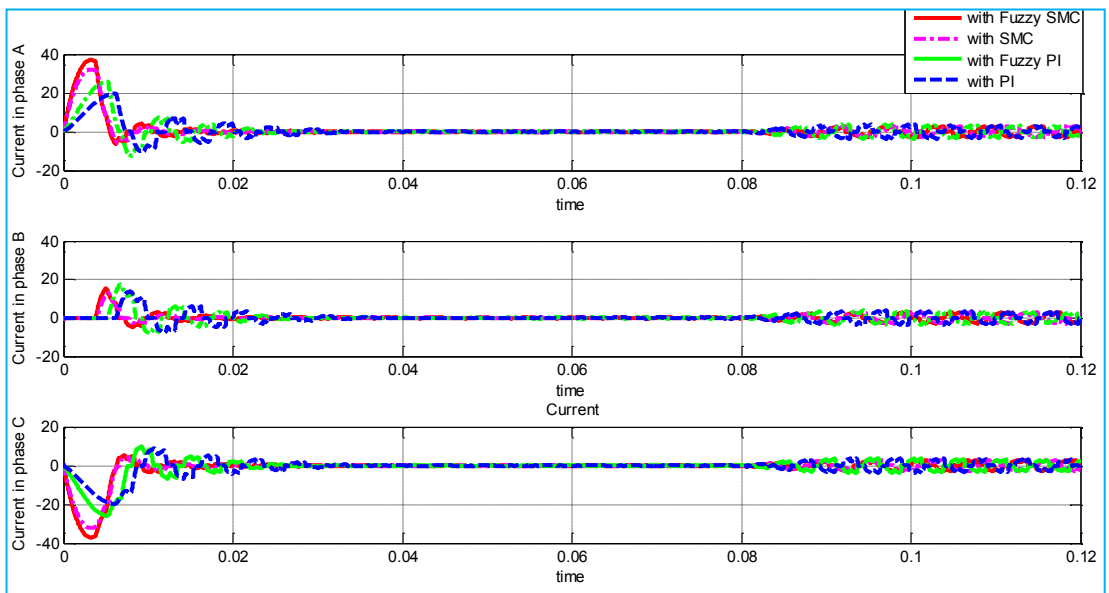


Fig 5.29 Current in the three phases of BLDC motor

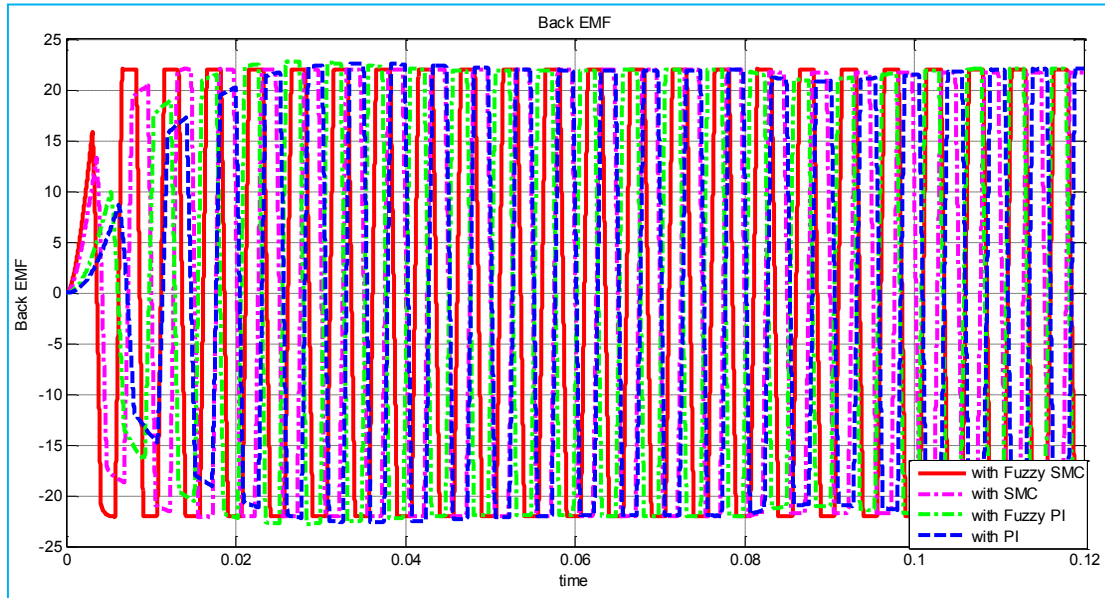


Fig 5.30 Back EMF in the three phases of BLDC motor

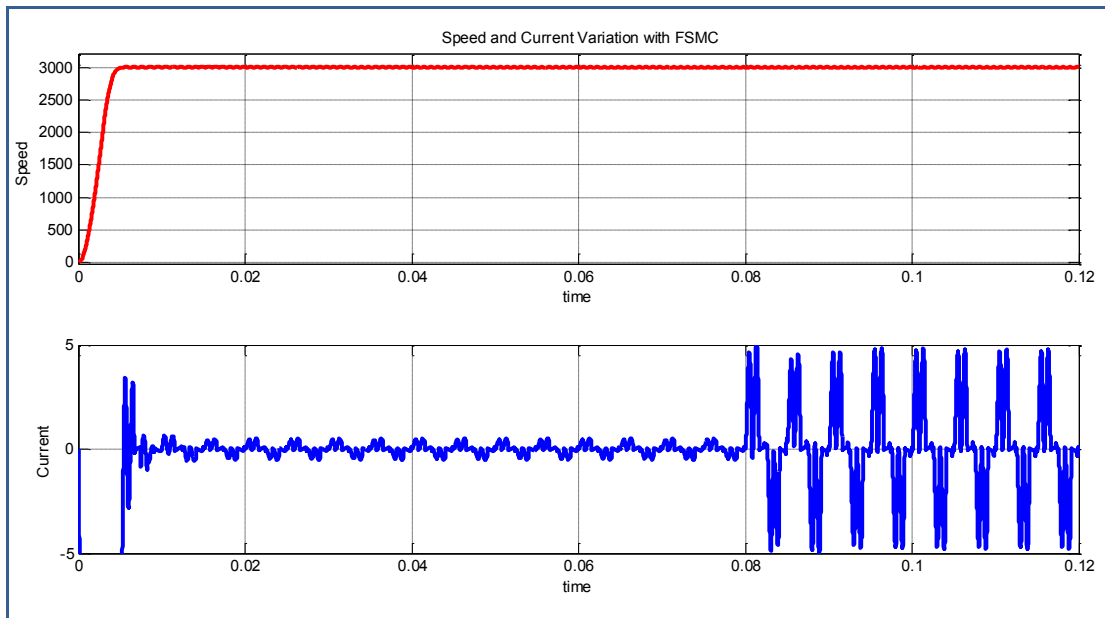


Fig 5.31 Variation of speed and current with FSMC

Table 5.17 Performance comparison

	Fuzzy SMC	Modified SMC	Fuzzy PI	PI
Rise time (ms)	8	15	20	25
Peak overshoot (%)	0	0	2.5	3
Settling time (ms)	8	15	38	46
Steady state error (%)	0.02	0.04	0.05	0.06
Speed variations when suddenly load is applied (%)	0	3	4	5

5.4 SPEED CONTROL OF SWITCHED RELUCTANCE MOTOR

The block diagram for the speed control scheme of an SRM is given in fig 5.32.

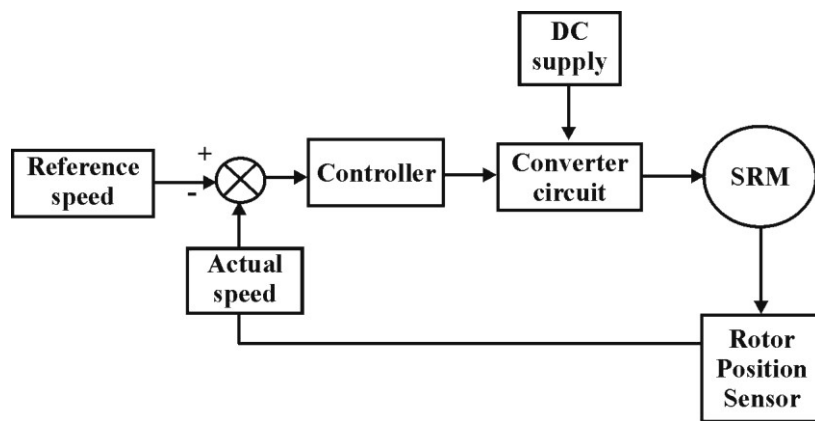


Fig.5.32 Block diagram of SRM speed control

Table 5.18 Parameters of SRM

Motor Parameters of SRM	Value
Rated Power	3.6kW
Rated phase to phase voltage	240V
Rated current	15A
Rated speed	2000 rpm
No of stator poles	6
Stator Resistance (R)	0.01ohm
Stator inductance	0.00067 H
Maximum flux linkage (ψ_m)	0.486 Wb
Moment of inertia (J)	0.0082 Kg-m
Viscous friction coefficient (B)	0.01

The rotor position sensor senses the speed and provides the signal corresponding to the output to the error detector which in turn compares it with the reference speed to generate an error signal that acts as an input to the controller. The resulting output signal controls the speed of the motor by the excitation of their corresponding windings. The simulation is conducted on a 3.6 kW SRM whose parameters are given in table 5.18. The controller output signal is fed to the converter which generates the excitation required as applicable to a particular winding of the SRM for its required speed.

5.4.1 Stability Analysis of the system

The stability of the system model is ensured using Lyapunov stability theorem before considering the implementation of controllers. The state variables of the SRM are $x_1 = i$, $x_2 = \omega$ and $x_3 = \theta$. The positive definite Lyapunov function, $V(x)$ for the stability analysis is taken as

$$V(x) = x_1^2 + x_2^2 + x_3^2 \quad (5.5)$$

Then the derivative of the Lyapunov function is given by

$$\dot{V}(x) = 2x_1\dot{x}_1 + 2x_2\dot{x}_2 + 2x_3\dot{x}_3 \quad (5.6)$$

By substituting the state variables and its derivatives in the above equation it is found that $\dot{V}(x) = -816$ is negative definite and hence, the system is stable according to Lyapunov stability criterion.

Controller design is carried out after verifying the controllability and observability of the system using Kalman's test with controllability matrix Q_c and observability matrix Q_o respectively.

$$Q_c = [B \quad AB \quad A^2B] = \begin{bmatrix} 100 & -1493 & 2290 \\ 0 & -1.2 & 1.44 \\ 0 & 0 & -1.2 \end{bmatrix}$$

$$Q_o = [C^T \quad A^T C^T \quad A^{T^2} C^T] = \begin{bmatrix} 0 & 1 & 0 \\ 1 & -1.2 & 1.44 \\ 0 & 1 & 1 \end{bmatrix}$$

It is found that $|Q_c| = 144 \neq 0$ and $|Q_o| = -1 \neq 0$ and rank of the matrix is equal to the dimension of the system and hence it is completely state controllable and observable.

5.4.2 PI Controller

The controller constants K_p and K_i of the PI controller are tuned according to the Ziegler- Nichols tuning method for quarter decay response and their values are $K_p = 3.8$ and $K_i = 32.4$ respectively.

5.4.3 Fuzzy PI Controller

The performance of the PI controller is improved by suitably varying the proportional constant K_p and integral time constant T_i using a FIS. The gain of the controller K_p is varied according to the error e and the rate of error \dot{e} . The inputs to the fuzzy system for the adaptive fuzzy controller are e and \dot{e} and the output is the gain K_p . The input and output membership functions are shown in fig 5.33 (a) and (b) and 5.34 respectively and the universe of discourse are taken according to the maximum range variation of each variable and the corresponding fuzzy rules are given in in table 5.19.

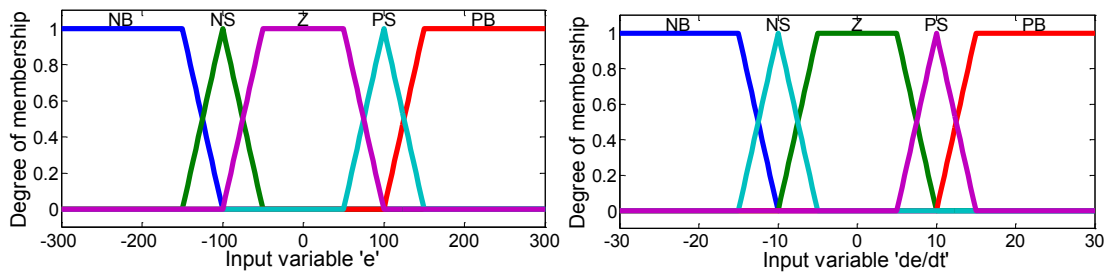


Fig 5.33 (a) Input membership function e Fig 5.33 (b) Input membership function \dot{e}

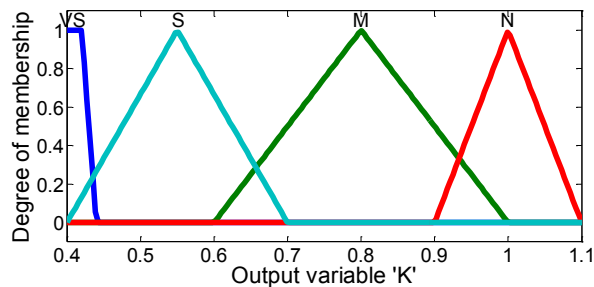


Fig. 5.34 Output membership function k

Table 5.19 Fuzzy Rules

$\dot{e} \backslash e$	<i>NB</i>	<i>NS</i>	<i>Z</i>	<i>PS</i>	<i>PB</i>
<i>NB</i>	VS	S	M	M	VS
<i>NS</i>	VS	S	N	M	VS
<i>Z</i>	VS	S	N	S	VS
<i>PS</i>	VS	M	N	S	VS
<i>PB</i>	VS	M	M	S	VS

5.4.4 Modified Sliding Mode Controller (SMC)

The modified SMC for the speed control of DC servo motor is designed. The control law of SMC is $u = -ksat(s)$ as explained in section 4.3.2. The sliding surface is given by $s = \dot{e} + \lambda_1 e + \lambda_2 \int e dt$ where $\lambda_1, \lambda_2 > 0$ are a strictly positive real constant. The value of λ_1, λ_2 and k are selected as 9, 1.1 and 8.2 respectively by proper tuning. Also the value of ϕ is taken as unity.

5.4.5 Fuzzy SMC (FSMC)

Control law of chatter free SMC is $u = -ksat(s/\phi)$ where the gain k is constant. The performance of the sliding mode controller is improved further if the constant k in the control law is suitably varied according to the variation in the error signal and the rate of change of the error signal. For this purpose the error signal e and its rate of change \dot{e} are taken as the input and the value of k as the output for the fuzzy system.

The input membership function for e and \dot{e} are given in fig. 5.35(a) and (b) respectively. Triangular and trapezoidal membership functions are used and the universe of disclosure is taken as -200 to 200 for e and -10 to 10 for \dot{e} . The output

membership function is given in fig.5.36. Triangular and trapezoidal membership functions are used as output membership functions for de-fuzzification and the universe of discourse is taken as and 0.5 to 1.8. The fuzzy rules corresponding to this are listed in in table 5.20.

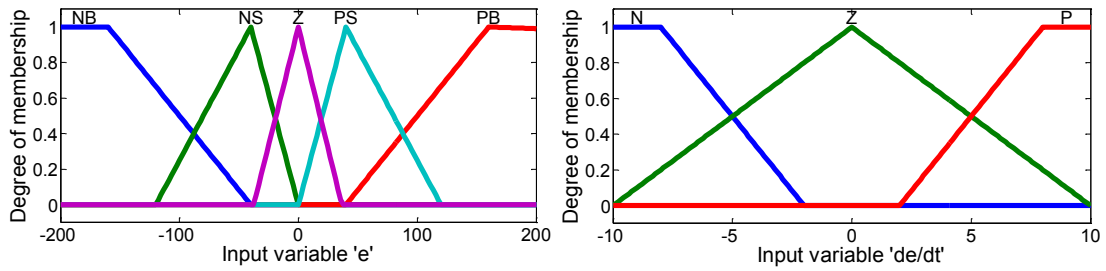


Fig.5.35 (a) Input membership function e Fig. 5.35(b) Input membership function \dot{e}

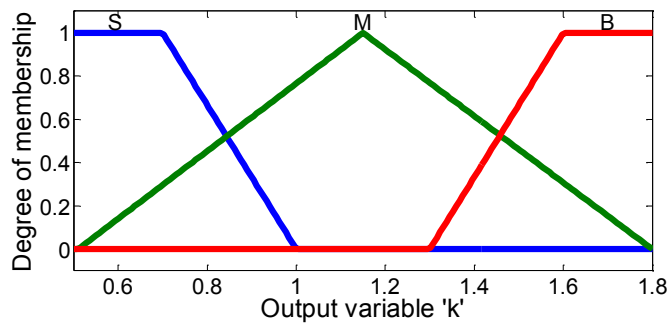


Fig .5.36 Output membership function k

Table 5.20 Fuzzy Rules

$\dot{e} \backslash e$	<i>NB</i>	<i>NS</i>	<i>Z</i>	<i>PS</i>	<i>PB</i>
<i>N</i>	B	B	M	S	B
<i>Z</i>	B	M	S	M	B
<i>P</i>	B	S	M	B	B

5.4.6 Results & Discussions

Speed control of SRM is used in industrial applications like electric vehicle, fans, aerospace and industrial automation. Hence considering the importance of the speed control of this machine a Fuzzy Sliding Mode Controller is simulated in MATLAB/Simulink and the results are compared with that of a conventional chatter free SMC, Fuzzy PI and conventional PI controller. In order to achieve appropriate variations of gain k , suitable membership function with universe of discourse is selected for the fuzzy system and proportional gain (K_p) and integral time constant (T_i) are calculated for the PI controller.

Step response of the SRM with Fuzzy SMC, chatter free SMC, Fuzzy PI and conventional PI controller for a reference speed of 2000 rpm is shown in fig 5.37. A load torque of 20 Nm is applied at 0.15 seconds after starting. Fig 5.38 shows the enlarged view of the step response near 2000 rpm from which the speed variation while loading becomes more clear. The performance comparison of rise time, peak overshoot, settling time and speed variation while loading, are given in table 5.21. It is observed that the rise time with proper tuning of PI controller is 62ms which is reduced to 60ms with fuzzy PI and is again reduced to 45ms with modified SMC and is further improved by FSMC to a value of 25ms. The peak overshoot is completely eliminated with FSMC and modified SMC which is 0.4% and 1.25% respectively with Fuzzy PI conventional PI controller. Moreover the settling time of 100ms with PI controller is reduced to 80ms with fuzzy PI and which is again reduced to 45ms

with SMC and is improved by FSMC to 25ms. The steady state error is also eliminated with FSMC and modified SMC whereas it is 0.1% each with Fuzzy PI conventional PI controller. The speed variation while loading was also improved to 0.5% with FSMC from 1% with SMC, 2% with Fuzzy PI and PI controllers. From the results it is observed that transient performance of the fuzzy sliding mode controller is greatly improved in terms of rise time, peak overshoot, settling time and steady state error compared to that of modified SMC, Fuzzy PI and PI controllers. Also the speed variation while loading is minimum with Fuzzy sliding mode controller when compared with the other controllers. The improvement in the performance of FSMC is achieved by suitably modifying the control law of SMC as well as adjusting the gain k of the controller using FIS.

Even though the FSMC algorithm is more complex and hence computationally expensive, it results in the improvement of its transient as well as steady state performances that leads to better precision and quality of the product when used practically for industrial applications.

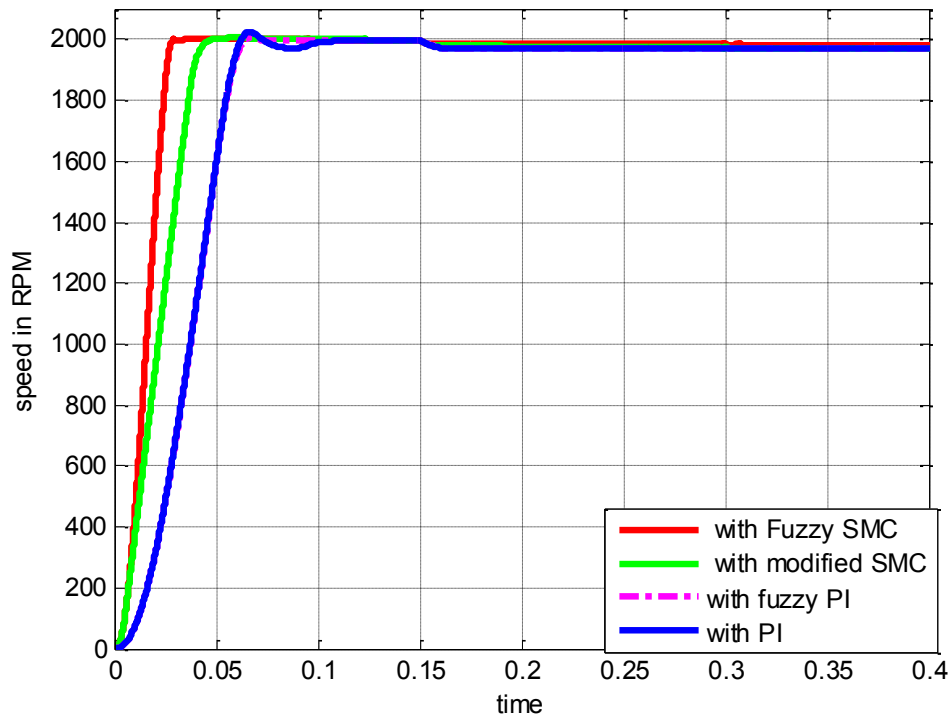


Fig.5.37 Step response of SRM with Fuzzy SMC and other controllers

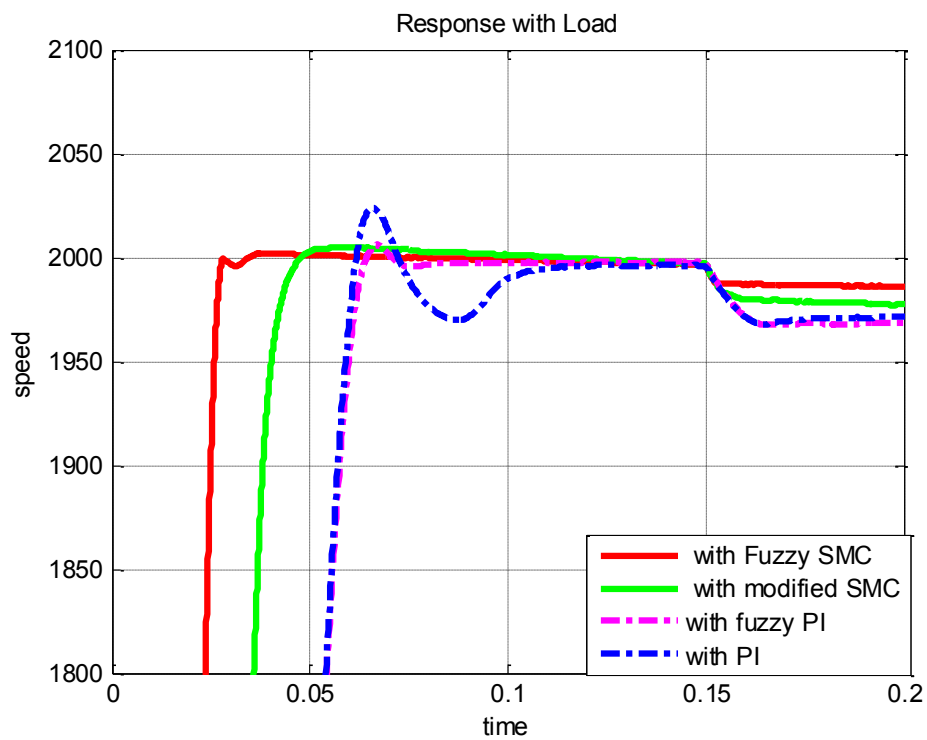


Fig 5.38 Response while loading with Fuzzy SMC and other controllers

Table 5.21 Performance comparison

Performance Indices	Fuzzy SMC	Modified SMC	Fuzzy PI	PI
Rise time (s)	0.025	0.045	0.06	0.062
Peak overshoot (%)	0	0	0.4	1.25
Settling time (s)	0.025	0.045	0.08	0.1
Steady state error (%)	0	0	0.1	0.1
Speed Variation with rated load (%)	0.5	1	2	2

The comparison of the performance indices of selected DC drives with various controllers are represented in fig. 5.39 (a), (b), (c) and (d) respectively. Among the widely used DC drives of DC servo motor, BLDC motor and PMSM, the proposed FSMC produces minimum values of rise time, peak over shoot, settling time and steady state error compared to modified SMC, Fuzzy PI and PI controllers. The improvement in the performance of FSMC compared to other controllers is highly significant in spite of its design complexity.

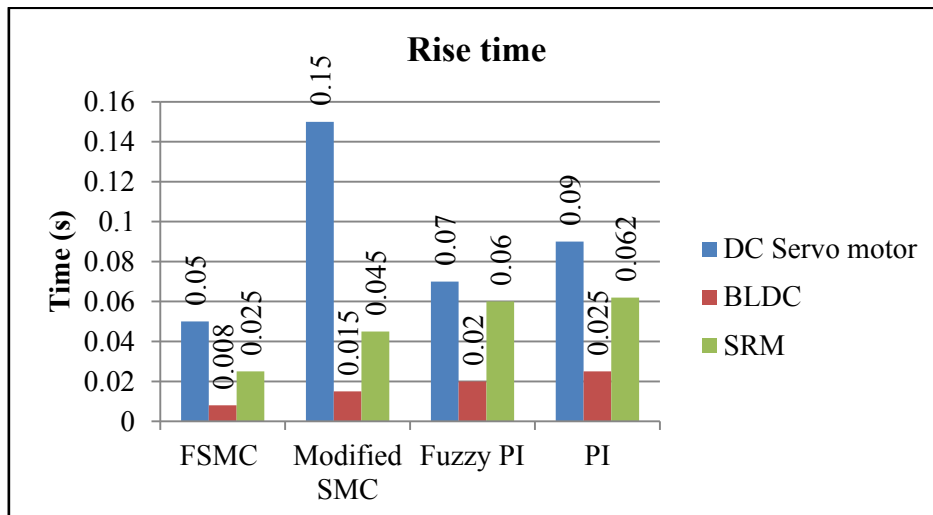


Fig. 5.39 (a) Comparison of rise time for DC servo motor, BLDC and SRM with FSMC, Modified SMC, Fuzzy PI and PI controllers

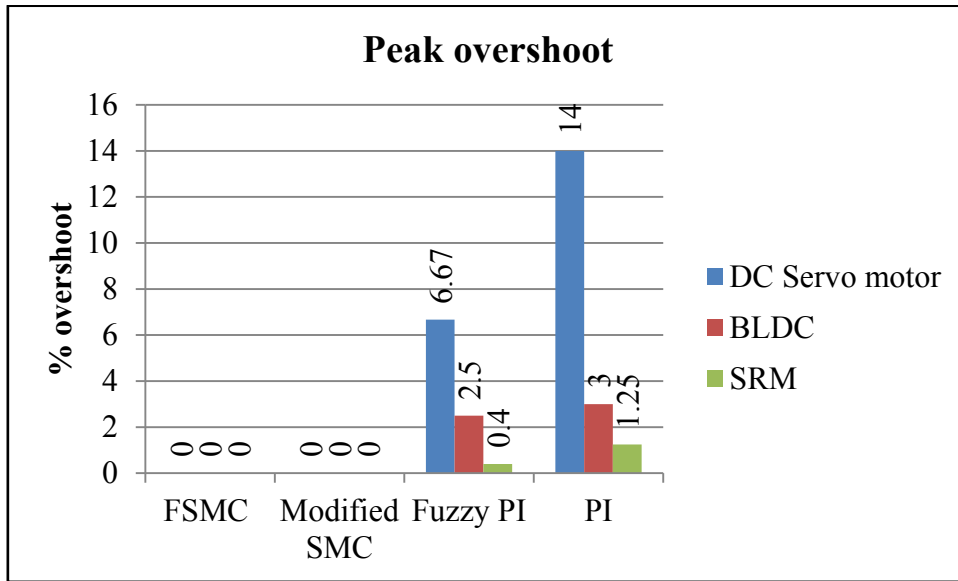


Fig. 5.39(b) Comparison of peak overshoot for DC servo motor, BLDC and SRM with FSMC, Modified SMC, Fuzzy PI and PI controllers

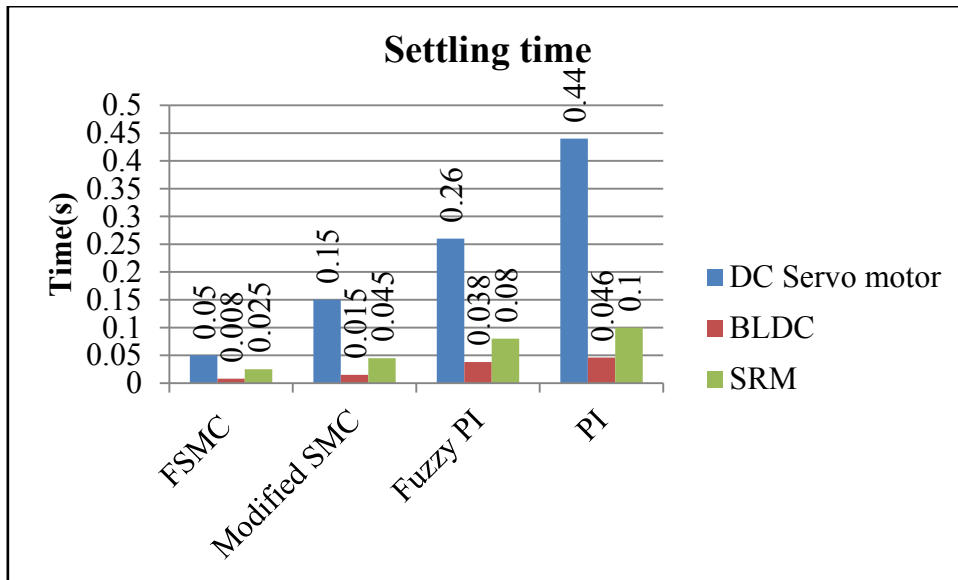


Fig. 5.39(c) Comparison of settling time for DC servo motor, BLDC and SRM with FSMC, Modified SMC, Fuzzy PI and PI controllers

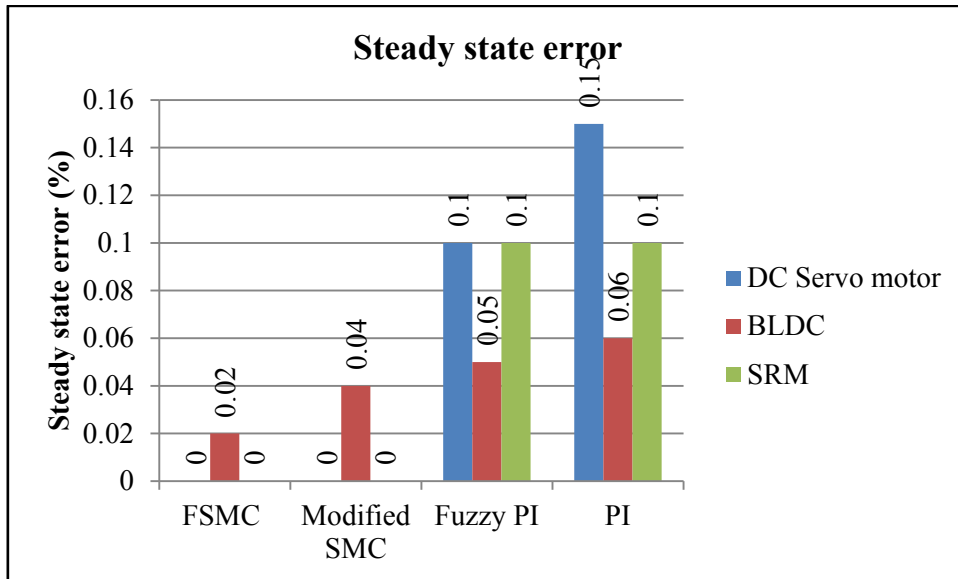


Fig.5.39 (d) Comparison of steady state error for DC servo motor, BLDC and SRM with FSMC, Modified SMC, Fuzzy PI and PI controllers

CHAPTER 6

NON-LINEAR INTELLIGENT CONTROL OF AC DRIVES

Permanent magnet synchronous motors (PMSM) are extensively used for many industrial applications like Computer Numerical Control (CNC) machine tools, industrial robots, hybrid electric vehicle etc. due to high torque to weight ratio, high power density, high efficiency, reliability and ease of maintenance (Sain *et al.*, 2016). For the precise and accurate speed control of PMSM, various control techniques using FSMC, modified SMC, Fuzzy PI and conventional PI control are designed and their transient and steady state performances are compared to decide the most suitable controller.

6.1 FIELD ORIENTED CONTROL OF PMSM

The control of AC drives become equivalent to that of DC drives due to the introduction of Field Oriented Control (FOC) or vector control, in which the torque and flux are controlled independently. To achieve high precision and accuracy in performance, the vector control is employed in the PMSM drive. However, system non-linearity, motor parameters variation and load torque variation make it difficult to control the speed of the motor precisely. These problems can be solved by incorporating a suitable control scheme capable of dealing with such cases.

Vector control is the most widely used control technique of AC motors (Krishnan, 2001). The main objective of the vector control of AC motors is to independently control the torque and the flux where the control is usually performed in the reference frame (d-q) attached to the rotor flux space vector. Hence the implementation of

vector control requires information on the modulus and the space angle (position) of the rotor flux space vector. The stator currents of the AC machine are separated into flux and torque producing components by utilizing transformation to the d-q coordinate system, whose direct axis (d) is aligned with the rotor flux space vector making the q-axis component of the rotor flux space vector always zero. Various steps in the field oriented control are listed below:

1. Measure the motor quantities (phase voltages and currents).
2. Transform them to the 2-phase system (α, β) using a Clarke transformation.

$$\begin{bmatrix} v_\alpha \\ v_\beta \end{bmatrix} = \begin{bmatrix} 2/3 & -1/3 & -1/3 \\ 0 & 1/\sqrt{3} & -1/\sqrt{3} \end{bmatrix} \begin{bmatrix} v_a \\ v_b \\ v_c \end{bmatrix} \quad (3.29)$$

3. Calculate the rotor flux space vector magnitude and position angle.
4. Transform stator currents to the d-q coordinate system using a Park transformation.

$$\begin{bmatrix} v_q \\ v_d \end{bmatrix} = \begin{bmatrix} \cos \theta_e & -\sin \theta_e \\ \sin \theta_e & \cos \theta_e \end{bmatrix} \begin{bmatrix} v_\alpha \\ v_\beta \end{bmatrix} \quad (3.30)$$

Where θ_e is the rotor position

5. The torque producing component (i_q) and flux producing component (i_d) of stator current are separately controlled.
6. The output stator voltage space vector is calculated using the decoupling block.
7. An inverse Park transformation transforms the stator voltage space vector back from the d-q coordinate system to the 2-phase system fixed with the stator.
8. Using the space vector modulation, the output 3-phase voltage is generated.

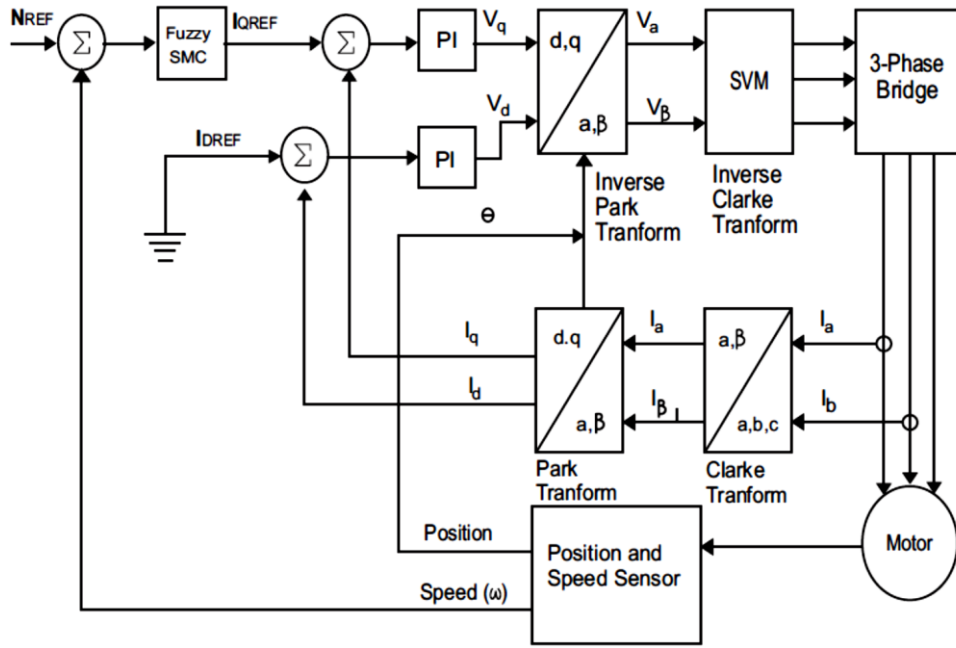


Fig 6.1 Block diagram of the vector control of PMSM

The block diagram of the vector control of PMSM using a suitable controller is shown in fig 6.1. Here the phase currents of the motor are measured and transformed to the direct axis and quadrature axis components (i_d and i_q) respectively by using Clarke and Park transforms. In order to make the PMSM system linear, the reference value of d axis current is set to zero. The actual i_d is compared with the reference i_d and the resulting error signal is given as the input to the i_d controller that generates the required value of v_d . Similarly the actual speed is compared with the reference speed and the corresponding error signal is given as the input to the speed controller that generate the reference i_q value. The actual i_q is compared with the reference i_q and the resulting error signal is applied to the i_q controller that generates the required value of v_q . From v_q and v_d thus generated, the required voltage is estimated by using inverse of Clarke and Park transforms. The triggering of the three phase bridge converter is established according to this voltage levels which in turn controls the speed of the motor by varying its stator voltage and frequency.

The PMSM control system by vector control is simulated for a 3.6 kW with motor parameters listed in table 6.1

Table 6.1 PMSM parameters

Motor Parameters	Value
Rated Power	3.6 kW
Rated phase to phase voltage	300V
Rated current	12A
Rated speed	1000 rpm
Rated torque	20 N m
No of poles	6
Stator Resistance (R)	0.129
Direct axis inductance (L_d)	0.00153 H
Quadrature axis inductance (L_q)	0.00153 H
Permanent magnet flux	0.1821 Wb
Moment of inertia (J)	0.003334Nms ² /rad
Viscous friction coefficient (B)	0.0004254Nms/rad

6.2 STABILITY ANALYSIS OF THE SYSTEM

Stability of the system model is ensured using Lyapunov stability theorem before considering the implementation of controllers. The state variables of the motor model are $x_1 = i_d$, $x_2 = i_q$, $x_3 = \omega_r$ and $x_4 = \theta_r$. The Lyapunov function, $V(x)$ that is positive definite and is selected as

$$V(x) = x_1^2 + x_2^2 + x_3^2 + x_4^2 \quad (5.1)$$

Then the derivative of the Lyapunov function is given by

$$\dot{V}(x) = 2x_1\dot{x}_1 + 2x_2\dot{x}_2 + 2x_3\dot{x}_3 + 2x_4\dot{x}_4 \quad (5.2)$$

By substituting the state variables and its derivatives in the above equation it is found that $\dot{V}(x) = -664312$ which is negative definite and hence, the system is stable according to Lyapunov stability criterion.

Controllability and observability tests are carried out for the model using Kalmans test using the controllability and observability matrices Q_C and Q_O respectively.

$$Q_c = [B \quad AB \quad A^2B \quad A^3B] = \begin{bmatrix} 653.5 & 5.5 \times 10^5 & 4.64 \times 10^8 & 3.951 \times 10^{11} \\ 0 & 1 & 1 & -1.53 \\ 0 & 0 & -1 & 1 \\ 0 & 0 & 0 & -1.53 \end{bmatrix}$$

$$Q_o = [C^T \quad A^T C^T \quad A^{T^2} C^T \quad A^{T^3} C^T] = \begin{bmatrix} 0 & 0 & -1.53 & 1.53 \\ 0 & 2.69 \times 10^3 & -2.753 \times 10^6 & -2.843 \times 10^9 \\ 1 & -1.53 & -1.7640 \times 10^6 & 1.487 \times 10^9 \\ 0 & 1 & 0 & 0 \end{bmatrix}$$

It is found that $|Q_C| = 999 \neq 0$ and $|Q_O| = 4.354 \times 10^9 \neq 0$ indicating its non-singular nature and rank of the matrix is 3 which is equal to the dimension of the system. Hence the system is completely state controllable and observable.

6.3 PI CONTROLLER

In order to compare the improvement in performance of FSMC, modified SMC Fuzzy PI controller, a conventional PI controller is also simulated. The PI controller parameters are selected using Ziegler- Nichols tuning method for the Quarter Decay Response (QDR) as described in chapter 4. For the PMSM system the ultimate gain K_u and the time period P_u are obtained as $K_u= 6.8$ and $P_u=0.14\text{sec}$ and the corresponding PI controller parameters are obtained as $K_p=3.1$ and $K_i= 33.2$.

6.4 FUZZY PI CONTROLLER

Constant values of proportional gain K_p and integral time T_i which are suitably varied using a fuzzy inference system to overcome the limitations of conventional PI controller. In this work the gain of the controller K_p is varied according to the error and the rate of error. The inputs to the fuzzy system are the error e and the rate of change of error \dot{e} and its output is the gain K_p . The input and output membership functions are shown in fig 6.2 (a) and (b) and 6.3 respectively. The universe of discourse is taken according to the maximum range variation of each variable and the fuzzy rules are given in table 6.2.

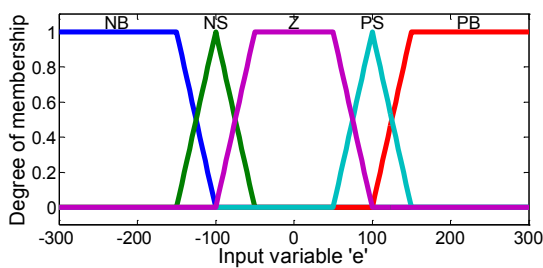


Fig 6.2 (a) Input membership function e

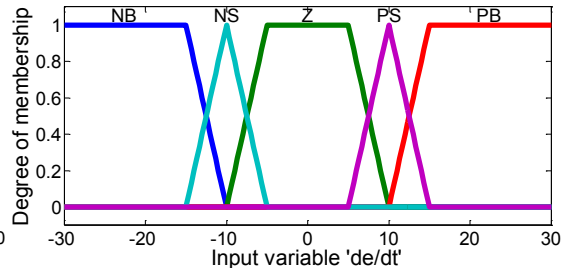


Fig 6.2 (b) Input membership function \dot{e}

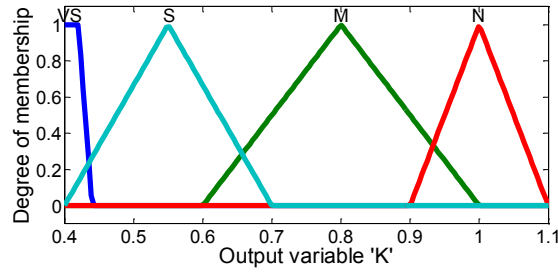


Fig. 6.3 Output membership function k

Table 6.2 Fuzzy Rules

\dot{e} \ e	NB	NS	Z	PS	PB
NB	VS	S	M	M	VS
NS	VS	S	N	M	VS
Z	VS	S	N	S	VS
PS	VS	M	N	S	VS
PB	VS	M	M	S	VS

6.5 MODIFIED SLIDING MODE CONTROLLER (SMC)

The Fuzzy SMC for the speed control of PMSM is designed by selecting suitable membership functions and fuzzy rules. The control law of chattering free SMC is $u = -ksat(s)$ as explained in section 5.1.2. The sliding surface is given by $s = \dot{e} + \lambda_1 e + \lambda_2 \int e dt$ where $\lambda_1, \lambda_2 > 0$ are a strictly positive real constant. The value of λ_1, λ_2 and k are selected as 8, 0.4 and 32.5 respectively by proper tuning. Also the value of ϕ is taken as unity.

6.6 FUZZY SMC (FSMC)

For designing the Fuzzy SMC, the error signal e and its rate of change \dot{e} are taken as the input to the fuzzy system and the value of k is selected as the output of the fuzzy system.

The input membership function for e and \dot{e} are given in fig 6.4 (a) and (b) respectively. Triangular and trapezoidal membership functions are used and the universe of discourse is taken as -200 to 200 for e and -10 to 10 for \dot{e} . The output membership function is shown in fig 6.5. Triangular and trapezoidal functions are used as output membership functions for defuzzification and the universe of discourse is taken as 0.5 to 1.8. The corresponding fuzzy rules are listed in table 6.3.

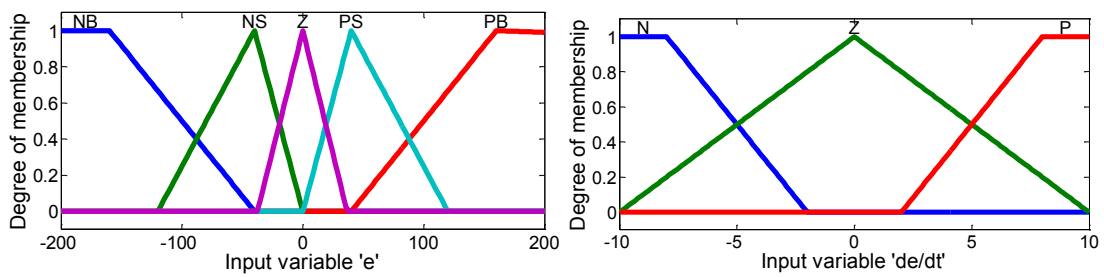


Fig. 6.4(a) Input membership function e Fig. 6.4 (b) Input membership function \dot{e}

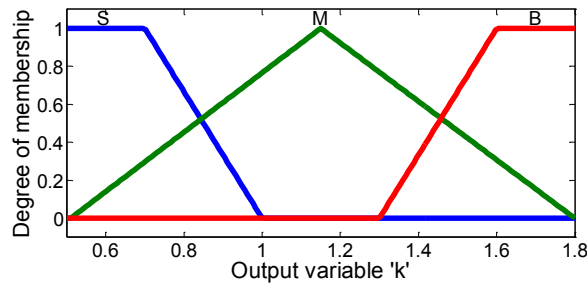


Fig. 6.5 Output membership function k

Table 6.3 Fuzzy Rules

$\dot{e} \backslash e$	<i>NB</i>	<i>NS</i>	<i>Z</i>	<i>PS</i>	<i>PB</i>
<i>N</i>	B	B	M	S	B
<i>Z</i>	B	M	S	M	B
<i>P</i>	B	S	M	B	B

6.6.1 Optimization of Controller Gain using Krill Herd Algorithm

In order to get the optimal values of controller gain to minimize rise time, peak overshoot, settling time and steady state error, Krill Herd algorithm is used which is explained in section 5.3.3. The objective function used to optimize the controller gain is $f(x) = 0.5t_r + 0.5t_s + 3.5M_p + \frac{1}{2}ss^2$ subjected to $0 \leq k \leq 46$ which ensures chatter free operation of the controller. The corresponding values of KH parameters are listed in table 6.4.

Table 6.4 Details of parameter values initialized in KH algorithm

KH Parameters	Value
Number of krills	30
Number of iterations	25
Foraging velocity	0.3
Inertia for foraging	0.4
Maximum diffusion	0.006
Maximum induced speed	0.2
Inertia for movement	0.1
Mutation	0.2

The values of the controller gain obtained using KH algorithm for various values of error are given in table 6.5. From the results, it is clear that optimal performance of the controller is achieved by varying the controller gain suitably according to the value of error.

Table 6.5 Optimized values of the controller gain

Error	Value of k
1000	36.15
800	35.16
500	33.25
100	31.67
50	29.32
10	27.85

6.7 RESULTS & DISCUSSION

The Fuzzy Sliding Mode Controller for the vector control of PMSM is simulated using MATLAB/Simulink and the results are compared with that of a modified chatter free SMC, conventional PI Controller and a fuzzy PI controller. The simulation is conducted on a 3.6 kW PMSM whose parameters are listed in Table 6.1. A load torque of 20 Nm is applied at 0.02 seconds after starting the motor. Fig 6.6 shows the step response of the system with Fuzzy SMC, chatter free SMC, fuzzy PI controller and conventional PI controller for a reference speed of 1000 rpm. Fig 6.7 shows the speed variation of the PMSM under loaded condition. The performances of all four controllers are compared and are detailed in table 6.6. The rise time is 4ms with FSMC and it is 6ms, 5ms and 5ms with chatter free SMC, Fuzzy PI and conventional PI controller respectively. The settling time is improved to 4ms with FSMC whereas the corresponding values with chatter free SMC, Fuzzy PI and conventional PI controllers are 6ms, 8ms and 12ms respectively. The peak overshoot is completely eliminated with FSMC and SMC which is 16% and 19.8 % with Fuzzy PI

and conventional PI controller respectively. The steady state error is the minimum of 0.04% with FSMC that is 0.06%, 0.07% and 0.1% respectively with chatter free SMC, Fuzzy PI and conventional PI controllers. It is also observed that the speed variation when sudden load is applied is only 0.7% with FSMC while the corresponding values are 1.7%, 1.7% and 2% respectively with chatter free SMC, Fuzzy PI and conventional PI controllers. It is clear from the results that the transient and steady state performance of the fuzzy PI controller is improved from that of the PI controller in terms of its peak overshoot and settling time. This improvement is achieved by suitably varying the controller gain within the selected range using FIS. SMC with modified control law gives a satisfactory output performance; a great improvement in output is achieved using a FSMC even though the control algorithm becomes more complex and difficult to implement.

The variation of controlled variable (speed) vs. the manipulated variable (current) is shown in fig.6.8. Rated load is applied at 0.02s and it is observed that in order to keep the controlled variable (speed) constant, the manipulated variable (current) is suitably adjusted by the controller according to the change in load.

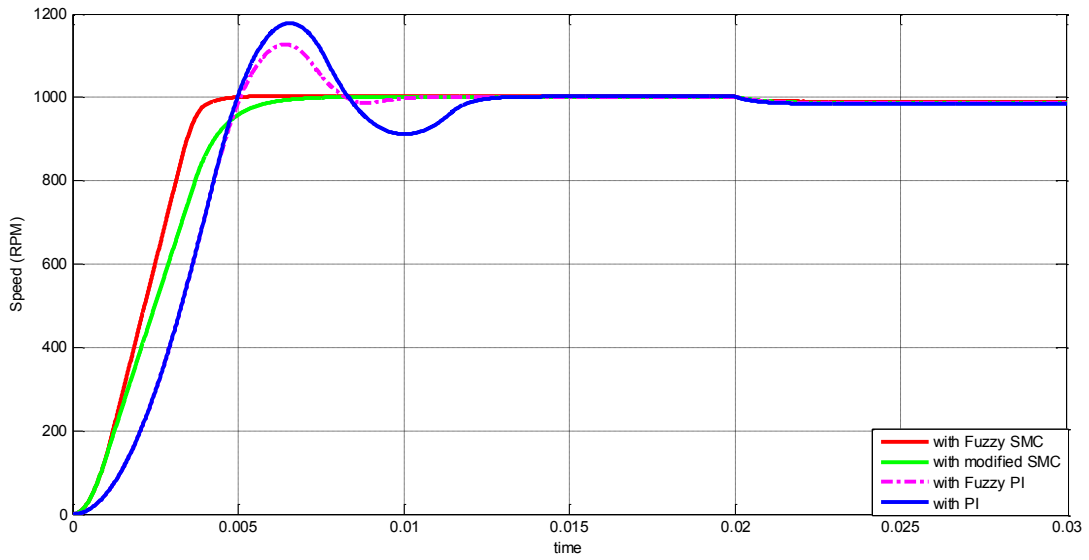


Fig. 6.6 Step response of PMSM with various controllers

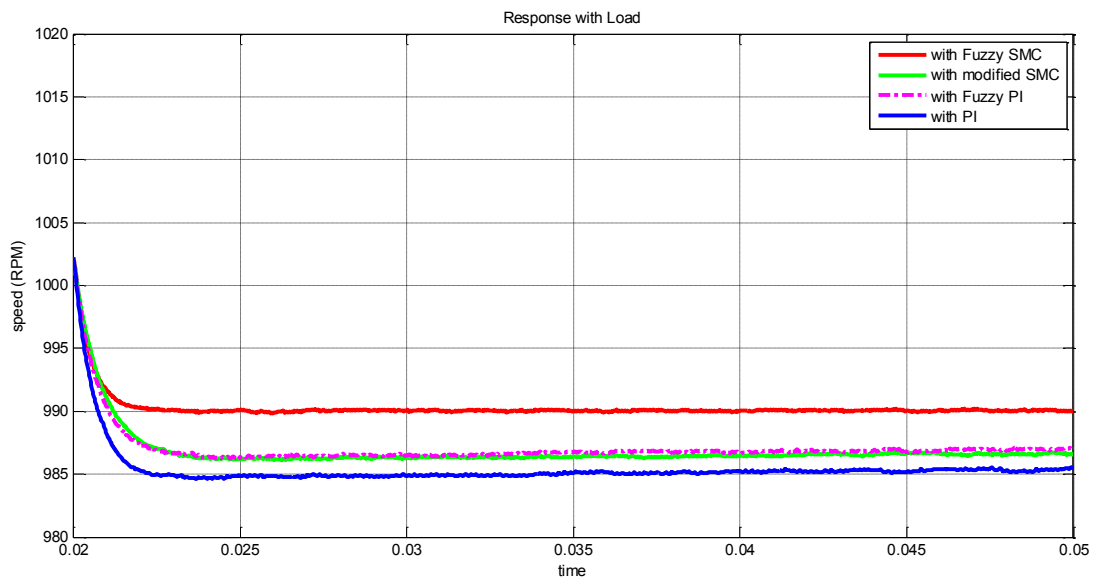


Fig. 6.7 Speed variation of PMSM under loaded condition

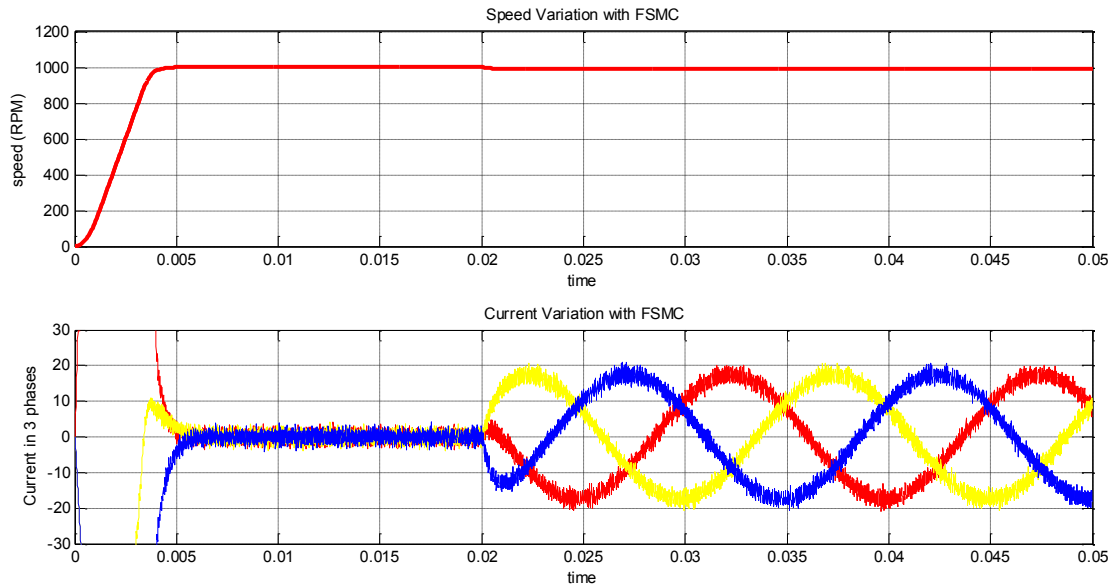


Fig. 6.8 Speed and Current variation of PMSM with FSMC

Table 6.6 Performance comparison

	Fuzzy SMC	Modified SMC	Fuzzy PI	PI
Rise time (ms)	4	6	5	5
Peak overshoot (%)	0	0	16	19.8
Settling time (ms)	4	6	8	12
Steady state error (%)	0.04	0.06	0.07	0.1
Speed Variation with rated load (%)	0.7	1.7	1.7	2

The PI controllers are very simple to design, easy to implement and also produce satisfactory performance under undisturbed conditions. But the performance is poor under disturbed condition like sudden changes in the reference speed and sudden variation load. PMSM with PI controller shows large overshoot, high settling time and comparatively large speed variation while loading. The output in terms of settling time and peak overshoot are improved by using a FIS integrated to PI controller that helps to achieve variable gains. But with this controller the speed variation while

loading becomes large and makes it unsuitable in many applications. The peak overshoot is completely eliminated with chatter free SMC where the control law is $u = -ksat(s/\phi)$ in which the controller gain k is constant. High values of k gives fast response of the system but results in high overshoot and also produce chatter. Low values of k reduce the effect of chattering and overshoot but results in slow speed of response. In order to get fast response without chattering and overshoot, the controller gain k is varied according the change in error signal using an FIS.

Fuzzy Sliding Mode Controller combines the intelligence of fuzzy logic with the modified SMC in which the controller gain k is appropriately varied using a fuzzy system. The peak overshoot is completely eliminated and the rise time and settling time are improved by the use of Fuzzy SMC for the speed control of PMSM. Speed variation while loading is also negligibly less with Fuzzy SMC.

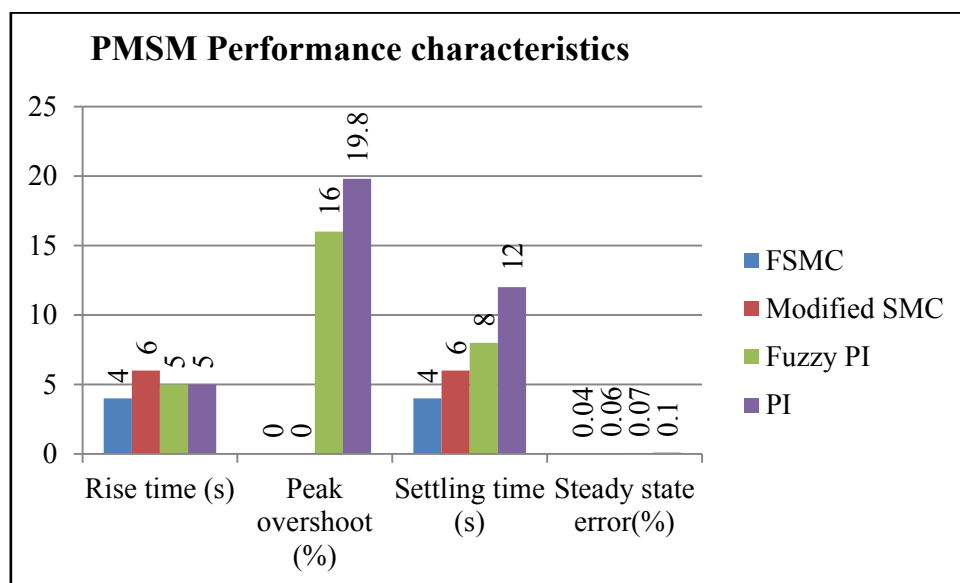


Fig.6.9 Comparison of performance indices of PMSM using FSMC, Modified SMC, Fuzzy PI and PI controllers

Comparison of rise time, peak overshoot, settling time and steady state error of PMSM using proposed FSMC, Modified SMC, Fuzzy PI and PI controllers are shown in fig. 6.9. It can clearly be observed that the improvement in performance of the proposed controller compared to other selected controllers is highly appreciable.

CHAPTER 7

FPGA IMPLEMENTATION OF CONTROL ALGORITHM IN INDUSTRIAL DRIVES

For the realization of any designed controller, Application Specific Integrated Chip (ASIC) and Field Programmable Gate Array (FPGA) provide a good solution for the hardware implementation. FPGA is a large-scale integrated circuit, for which the hardware configuration can be changed by programming after it is manufactured, whereas the ASIC like Digital Signal Processor (DSP) has a predetermined, unchangeable hardware function. The term "field-programmable" indicates that the hardware configuration of the device can be programmed in the field and the term "gate array" refers to a cluster of logic gates in an integrated chip. FPGA are semiconductor devices that are based around a matrix of configurable logic blocks (CLBs) connected via programmable interconnects for desired applications or functionality requirements and this feature makes it an ideal choice for different industrial applications (Mitra *et al.*, 2018; Lupon *et al.*, 2014).

FPGA configuration is generally specified using a hardware description language (HDL). The most popular HDL are Very High Speed Integrated Chip Hardware Description Language (VHDL) and Verilog. These two languages are standardized and provide the description with different levels and are portable and compatible with all FPGA technologies previously introduced. The speed, size and the number of inputs and outputs of a modern FPGA far exceeds that of a microprocessor or DSP processor.

The interest of FPGA technology is growing due to its applications in various fields such as telecommunication (Solanakis *et al.*, 2013), video signal processing (Meng *et al.*, 2005), embedded control systems (Shi *et al.*, 2009), and electric vehicle control systems (Poorani *et al.*, 2005). Presently, the density of FPGA components can achieve the equivalent of 10 million logic gates with switching frequencies of around 50MHz and this allows the implementation of complex algorithms in controls systems with very fast response time and hence makes it suitable for applications in drive systems used for industrial automation.

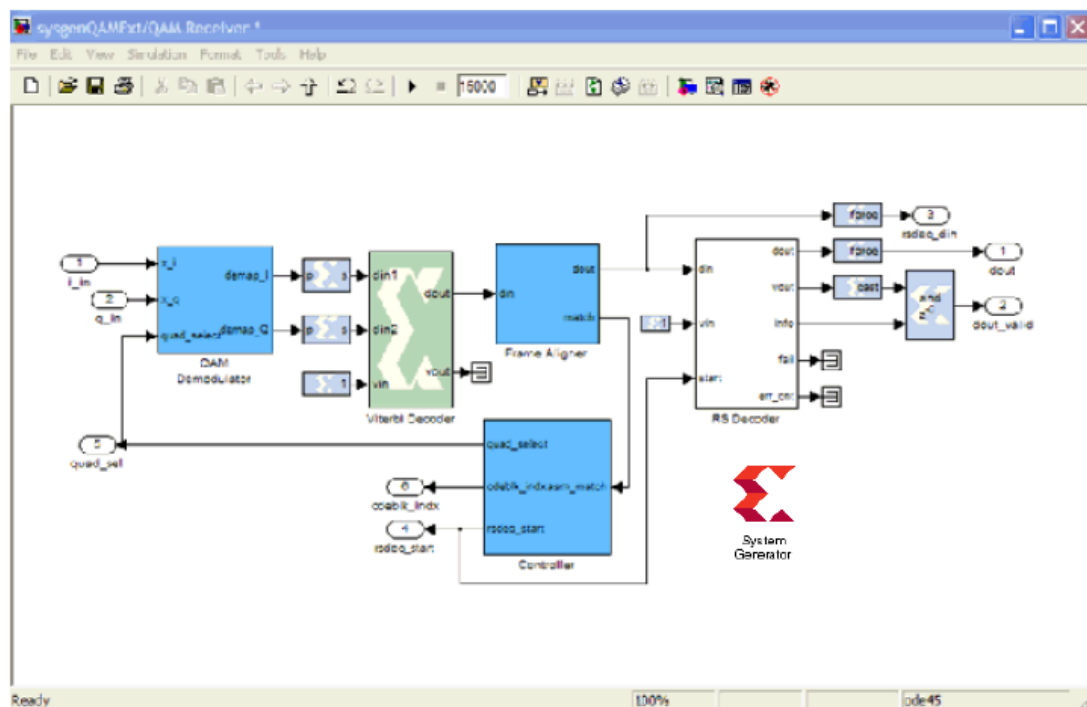


Fig. 7.1 Xilinx System generator window

The leading manufacturers of FPGA are Xilinx, Altera, Actel etc., out of these Xilinx is the most popular one. Software developed by Xilinx, Xilinx System Generator and Xilinx ISE design suite can be deployed for the implementation of Simulink models on the FPGA board. Xilinx System Generator is a DSP design tool from Xilinx that

enables the use of the Mathworks model-based Simulink design environment for FPGA design. All the downstream FPGA implementation steps including synthesis, place and route are automatically performed to generate an FPGA programming file. Over 90 DSP building blocks are provided in the Xilinx DSP block set for Simulink that include the complex DSP building blocks such as forward error correction blocks, FFTs, filters and memories in addition to the common ones such as adders, multipliers and registers. The window of a Xilinx system generator is shown in fig 7.1. This window contains the system generator token in the Simulink environment which is used for all the setting and other blocks like black box, counter, multiplier etc. The black box is used for including VHDL programs in the Simulink environment and the other system generator blocks can also be used along with Simulink by using the system generator. The required controller can be implemented using the proper interconnection of these building blocks and the VHDL code for programming the FPGA board can be generated.

7.1 IMPLEMENTATION OF MATLAB AND SIMULINK ALGORITHMS ON FPGAS

Matlab/Simulink algorithms are translated to VHDL using either a HDL Coder or a Xilinx system generator. In the former case the VHDL generated from the simulated model using Simulink and the HDL Coder is used to prototype the FPGA. The second method uses Xilinx System Generator that is based on Mathworks model-based Simulink design environment. In this work the second method is adopted due to its user friendly approach and efficiency. Also writing programs for complex algorithms in VHDL is computationally expensive and can lead to errors that need further verification before implementing and hence the application of Xilinx System

Generator is often used for the design of FPGA. Here the VHDL program is generated using Xilinx system generator and is transferred to the FPGA board using the Xilinx ISE Design suite.

Hardware Implementation of the control algorithm using Xilinx System Generator involves the following steps

- Develop the model using Xilinx System Generator blocks in Simulink
- Generate the VHDL Program
- Connect the FPGA board to system using J-Tag
- Program the FPGA board using Xilinx ISE Design Suite
- Implement Hardware in Loop Simulation (Hardware Co-Simulation)
- Assign the input and output pins using Xilinx ISE Design Suite for the actual Hardware implementation
- Connect the assigned pins to hardware components like inverter and sensors

7.2 IMPLEMENTATION OF CONTROLLER ON FPGA

Xilinx Virtex 4 FPGA board is used for the implementation of the designed and simulated FSMC, chatter free SMC and PI controllers. As the algorithm of fuzzy PI controller are complex and the output results are not as efficient as chatter free SMC, further analysis is carried out only using FSMC, modified SMC and PI controllers. Algorithms of these controllers are executed in Matlab/Simulink environment using Xilinx System Generator first and then it is translated automatically into VHDL programming language. This program is then embedded into the Xilinx FPGA application board.

7.3 HARDWARE IN THE LOOP SIMULATION

Hardware in the loop (HIL) or Hardware co-simulation is a concept that as revealed by the name uses the hardware in the simulation loop. Using this, the actual controller behaviour of the model of the drive system is tested and their outputs are verified. The VHDL code for the FPGA is generated using Xilinx System generator and the program is embedded with FPGA board using the Xilinx ISE design suite. The FPGA board is interfaced with the computer using the J-tag interface. After programming the board, the HIL simulation is conducted using the Xilinx System generator. The arrangement for the hardware in loop simulation is shown in fig. 7.2.

In HIL simulation, the computation of the controller part is executed by the FPGA board and the simulation of other parts like converter, motor, sensor are carried out in the Simulink environment of the PC.

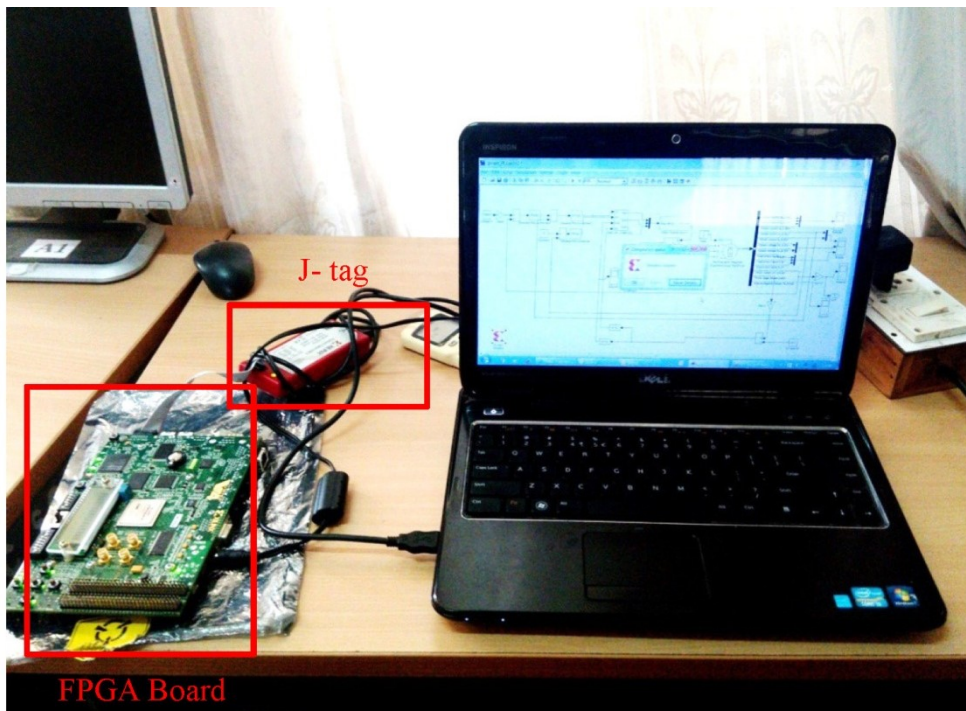


Fig. 7.2 Arrangement for the hardware in loop simulation

7.3.1 Hardware in the loop (HIL) Simulation for the speed control of PMSM

The block diagram for the FPGA implementation of FSMC for the speed control of PMSM is shown in fig. 7.3. The motor is fed by an inverter from a rectifier. The inputs to the FPGA board are the signals from speed and position sensors and two phase currents of the motor. The output of FPGA board is the PWM signals for the inverter corresponding to the reference speed.

HIL simulation for the vector control of PMSM is carried out using FPGA for FSMC, chatter free SMC and PI controllers. From the simulation results it is clear that the performance of Fuzzy PI is not greatly improved from that of conventional PI controller and hence only PI controller is considered instead of Fuzzy PI controller for HIL simulation. The rated load of 20 Nm is applied at 0.02 seconds after starting the motor. The performance comparison of FSMC obtained from HIL simulation with that of Simulink simulation is shown in fig. 7.4. Similar analysis is also carried out for modified SMC and PI controller and is shown in fig 7.5 and 7.6 respectively. The comparison of the transient response of all three controllers using HIL simulation and Simulink simulation is tabulated in table 7.1.

The rise time obtained with HIL simulation for FSMC, modified SMC and PI controller are 6ms, 8ms and 9ms respectively whereas the corresponding values are 4ms, 7ms and 8ms respectively with Simulink simulation. The rise time obtained is slightly higher for HIL simulation than that of Simulink simulation and it is due to the fact that the FPGA uses fixed point variables for its computation whereas floating point variables are used in Simulink. The peak overshoot is found to be negligible

with FSMC and modified SMC for both HIL simulation and Simulink simulation and the corresponding values for PI controller are 19% and 19.8% respectively. The Settling time obtained is 6ms, 8ms and 18ms respectively with FSMC, modified SMC and PI controllers for HIL simulation whereas these values are 4ms, 7ms and 14ms respectively for Simulink simulation. The values of steady state error are 0.06%, 0.08% and 0.12% respectively with FSMC, modified SMC and PI controllers for HIL simulation whereas these values are 0.04%, 0.06% and 0.1% respectively for Simulink simulation. Also the speed variation while loading is 0.7%, 1.8% and 2.2% respectively with HIL simulation for FSMC, modified SMC and PI controllers and the corresponding values with simulation are 0.7% , 1.7% and 2% respectively. From the results it can be observed that the values obtained for rise time, peak overshoot, settling time and speed variation due to loading with HIL simulation and simulation are almost comparable and the slight variation are mainly due to the fixed point variables used in the FPGA.

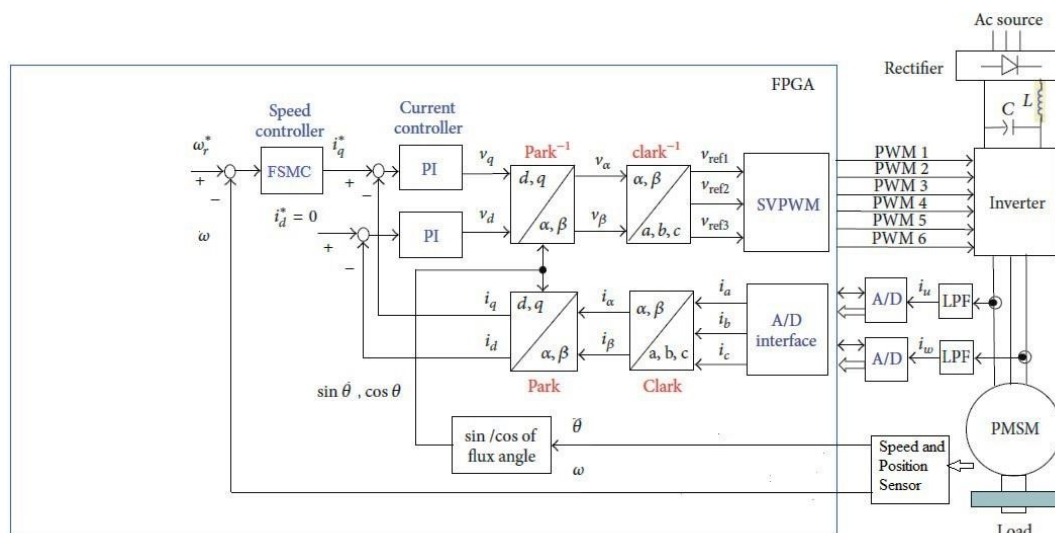


Figure 7.3 Block diagram of FPGA implementation of FSMC for the speed control of PMSM

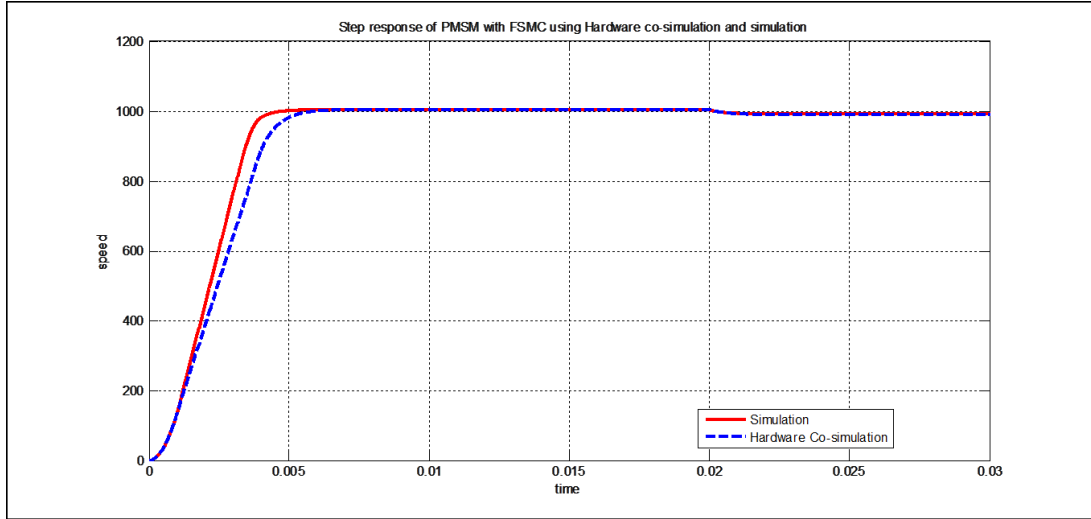


Fig. 7.4 Step response of PMSM with FSMC using HIL simulation and Simulink simulation

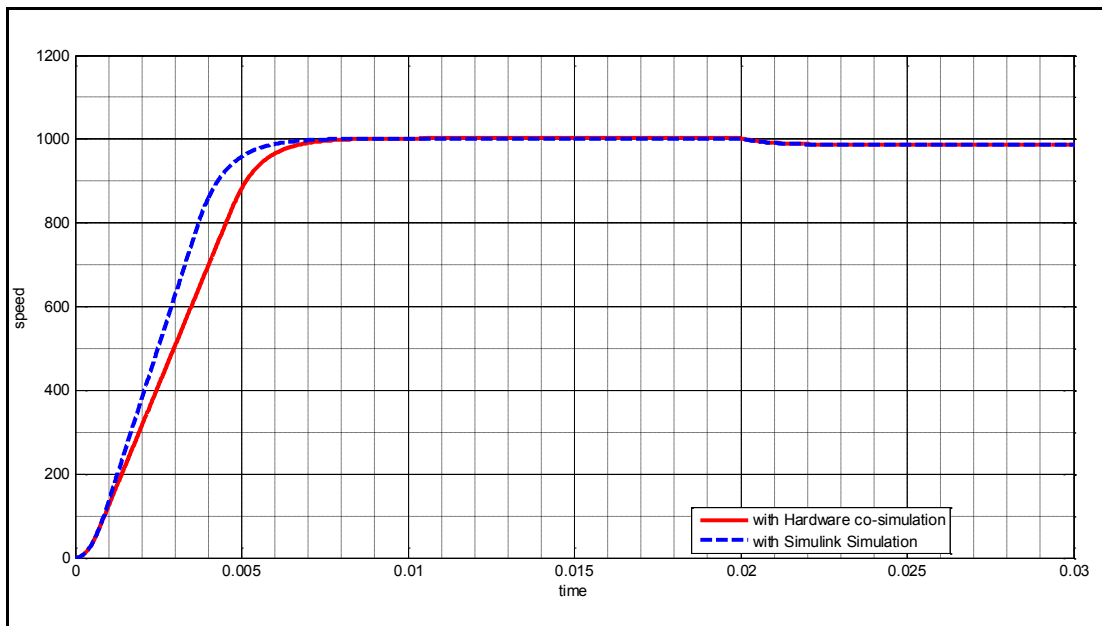


Fig. 7.5 Step response of PMSM with SMC using HIL simulation and Simulink simulation

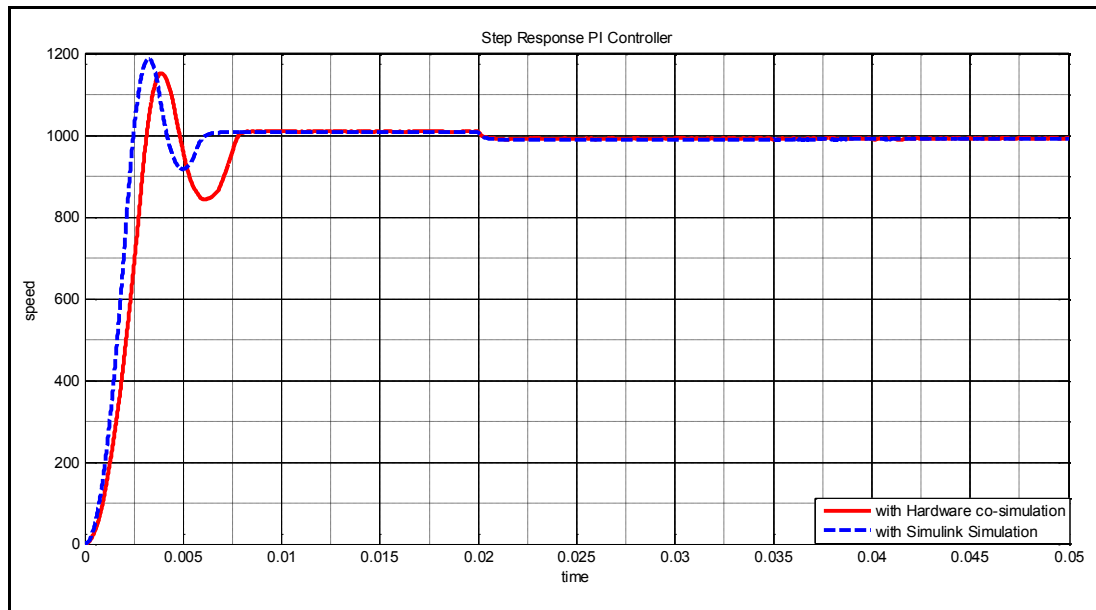


Fig. 7.6 Step response of PMSM with PI controller using HIL simulation and Simulink simulation

Table 7.1 Performance comparison of PMSM in HIL simulation and Simulink simulation

	Fuzzy SMC		Modified SMC		PI Controller	
	HIL simulation	Simulink simulation	HIL simulation	Simulink simulation	HIL simulation	Simulink simulation
Rise time (ms)	6	4	8	7	9	8
Peak overshoot (%)	0	0	0	0	19	19.8
Setting time (ms)	6	4	8	7	18	14
Steady state error	0.06	0.04	0.08	0.06	0.12	0.1
Speed variation while loading (%)	0.7	0.7	1.8	1.7	2.2	2

7.3.2 Hardware in the loop Simulation for the speed control of BLDC

The block diagram for the hardware implementation and HIL simulation of FSMC for the speed control of BLDC motor is shown in fig 7.7. The motor is supplied by a DC source through an inverter which is driven by the FPGA board. The input to the FPGA board is the signals from the Hall Effect sensors embedded with the BLDC motor corresponding to the rotor position of the motor and its output is the firing pulses applied to the inverter through a driver cum isolator circuit. The control algorithm is completed in Matlab/ Simulink environment using Xilinx System Generator block sets and is translated to VHDL programming language which is embedded into the Xilinx Virtex 4 FPGA application board. The HIL simulation of FSMC is conducted and the comparison of the step response with that of Simulink simulation is shown in fig. 7.8. The HIL simulation of the chatter free SMC and PI controllers are also carried out and the comparison with that of Simulink simulation is shown in fig 7.9 and 7.10 respectively. The performance indices of HIL simulation and Simulink simulation of all three controllers are listed in table 7.2.

The rise time from HIL simulation is obtained as 13ms, 19ms and 30ms with FSMC, modified SMC and PI controllers respectively whereas the corresponding values are 8ms, 15ms and 25ms respectively with Simulink simulation. From the results it is observed that the values are slightly higher for HIL simulation than that of Simulink simulation and this is due to the fact that the FPGA uses fixed point variables for its computation whereas floating point variables are used for the Simulink simulation. The peak overshoot is negligible with FSMC and modified SMC for both HIL

simulation and conventional Simulink simulation and corresponding values for PI controller are found to be 5.8% and 1.8% respectively. The values of settling time with HIL simulation are 13ms, 19ms and 40ms respectively with FSMC, modified SMC and PI controllers whereas the values with simulation are 8ms, 15ms and 43ms respectively. The speed variation while loading with HIL simulation are 1%, 3% and 5% respectively for FSMC, modified SMC and PI controllers whereas values obtained with simulation are 0.1%, 3% and 5% respectively. The steady state error with HIL simulation are 0.03%, 0.05% and 0.08% respectively for FSMC, modified SMC and PI controllers whereas corresponding values obtained with simulation are 0.02% , 0.04% and 0.06% respectively. The rise time and settling time are slightly increased with hardware co-simulation and the other performance indices are almost comparable. From the results obtained, it can be observed that the rise time, peak overshoot, settling time and speed variation due to loading with HIL simulation and Simulink simulation are almost comparable and the slight variation of the values are mainly due to the fixed point variables used in the FPGA. It is also clear from these results that FSMC outperform the other two controllers for its transient as well as steady state behaviour. Moreover, the speed variation with sudden changes in load is also negligibly less for FSMC. Hence it is desirable to analyse the performance of BLDC motor using the FSMC implemented for its speed control.

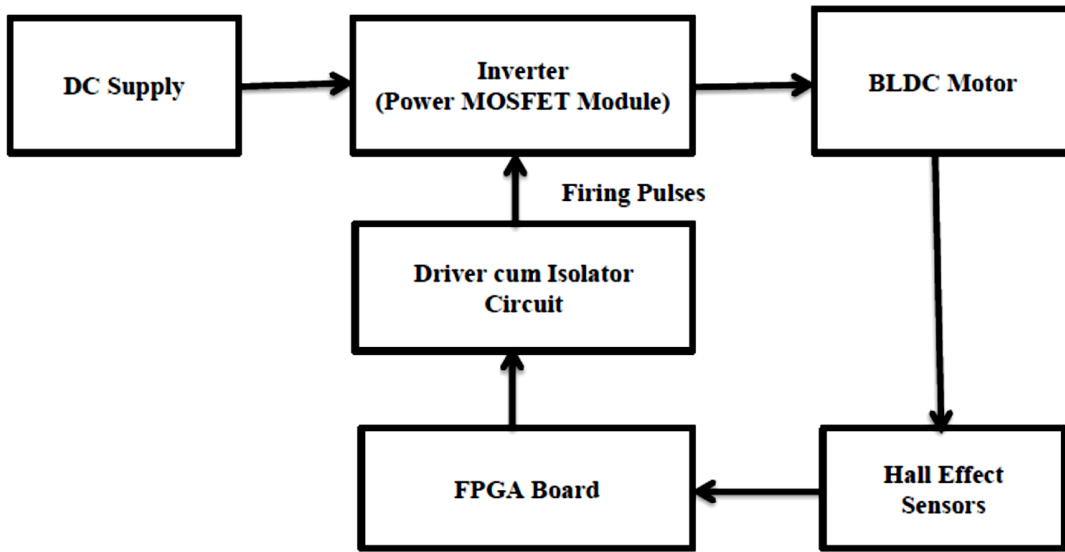


Fig 7.7 Block diagram of hardware implementation for the speed control of BLDC motor using FPGA

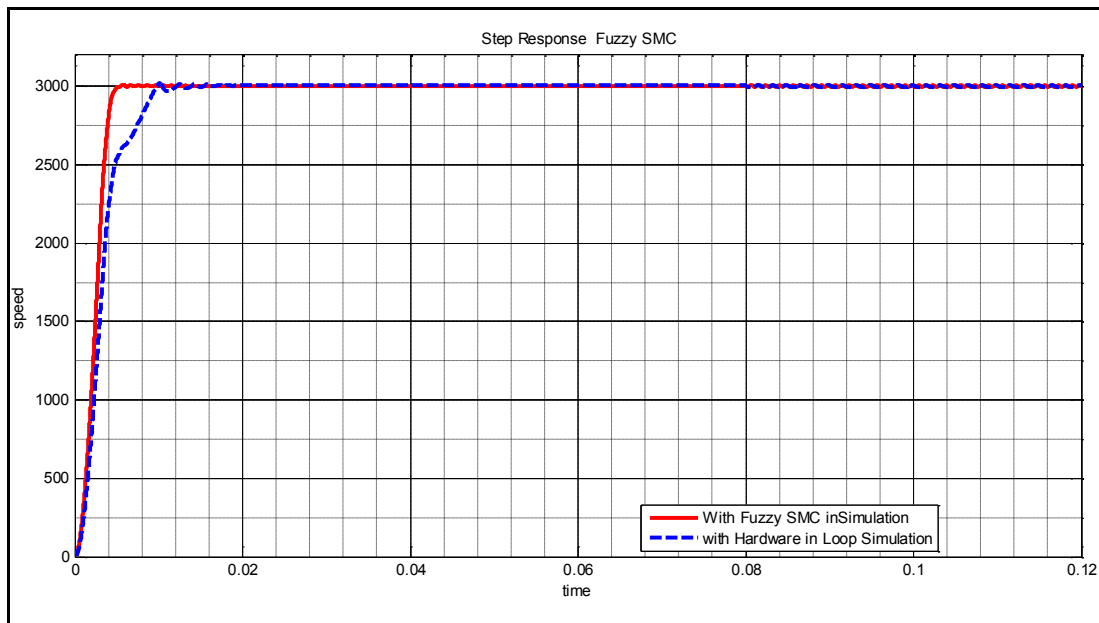


Fig. 7.8 Step response of BLDC motor with FSMC using HIL simulation and Simulink simulation

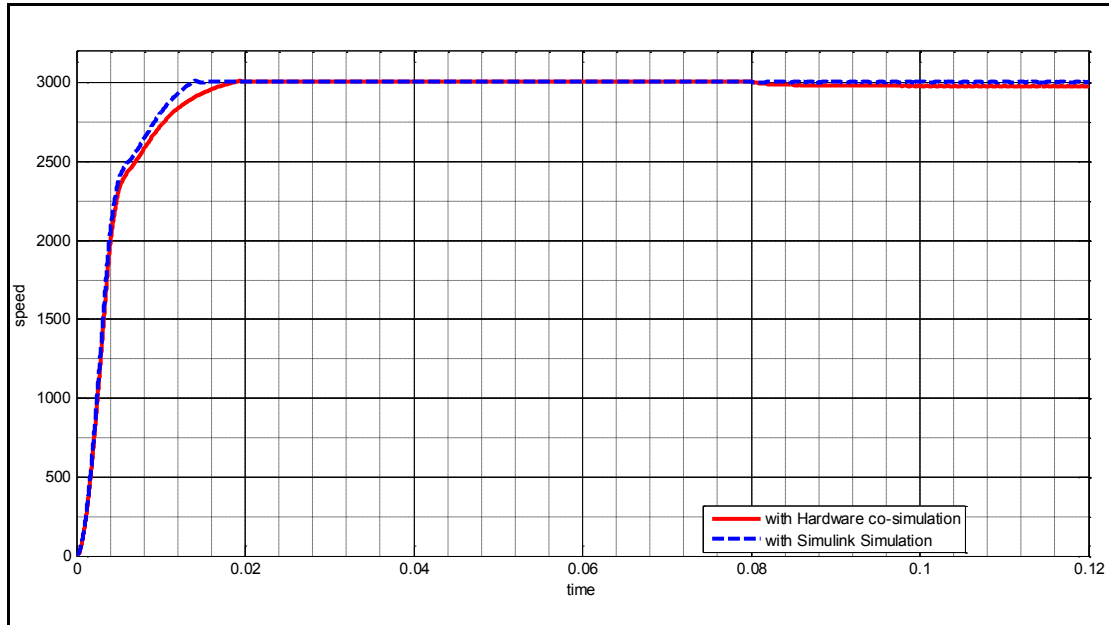


Figure 7.9 Step response of BLDC motor with SMC using HIL simulation and Simulink simulation

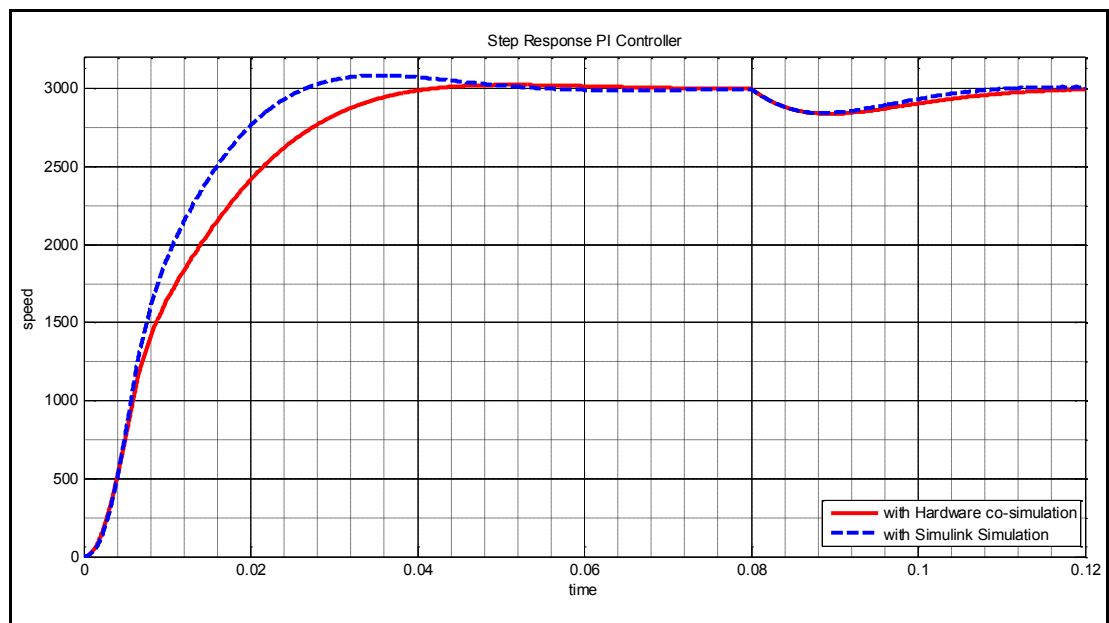


Figure 7.10 Step response of BLDC motor with PI controller using HIL simulation and Simulink simulation

Table 7.2 Performance comparison of BLDC motor in HIL simulation and Simulink simulation

	Fuzzy SMC		Modified SMC		PI Controller	
	HIL simulation	Simulink simulation	HIL simulation	Simulink simulation	HIL simulation	Simulink simulation
Rise time (ms)	13	8	19	15	40	25
Peak overshoot (%)	0	0	0	0	5.8	1.8
Settling time (ms)	13	8	19	15	40	43
Steady state error	0.03	0.02	0.05	0.04	0.08	0.06
Speed variation while loading (%)	0.28	0.25	3	3	5	5

7.4 HARDWARE IMPLEMENTATION OF FSMC OF BLDC

The block diagram for the hardware implementation of FSMC for the speed control BLDC motor is carried out as per the block diagram shown in fig 7.7. The BLDC motor is supplied using a three phase power MOSFET inverter circuit which is controlled by the PWM signals from the Xilinx FPGA chip. The speed and position of rotor are measured from the signals of Hall Effect sensors embedded in the motor. The input to the inverter is 24V DC generated from 230 V, 50 Hz AC supply by using a transformer, rectifier and filter. The circuit diagram of the inverter is shown in fig.7.11.

The signals from the Hall Effect sensors are used for the measurement of the motor speed and for the electronic commutation. The PWM pulses generated corresponding to the control action using FPGA are applied to a driver circuit. The function of the

driver circuit is to amplify the PWM pulses and to give electrical isolation between the FPGA board and the gate of the MOSFETs. The driver circuit shown in fig. 7.12 uses the TPL 250 opto-coupler IC for the electrical isolation. The output of each driver is given to the gate of corresponding power MOSFET. Fig. 7.13 shows the complete hardware setup for the implementation of FSMC for the speed control of the BLDC motor. The motor is run at its rated speed of 3000 rpm and a load of 0.16 Nm is applied at 0.08s after starting. From step response, the transient as well as steady state performance analysis of the motor is carried out.

7.5 RESULT AND DISCUSSION

HIL simulation of FSMC, modified SMC and PI control of PMSM and BLDC motor are carried out using FPGA and their performance are compared with corresponding results obtained from Simulink simulation. From the results obtained it is clear that the performance of FSMC is greatly improved when the control law of conventional SMC is modified using saturation function and the gain is made variable using FIS. Hence the hardware for the FSMC is designed and implemented using FPGA for the speed control of BLDC motor. The performance obtained from the actual hardware implementation is compared with that of HIL simulation as well as Simulink simulation.

Step response of the performance of FSMC using real implementation, HIL simulation and Simulink simulation for the speed control of BLDC motor is shown in fig. 7.14. Fig. 7.15 shows the corresponding speed variation with rated load applied to it. The comparison of various performance indices is shown in the table 7.3. The rise

time and settling time obtained with actual FSMC implemented on the motor are 15ms each whereas the values with HIL simulation are 13ms each and these results are very much comparable. The peak overshoot is negligible in all three cases. The steady state error observed for the real hardware is 0.05% whereas it is 0.03% and 0.02% respectively with HIL simulation and Simulink simulation. The speed variation while loading is 0.33% with original hardware which is 0.28% with HIL simulation and 0.25% with Simulink simulation. From the experimental results it is observed that the performance indices are almost similar with the simulation and HIL simulation which validate the design of FSMC for the speed control of BLDC motor. Even though these results are comparable, the values obtained from the hardware setup are slightly higher than that of HIL simulation and Simulink simulation. This is due to the small variation of actual parameter from that of the designed values. Also the variation is due to the fact that FPGA uses fixed point variables for both HIL simulation and hardware implementation while floating point variables are used for Simulink simulation.

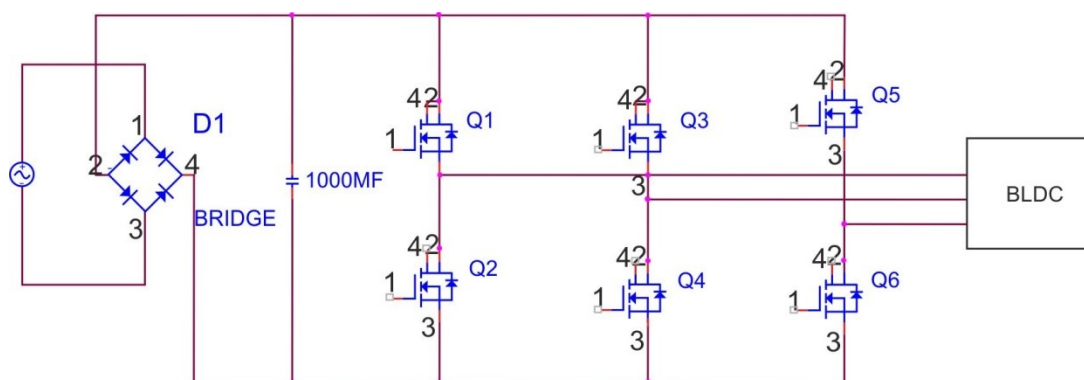


Fig .7.11 Circuit diagram of 3 phase inverter

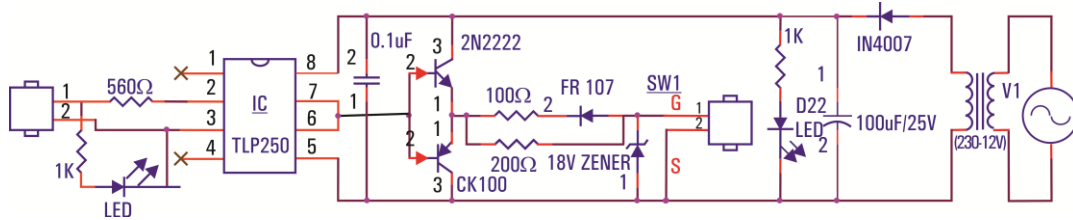


Fig 7.12 Driver cum isolation circuit

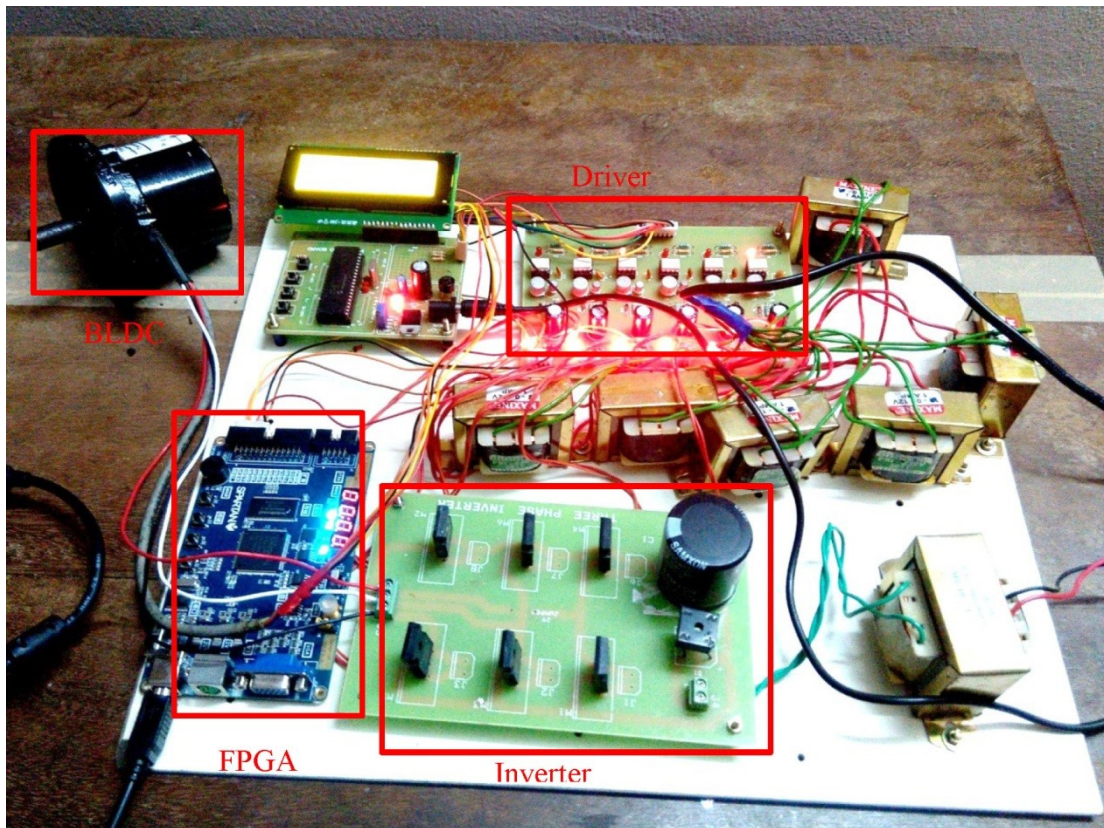


Fig 7.13 The Hardware setup for the speed control of BLDC motor using FSMC

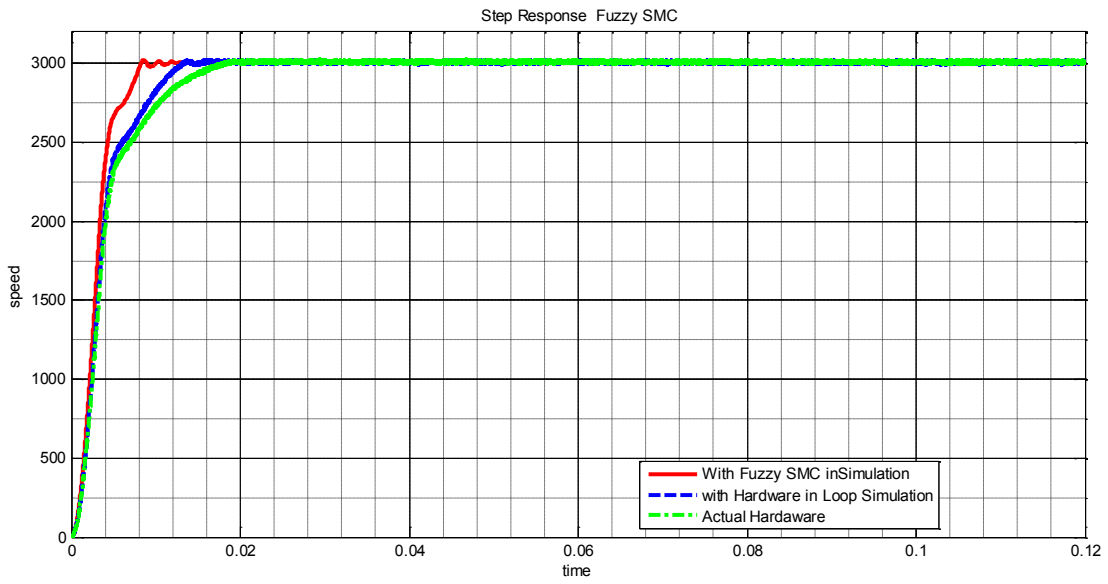


Fig 7.14 Step Response of Hardware, HIL simulation and Simulation of BLDC motor

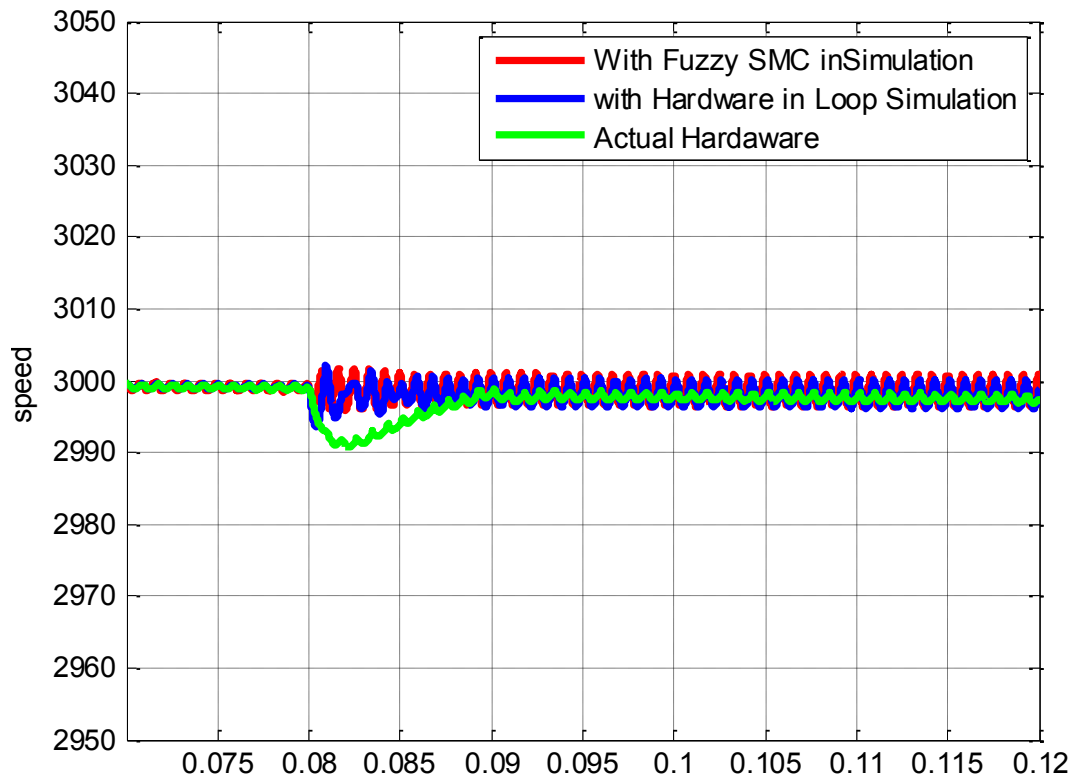


Fig. 7.15 Speed variation of BLDC motor when load is applied at 0.08 s with Hardware, HIL simulation and Simulation

Table 7.3 Performance comparison of Simulink simulation HIL Simulation and actual hardware

	Simulink Simulation	HIL Simulation	Actual Hardware
Rise time (ms)	8	13	15
Peak overshoot (%)	0	0	0
Settling time (ms)	8	13	15
Steady state error	0.02	0.03	0.05
Momentary Speed while variation while loading (%)	0.25	0.28	0.33

CHAPTER 8

CONCLUSION AND FUTURE DIRECTIONS

Advanced manufacturing and automation in industries require high precision and accuracy in machining which in turn demands fast and efficient speed control technique for the drive system used in it. Conventional DC servo motor, BLDC motor, SRM and PMSM are popularly used as special electric drives in aerospace, antenna positioning, solar tracking, electric and hybrid electric vehicle and robotics. Speed control of electric machines has become very efficient and popular with the introduction of power converters using power electronic switches, capable of converting the power from AC to DC and vice-versa. Nonlinear models incorporating the saturation effect of the magnetic core of these motors are more precise than their corresponding linear models. Hence various efficient speed control techniques are designed for these models and simulated to identify the most suitable controller and realized it using FPGA for the selected motors.

8.1 CONCLUSIONS

Nonlinear models of DC servo motor, BLDC motor, SRM and PMSM are developed and their stability is ensured using Lyapunov theorems. The system's controllability and observability are also verified using Kalman's test. FSMC, chatter free SMC, conventional PI controller and Fuzzy PI controller are designed for each of these models and their transient and steady state behaviour under no load as well as loaded condition are evaluated.

- **DC servo motor:** Position control of DC servo motors are widely used in industrial systems, such as robotic manipulators and servo systems like antenna positioning and solar tracking because of their relatively simple control and reliability for a wide range of operating conditions. FSMC, chatter free SMC, FLC, Fuzzy PI controller and conventional PI controller are designed and simulated for the nonlinear model of the DC servomotor for its position control . From the results it is observed that the rise time, peak overshoot and settling time are improved with Fuzzy PI controller than that of conventional PI controller. The peak overshoot is completely eliminated and settling time is reduced with FLC, but it has increased rise time. A conventional SMC, that has high frequency chattering effect in the output, is modified using a saturation function in the control law to eliminate the unwanted oscillations. With this modified SMC the peak overshoot is completely eliminated and it provides improved rise time and settling time than that of FLC, Fuzzy PI and PI controllers. Further improvement in the transient performance characteristics is achieved using FSMC in which the controller gain of chatter free SMC is varied with in an optimized range using FIS.

The speed control of DC motor is used in numerous applications such as rolling mills, cranes, hoists, elevators, machine tools and locomotive drives. All the above controllers are designed and simulated for the speed control of DC servomotor also. From the simulation results it is observed that rise time, peak overshoot, settling time, steady state error and speed variation while loading are improved with Fuzzy PI controller than that of conventional PI controller. Even though the modified SMC has increased rise time, all other

steady state and transient parameters are improved and peak overshoot is completely eliminated. It is clear that FSMC outperforms all of these controllers in terms of its rise time, peak overshoot, settling time, steady state error and speed variation while loading.

- **Switched Reluctance Motor (SRM):** Simplicity, ruggedness, and low cost of a SRM makes it a viable candidate for various general-purpose, adjustable-speed and servo type applications. The mathematical model of SRM is inherently nonlinear due to the coupling effect of its state variables. Performance comparison of the speed control of SRM using FSMC, chatter free SMC, Fuzzy PI controller and conventional PI controller is carried out. The results indicate that all the transient as well as steady state performance are improved with Fuzzy PI controller compared with that of conventional PI controller and is further enhanced by the modified SMC in its speed variation while loading. Finally it is observed that all the performance indices and the speed variation while loading is greatly improved with FSMC as compared with all other controllers, making it more suitable for industrial applications.
- **Brushless DC motor (BLDC):** BLDC motors are increasingly gaining importance in various application fields such as aerospace, automotive, medical, industrial and consumer equipment, machine tool, fans and hybrid electric vehicles. The mathematical model of BLDC motor is inherently nonlinear due to its trapezoidal back EMF. FSMC, chatter free SMC, Fuzzy PI controller and conventional PI controller are designed and simulated for the speed control of BLDC motor and the performance comparison is carried out. From the results it

is clear that all the transient as well as steady state performance are improved with Fuzzy PI controller than that of conventional PI controllers. The speed variation with sudden application of rated load is also improved with this controller. A further improvement in the performance characteristics and speed variation with sudden loading is obtained using modified SMC. Finally the design of FSMC, optimized using KH algorithm to vary the gain of modified SMC using FIS in a suitable range, to obtain an outstanding performance is carried out. This controller outperforms all other controllers in terms of all the steady state and transient performance indices including its speed variation with sudden loading and becomes an excellent choice among the other ones. FSMC algorithm is implemented using FPGA and its performance is evaluated using both HIL simulation and its actual hardware implementation with the motor connected. The output results validate the effectiveness of this controller for the speed control of BLDC motor.

- **Permanent magnet synchronous motor (PMSM):** PMSM are very popularly used for many industrial applications like CNC machine tools, industrial robots, electric vehicle etc. due to high torque to weight ratio, high power density, high efficiency, reliability and ease of maintenance. Mathematical model of the motor is developed and the design and simulation for the vector control of PMSM using FSMC, chatter free SMC, Fuzzy PI controller and conventional PI controller are carried out. From the results it is observed that peak overshoot, settling time, steady state error and speed variation with sudden loading are improved with Fuzzy PI controller than that of conventional PI controller even though the rise time remains the same.

These parameters are further improved with a modified SMC while it shows a slight increase in the rise time. FSMC produces the best output performance, compared to other controllers, under steady state and transient conditions with PMSM, similar to the other motors. The speed variation with sudden loading is also greatly improved with FSMC. Hence the implementation of FSMC using FPGA is carried out using the HIL simulation and the results validate the performance of this controller for the speed control of PMSM.

PI Controller is the most widely used technique for the speed control of industrial drives due to its simple design and ease of implementation. This controller gives satisfactory performance only under undisturbed conditions and its performance is poor with sudden changes in the reference speed and load variations. Various DC and AC drives with PI controller shows large overshoot, high settling time and comparatively large speed variation while loading. The output in terms of settling time and peak overshoot are improved by the Fuzzy PI controller where the gain is made variable using FIS. But with this controller, the peak overshoot is not completely eliminated and shows large speed variation while loading which is overcome using chatter free SMC with modified control law that uses a saturation function instead of signum function in the conventional SMC. The performance is further improved using a FSMC, which integrates the intelligence of fuzzy logic with the Sliding Mode technique for appropriately varying the controller gain within an optimized range.

The realization of the FSMC is carried out using FPGA which has complex computational ability and high speed of calculation. The FPGA based algorithm of the FSMC for the speed control of PMSM and BLDC motor are developed and their

HIL simulation is carried out. The results are compared with chatter free SMC, conventional PI controllers and Fuzzy PI controllers. Also FPGA based FSMC for the speed control of a BLDC motor is implemented using Xilinx ISE design suite. The performance of speed control of BLDC motor, with FSMC implemented using FPGA, are compared with that of HIL simulation, Simulink simulation under no load as well as on load conditions. Even though the design and implementation of FSMC becomes more complex compared to other controllers, the transient and steady state performances are greatly improved and speed variations with change in load is reduced for all DC as well as AC drives considered here. These results validate the effectiveness of the intelligent FSMC for the efficient speed control applications of drive systems in industries.

8.2 RESEARCH CONTRIBUTIONS

With the aim of improving the transient and steady state performance of widely used electrical drives in industrial applications, a fuzzy based intelligent FSMC with adaptable gains and modified control law is designed and developed. To establish the effectiveness of this controller for the speed/position control of DC servo motor, BLDC motor, SRM and PMSM, their non-linear models are considered and the performance of FSMC with modified SMC, Fuzzy PI and conventional PI controller is compared. Also the FSMC algorithm for PMSM and BLDC motor are developed using FPGA and tested with hardware in the loop simulation. Hardware implementation of FSMC with BLDC motor connected for its speed control is successfully carried out using FPGA and the results are validated.

This work clearly brings out the effectiveness of FSMC for the accurate speed control of both AC and DC drives used in industrial applications.

8.3 FUTURE DIRECTIONS

Some of the possible extensions of the work that maybe pursued are listed below.

- Hardware implementation of FSMC for motors like PMSM and SRM can be carried out using FPGA and their performance can be evaluated to verify its suitability for speed control applications in industries.
- Artificial Neural Network can be deployed for varying the controller gain instead of fuzzy inference system used in the present work. Performance from the hardware implementation of ANN based SMC can be compared with FSMC to verify its suitability in motor control.
- Design and performance evaluation of H-infinity, Adaptive and Robust controllers for various drives can be developed.
- Suitable combinations of various controllers will further improve their performance and can lead to an ideal controller suitable for industrial automation.

REFERENCES

1. **Abianeh, Ali Jafarian** (2011) Sliding mode speed control of direct torque fuzzy controlled IPM synchronous motor drive. *6th IEEE Conference on Industrial Electronics and Applications*, 657-662.
2. **Adam, A. A. and K. Gulez**, (2008) Fast response adaptive fuzzy logic controller for sensor less direct torque control of PMSM with minimum torque ripple. *COMPEL-27*, 2, 534-550.
3. **Ali, H.I., S. B. Mohd. Noor, S. M. Bashi and M. H. Marhaban** (2010) Design of H-infinity based robust control algorithms using particle swarm optimization method. *The Mediterranean Journal of Measurement and Control*, **6(2)**, 70-81.
4. **Ali, T., A. Y. M. Abbas and E. H. A. Osman** (2014) Control of Induction Motor Drive using Artificial Neural Network. *SUST Journal of Engineering and Computer Science (JECS)*, **15 (2)**
5. **Alma, M., John J. Martinez, Ioan D. Landau and Gabriel Buche** (2012) Design and Tuning of Reduced Order H_{∞} Feed forward Compensators for Active Vibration Control. *IEEE Transactions on Control Systems Technology*, **20(2)**, 554-561.
6. **Ang, K., G. Chong, and Y. Li** (2005) PID control system analysis, design, and technology, *IEEE Trans. on Control System Technology*, 13, 559- 576.
7. **Astrom, K. J. and B. Wittenmark**, *Adaptive control*, Prentice-Hall Inc., Upper Saddle River, NJ:, Third edition, 1997.
8. **Astrom, K.J., U. Borisson, L. Ljung and B. Wittenmark** (1977) Theory and applications of self-tuning regulators, *Automatica*, **13**, 457-476.
9. **Athans, Michael** (1971) The Role and use of the Stochastic Linear Quadratic Gaussian Problem in Control System Design. *IEEE Transactions on Automatic Control*, **16(6)**, 529-552.
10. **Balamurugan, S., P Venkatesh and M Varatharajan** (2017) Fuzzy sliding-mode control with low pass filter to reduce chattering effect: an experimental validation. *Quanser SRIP*, **42(10)**, 1693–1703.
11. **Bansal, H.O., R. Sharma, and P. R. Shreeraman** (2012). PID Controller Tuning Techniques: A Review. *Journal of Control Engineering and Technology (JCET)*, **2(4)**, 168-176.

12. **Baroud, Z., A. Benalia and C. Ocampo-Martinez** (2018) Robust fuzzy sliding mode control for air supply on PEM fuel cell system. *Int. J. Modelling, Identification and Control*, **29(4)**, 341-351.
13. **Barrero, F. and M. J. Duran**, (2016) Recent Advances in the Design, Modelling and Control of Multiphase Machines - Part I. *IEEE Transactions on Industrial Electronics*, **63 (1)**, 449-458.
14. **Bassi, S. J., M. K. Mishra and E. E. Omizegba** (2011) Automatic Tuning of Proportional–Integral–Derivative (PID) Controller using Particle Swarm Optimization (PSO) Algorithm. *International Journal of Artificial Intelligence & Applications (IJAI)*, 2(4), 25-34.
15. **Basu, J.K., D. Bhattacharyya and Tai-hoon Kim** (2010) Use of Artificial Neural Network in Pattern Recognition. *International Journal of Software Engineering and Its Applications*, **4(2)**, 23-34.
16. **Batzel, T. D. and K. Y. Lee** (2000) A diagonally recurrent neural network approach to sensor less operation of the permanent magnet synchronous motor. *Proc. of IEEE Power Engineering Society Summer Meeting*, Seattle, WA, **4**, 2441-2445.
17. **Baños A, F. L. Lagarrigue, and F.J.Montoya** (2001). Advances in the control of nonlinear systems: *Springer Science & Business Media*,
18. **Bencsik, Attila L.** (2004) Appropriate Mathematical Model of DC Servo Motors Applied in SCARA Robots. *Acta Polytechnica Hungarica*, **I(2)**, 99-111.
19. **Bernat, J. and S. Stepien** (2011) The adaptive speed controller for the BLDC motor using MRAC technique. *Proceedings of the 18th World Congress The International Federation of Automatic Control*, Milano (Italy).
20. **Bolognani, S., L. Tubiana, and M. Zigliotto** (2003) Extended Kalman filter tuning in sensorless PMSM drives. *IEEE Trans. on Industrial Applications*, **39(6)**, 1741-1747.
21. **Bose, B.K.** (2009) Power Electronics and Motor Drives Recent Progress and Perspective. *IEEE Transactions on Industrial Electronics*, **56(2)**, 581-588.
22. **Bousserhane, I.K., A.Hazzab, M.Rahli, B.Mazari and M.Kamli**, (2009) Mover position control of linear induction motor drive using adaptive backstepping control with integral action. *Tamkang Journal of Science and Engineering*, **12(1)**, 17-28.
23. **Brezina, Lukas and Tomas Brezina** (2011) H-Infinity Controller Design for a DC Motor Model with Uncertain Parameters. *Engineering Mechanics*, **18(5)**, 271–279.

24. **Cai, J. C. Wen, H. Su, Z. Liu and L. Xing** (2017) Adaptive Back stepping Control for a Class of Nonlinear Systems with Non-triangular Structural Uncertainties. *IEEE Transactions on Automatic Control*, **62(10)**, 5220 – 5226.
25. **Camorali, D., G.A. Magnani, P. Rocco, and A. Rusconi** (2006) Position/Torque Control of a Space Robotics Arm. *IFAC Proceedings*, **39(16)**, 283-288
26. **Chaiyaratana, N. and A.M.S. Zalzala** (1997) Recent developments in evolutionary and genetic algorithms: Theory and applications. *Proceedings of 1997 IEE Conference on Genetic Algorithms in Engineering Systems: Innovations and Applications*. 270-277.
27. **Chakaravarthi, P.V. and P.Karpagavalli** (2016) Speed Control of PMSM Motor Using Fuzzy and PID Controller. *International Journal of Innovative Science, Engineering & Technology*, **3(1)**, 526-534.
28. **Chander, S., Agarwal P. and Gupta I.** (2010) FPGA-based PID controller for DC-DC converter. *Power India Joint International Conference on Power Electronics, Drives and Energy Systems (PEDES)*, **1(6)**, 20-23.
29. **Chaoui, H., P. Sicard and Wail Gueaieb** (2009) ANN-Based Adaptive Control of Robotic Manipulators with Friction and Joint Elasticity. *IEEE Transactions on Industrial Electronics*, **56(8)**, 3174-3187.
30. **Chen, Hao, Dong Zhang, Zi-Yue Cong and Zhi-Feng Zhang,** (2002) Fuzzy logic control for switched reluctance motor drive. *Proceedings of IEEE International Conference on Machine Learning and Cybernetics*.
31. **Chen, C. Y, W.C. Chan, T.C. Ou, S.H. Yu, and T.-W. Liu** (2009) Sliding Mode Speed Control of Brushless DC Motor Using Pulse-Width-Modulated Current Regulator. *IEEE/ASME International Conference on Advanced Intelligent Mechatronics*, 1395-1399.
32. **Chou, H.-H., Y.-S. Kung, N. Vu Quynh, and S. Cheng** (2013) Optimized FPGA design, verification and implementation of a neuro-fuzzy controller for PMSM drives. *Mathematics and Computers in Simulation*, **90**, 28–44.
33. **Cirstea, M.N., A. Dinu, J.G. Khor and M. McCormick,** *Neural and Fuzzy Logic Control of Drives and Power Systems*. Newnes- An imprint of Elsevier Science, Linacre House, Jordan Hill, Oxford, 2002.
34. **Coban, R.** (2018) Back stepping integral sliding mode control of an electromechanical system. *Automatika Journal for Control, Measurement, Electronics, Computing and Communications*, **58(3)**, 266–272.

35. **Corradini, M.L. G.Ippoliti, S.Longhi and G.Orlando** (2012) A quasi-sliding mode approach for robust speed control and speed estimation of PM synchronous motor. *IEEE Transactions on Industrial Electronics*, **59(2)**, 1096-1104..
36. **Damiano, A., G.L.Gatto, I.Marongia and A. Pisano** (2004) Second order sliding mode control of DC drives. *IEEE Transactions on Industrial Electronics*, **51 (2)**, 364-373.
37. **Decarlo, R.A, S.H. Zak and G.P. Matthews**, (1988) Variable Structure Control of Nonlinear Multivariable Systems: A Tutorial,” *Proceedings of the IEEE*, **76(3)** , 212-232
38. **Dey, A., Singh B, Dwivedi B and Chandra D.** (2009) Vector controlled induction motor drive using genetic algorithm tuned PI speed controller *Electrical Power Quality and Utilisation*, **15(1)**, 3-8.
39. **Dong, W., Song, J., Cheng, S., Yu, L. and Lu, Z.** (2018) Speed Control of BLDC Motor in Electro-Hydraulic Power Steering System Based on Fuzzy-PI Controller. *SAE International University Technical Paper*.
40. **Dorigo, M. , Maniezzo V., and Colorni A.**, (1996) The ant system: optimization by a colony of cooperating agents. *IEEE Transactions on System, Man and Cybernetics*, **26(1)**, 29–41.
41. **Drakunov, S. V. and Utkin, V. I.** (1992) Sliding mode control in dynamic systems. *Int. Journal of Control*, **55**, 1029-1037.
42. **Dumanay, A.B, A. Istanbulu and M. Demirtas** (2016) Comparison of PID and SMC Methods in DC Motor Speed Control. *IOSR Journal of Electrical and Electronics Engineering*, **11(6)**, 10-16.
43. **Eberhart, R.C., and Kennedy J.** (1995) A new optimizer using particle swarm theory, *Proceedings of the sixth international symposium on micro machine and human science*, 1942-1948.
44. **Eide, R., P. M. Egelid, A. Stamso and H. R. Karimi** (2011) LQG Control Design for Balancing an Inverted Pendulum Mobile Robot. *Intelligent Control and Automation*. **2(2)**, 160-166.
45. **Elgammal, Adel A. A.** (2014) Adaptive Fuzzy Sliding Mode Controller for Grid Interface Ocean Wave Energy Conversion. *Journal of Intelligent Learning Systems and Applications*, **6**, 53-69.
46. **El-Sharkawi, Mohamed A.** *Fundamentals of Electric Drives*. Brookes/Cole Publishing Company, USA., 2000.
47. **El-Sousy, F.F.M.** (2011) Robust wavelet-neural network sliding mode control system for permanent magnet synchronous motor drive. *IET Electronics and Power Applications*, **5(1)**, 113-132.

48. **Emhemed, Abdul Rahman A.A.** (2013) Fuzzy Control for Nonlinear Ball and Beam System. *International Journal of Fuzzy Logic Systems*, **3(1)**, 25-31.
49. **Feng, J., Q. Gao, W. Guan and X. Huang** (2017) Fuzzy sliding mode control for erection mechanism with unmodelled dynamics. *Automatika Journal for Control, Measurement, Electronics, Computing and Communication*, **58(2)**, 131–140.
50. **Gandomi, A. H. and A. H. Alavi** (2012) Krill herd: A new bio-inspired optimization algorithm. *Communication in Nonlinear Science and Numerical Simulation*, **17(4)**, 4831-4845.
51. **Ganesh, C., M.Prabhu, M.Rajalakshmi, G.Sumathi, Virender Bhola and S.K.Patnaik** (2012) ANN Based PID Controlled Brushless DC drive System. *ACEEE Int. J. on Electrical and Power Engineering*, **3(1)**, 45-48.
52. **Gharieb, W., and Nagib G.** (2001) Fuzzy intervention in PID controller design. *IEEE ISIE*.
53. **Guillemin, P.** (1996) Fuzzy logic applied to motor control. *IEEE Transactions on Industry Applications*, **32(1)**, 51-56.
54. **Hartley, E., J. L. Jerez, A. Suardi, J. M. Maciejowski, E. C. Kerrigan, and G. A. Constantinides** (2014) Predictive control using an FPGA with application to aircraft control. *IEEE Transactions on Control Systems Technology*, **22(3)**, 1006-1017.
55. **Hasirci, U., A.Balikci and A.Ozturk** (2009) Nonlinear adaptive back stepping control of linear induction motor. *5th International Advanced Technologies Symposium (IATS'09)*, 2009.
56. **Haykins, Simon**, *Neural Networks*. Prentice-Hall of India, New Delhi, 1999.
57. **Holland, J. H.** (1967) Genetic Algorithms. *Scientific American*, **267**, 66-72.
58. **Hu, B., George K. I. Mann, and Raymond G. Gosine** (1999) New Methodology for Analytical and Optimal Design of Fuzzy PID Controllers. *IEEE Transactions on Fuzzy Systems*, **7(5)**, 521-539.
59. **Huang, Y. and Cheng P.** (2004) Using Fuzzy Inference Method to Automatically Detect and Identify Intruders from the Security System. *IEEE International Conference on Networking, Sensing & Control*.
60. **Hung, John Y., Weibing Gao and James C. Hung** (1993) Variable structure Control: A Survey, *IEEE Transactions on Industrial Electronics*, **40(1)**, 2-22.

61. **Husain, Iqbal and Syed A. Hossain** (2005) Modeling, Simulation, and Control of Switched Reluctance Motor Drives. *IEEE Transactions on Industrial Electronics*, **52(6)**, 1625-1634.
62. **Ibrahim, H. E. A. and, Ahmed A. Hakim Mahmoud** (2014) DC Motor Control Using PID Controller Based on Improved Ant Colony Algorithm. *International Review of Automatic Control*, **7(1)**, 1-6.
63. **Iqbal, J., Ullah, M., Khan, S., et al.** (2017). Nonlinear control systems: A brief overview of historical and recent advances. *Nonlinear Engineering*, **6(4)**, pp. 301-312.
64. **Jain, Manu, Mukhtiar Singh, Ambrish Chandra, and Sheldon S. Williamson** (2011) Sensorless Control of Permanent Magnet Synchronous Motor using ANFIS Based MRAS. *IEEE International Electric Machines and Drives conference (IEMDC)*, 599-606.
65. **Jain, Priyank and M.J. Nigam** (2013) Design of a Model Reference Adaptive Controller Using Modified MIT Rule for a Second Order System. *Advance in Electronic and Electric Engineering*, **3(4)**, 477-484.
66. **Jang, J.-S. R., C.-T. Sun, and E. Mizutani** *Neuro-Fuzzy and Soft Computing*, Prentice-Hall, Upper Saddle River, NJ, 1997.
67. **Joseph, A., and S.Geetha** (2007) Application of back stepping for control of launch vehicle. *IE (I) Journal-AS*, **88**, 13-19.
68. **Kaliappan, E., and C. Chellamuthu** (2012) Modelling, Simulation and Experimental Analysis of Permanent Magnet Brushless DC Motors for sensor less operation. *Archives of Electrical Engineering*, **64(4)**, 499-515.
69. **Kamble, B.C.** (2016) Speech Recognition Using Artificial Neural Network – A Review. *International Journal of Computing, Communications & Instrumentation Engg. (IJCCIE)*, **3(1)**, 1-4.
70. **Kara, Tolgay and Ilyas Eker** (2003) Nonlinear modeling and identification of a DC motor for bidirectional operation with real time experiments. *Energy Conversion and Management*, **45(7)**, 1087-1106.
71. **Khamis, Mustafa A.** (2013) Design and Simulation of Self Tuning Controller for DC Servo Motor. *Diyala Journal of Engineering Sciences*, **6(4)**, 107-119.
72. **Kirkpatrick, S., C.D. Gelatt Jr., and M.P. Vecchi** (1983) Optimization by simulated annealing. *Science*, **220**, 671–680.
73. **Kokotovic, P.V., M. Krstic and I. Kannellakopoulous** (1995) *Non-linear and Adaptive Control Design*, Wiley-Inter science, New York.

74. **Krishnan, R.** *Electric motor drives: modelling, analysis, and control*, Prentice-Hall, New-Jersey, 2001.
75. **Kulcsar, Balazs** (2000) LQG/LTR Controller Design for an Aircraft Model. *Periodica Polytechnica Ser. Transp. Eng.* **28(1)**, 131–142.
76. **Kumar, Y.N., P.Eswara Rao, P. Vijay Varma, V. V. Ram Vikas and P. Kasi Naidu** (2014) Speed Control of BLDC Motor Drive By Using PID Controllers. *International Journal of Engineering Research and Applications.* **4(4)**, 37-41.
77. **Kung, Y.-S.** and **M.-H. Tsai** (2007) FPGA-based speed control IC for PMSM drive with adaptive fuzzy control. *IEEE Transactions on Power Electronics*, **22(6)**, 2476–2486.
78. **Kunto, W.W.** and **J. Seok-kwon** (2013) Genetic algorithm tuned PI controller on PMSM simplified vector control. *Springer Journal of Central South University*, **20(11)**, 3042–3048.
79. **Lawrence, D. A.** and **W. J. Rugh** (1995) Gain scheduling dynamic linear controllers for a nonlinear plant. *Automatica*, **31**, 381-390.
80. **Lee, H.** and **V. I. Utkin** (2007) Chattering suppression methods in sliding mode control system,” *Annual Review in Control*, **31**, 179-188.
81. **Leonhard, W.** *Control of Electric Drives*. Springer Verlag, Berlin, Germany, 1984
82. **Li, C.** and **M. Elbuluk**, (2001) A sliding mode observer for sensorless control of permanent magnet synchronous motors. *Proc. IEEE Industry Applications Society Annual Meeting*, Chicago, IL. 2, 1273-1278.
83. **Li, J-H.** and **J-S. Chiou**, (2014) Two-Dimensional Fuzzy Sliding Mode Control of a Field-Sensed Magnetic Suspension System. *Mathematical Problems in Engineering*, **1**, 1-10.
84. **Li, N., X. Lin-Shi, P. Lefranc, E. Godoy and A. Jaafar** (2011) FPGA based sliding mode control for high frequency SEPIC. *IEEE International Symposium on Industrial Electronics*.
85. **Li, Y.** and **H. Zhu** (2008) Sensorless control of permanent magnet synchronous motor—a survey. *Proc. of IEEE Vehicle Power and Propulsion Conf.*, Harbin, China, 1-88.
86. **Liang, Y.** and **Y. Li** (2003) Sensor less control of PM synchronous motors based on MRAS method and initial position estimation. *Proc. Of IEEE International Conf. on Electrical Machines and Systems*, Beijing, China, 1, 96-99.

87. **Lin, C. L., H. Y. Jan, and N. C. Shieh**, (2003) GA-based multi-objective PID control for a linear brushless DC motor. *IEEE/ASME Trans. Mechatronics*, **8(1)**, 56-65.
88. **Lin, C.K., L.C.Fu, T.H.Liu and B.H.Chou** (2011b) Passivity based adaptive back stepping PI sliding mode position control for synchronous reluctance motor drives. *Proceedings of 8th Asian Control Conference (ASCC)*, 245-250.
89. **Lin, C.K., T.H.Liu and L.C.Fu** (2011a) Adaptive back stepping PI sliding mode control for Interior permanent magnet synchronous motor drive systems. *Proceedings of American Control Conference*, 4075-4080.
90. **Lin, C.-L. and H.-Y. Jan** (2002) Evolutionarily multi-objective PID control for linear brushless DC motor. *Proc. IEEE Int. Conf. Industrial Elect. Society*, 39-45.
91. **Lin, Chih-Hong and Chih-Peng Lin** (2009) Adaptive Backstepping FNN control for a Permanent magnet synchronous motor drive. *IEEE-ICIEA-2009*, pp.2712-2717.
92. **Lin, F.J, C.K. Chang and Po-Kai Huang** (2007) FPGA-Based Adaptive Back stepping Sliding-Mode Control for Linear Induction Motor Drive. *IEEE Transactions on Power Electronics*, **22(4)**, 1222-1231.
93. **Lin, H., W.Yan, J.Wang, Y.Yao and B.Gao** (2009a), Robust nonlinear speed control for a brushless DC motor using model reference adaptive back stepping approach. *Proceedings of the IEEE international conference on Mechatronics and Automation*, 335-339.
94. **Lin, H., W.Yan, M.Li, P.Wen, C.Zhang and Mei Li** (2009b) Direct torque control of an IPM synchronous motor drive using model reference adaptive back stepping approach. *Proceedings of the IEEE international conference on Robotics and Biomimetics*, 2119-2124.
95. **Liu, X. and B. Wang** (2006) ANN observer of permanent magnet synchronous motor based on SVPWM. *Proc. IEEE International Conf. on Intelligent Systems Design and Applications*, Jinan, China, 1, 95-100.
96. **Ltifi, A., M. Ghariani and R. Neji** (2014) Performance Comparison of PI, SMC and PI-Sliding Mode Controller for EV. *15th international conference on Sciences and Techniques of Automatic control STA'2014*, Hammamet, Tunisia.
97. **Lu, Renquan, Shukui Li and Lin Xue** (2008) Robust H_∞ Optimal Speed Control of DC Motor Using LMI Approach. *Proceedings of Chinese Control and Decision Conference*, 4350-4354.

98. **Luk, P. C. K., and C. K. Lee** (1994) Efficient modeling for a brushless DC motor drive. *20th International Conference on Industrial Electronics, Control and Instrumentation, IECON'94.*,
99. **Lupon, Emili, Sergio Busquets-Monge and Joan Nicolas-Apruzzese,** (2014) FPGA Implementation of a PWM for a Three-Phase DC–AC Multilevel Active-Clamped Converter. *IEEE Transactions on Industrial Informatics*, **10(2)**, 1296-1306.
100. **Ma, D., Hui Lin, and Bingqiang Li** (2017) Chattering-Free Sliding-Mode Control for Electromechanical Actuator with Backlash Nonlinearity. *Journal of Electrical and Computer Engineering*, **1(1)**, 1-9.
101. **Mahajan, Nayana P., and S.B. Deshpande** (2013) Study of Nonlinear Behavior of DC Motor Using Modeling and Simulation. *International Journal of Scientific and Research Publications* **3(3)**, 1-6.
102. **Mahendiran, T.V., P.Thangam, and K. Thanushkodi** (2011) A Comparative Study on Non Linear Drive Control for Separately Excited DC Motor Using Fuzzy Logic Controller, Fuzzy PI Controller and PSO Tuned Fuzzy PI Controller. *International Journal of Research and Reviews in Electrical and Computer Engineering*, **1(1)**, 32-38.
103. **Mamdani, E. H.** (1974) Application of fuzzy algorithms for the control of a dynamic plant. *Proceedings of IEE*, **121**, 1585-1588.
104. **Manjunath, T.C.** (1995) Design of Moving Sliding Surfaces in A Variable Structure Plant & Chattering Phenomena. *International Journal of Electronics, Circuits and Systems*, **1(3)**.
105. **Mao, Shang-Hsun and Mi-Ching Tsai** (2005) A novel switched reluctance motor with C-core stators. *IEEE Transactions on Magnetics*, **41(12)**, 4413-4420.
106. **Marino, R., S. Peresada, and P. Valigi** (1993) Adaptive input-output linearizing control of induction motors. *IEEE Transactions on Automatic Control*, **38(2)**, 208- 221.
107. **Masmoudi, M. S., N. Krichen, A. B. Koesdwiady, F. Karray and M. Masmoudi,** (2016) Design and FPGA Implementation of a Fuzzy-PI Controller for Omnidirectional Robot System. *Robot Intelligence Technology and Applications*, **447**, 141-152.
108. **Mathew, T. and Caroline Ann Sam** (2013) Closed Loop Control of BLDC Motor Using a Fuzzy Logic Controller and Single Current Sensor”, *International Conference on Advanced Computing and Communication Systems (ICACCS)*, December 19-21, Coimbatore, India. **2(13)**,

109. **Mehazzem, F., A.Reama and H.Benalla**, (2009) Sensorless nonlinear adaptive back stepping control of induction motor *ICGST-ACSE Journal*, **8(3)**, 1-8.
110. **Meng, H., N E Pears and C Bailey** (2005) FPGA Based Video Processing System For Ubiquitous Applications. *Proceedings:Conference on Perspectives in Pervasive Computing*, 57-63.
111. **Merzoug, M.S.** and H.Benalla (2010) Nonlinear back stepping control of permanent magnet synchronous motor. *International Journal of System control*, **1(1)**, 30-34.
112. **Minkova, M. D., D. Minkov , J.L. Rodgerson and R.G. Harley** (1998) Adaptive neural speed controller of a dc motor. *Department of Electrical Engineering, University of Natal, Durban 4014, South Africa*.
113. **Mirzaei, A., Moallem, M., Mirzaeian, B and Fahimi, B.** (2005) Design of an optimal fuzzy controller for antilock braking systems. *Vehicle Power and Propulsion, 2005 IEEE Conference*, **1**, 823 – 828.
114. **Mitra, Jubin and Tapan K. Nayak** (2018) An FPGA-Based Phase Measurement System. *IEEE Transactions on Very Large Scale Integration (VLSI) Systems*, **26 (1)**, 133-142.
115. **Mohanty, N. K. and R. Muthu** (2011) Implementation of proportional integral (PI) controlled DSP based cost effective inverter fed speed control of induction motor drive with VisSim/ embedded controls and developer (ECD). *International Journal of the Physical Sciences*, **6(20)**, 4790-4797.
116. **Monmasson, E. and M. N Cirstea** (2007) FPGA Design Methodology for Industrial Control Systems-a Review. *IEEE Transactions on Industrial Electronics*, **54**, 1824-1842.
117. **Monteiro, J. R. B. A. , C. M. R. Oliveira and M. L. Aguiar** (2015) Sliding mode control of brushless DC motor speed with chattering reduction. *IEEE International Symposium on Industrial Electronics (ISIE)*.
118. **Montiel, O., R.Sepulveda, P.Melin, O.Castillo, M.A.Porta and I.M.Meza** (2007) Performance of a simple tuned fuzzy controller and a PID controller on a DC motor. *Proceedings of the IEEE Symposium on Foundations of Computational Intelligence (FOCI 2007)*, 531-537.
119. **Mora, Luis, Ricardo Lugo, Carlos Moreno and Jhon Edgar Amaya** (2016) Parameters optimization of PID controllers using metaheuristics with physical implementation. *Proceedings of IEEE International Conference of the Chilean Computer Science Society (SCCC)*.

120. **Muruganatham, N. and S.Palani** (2010) State space modelling and simulation of sensor less permanent magnet BLDC motor. *International Journal of Engineering, Science and Technology*, **2(10)**, 5099-5106.
121. **Nagaraj, R. and B.K. Panigrahi** (2015) Simulation and Hardware Implementation of FPGA Based Controller for Hybrid Power System. *International Journal of Electrical Energy*, 3(2), 86-93.
122. **Nanda, A. B., Swagat Pati and Niti Rani** (2016) Performance comparison of a SRM drive with conventional PI, fuzzy PD and fuzzy PID controllers. *Proceedings of IEEE International Conference on Circuit, Power and Computing Technologies (ICCPCT)*.
123. **Nouri, Khaled , Rached Dhaouadi , and Naceur Benhadj Braiek** (2008) Adaptive control of a nonlinear dc motor drive using recurrent neural networks. *Elsevier, Applied Soft Computing*, 371–382.
124. **Ogata, Katsuhiko**, *Modern Control Engineering*, Prentice Hall of India, 2002
125. **Osornio-Rios, R. A.** (2017) FPGA Lead-lag Compensator Design for Industrial Control Systems. *Journal of Scientific and Industrial Research (JSIR)*, **76(11)**, 733-736.
126. **Parker, Horacio Vasquez Joey K.** (2004) A new simplified mathematical model for a switched reluctance motor in a variable speed pumping application. *Mechatronics*, **14**, 1055–1068.
127. **Pham, D. T., A. Ghanbarzadeh, E. Koc, S. Otri, S. Rahim and M. Zaidi** (2005) The Bees Algorithm. *Technical Note, Manufacturing Engineering Centre, Cardiff University, UK*.
128. **Pillay, P and R. Krishnan** (1989a) Modeling, Simulation, and Analysis of Permanent Magnet Motor Drives, Part I: The Permanent Magnet Synchronous Motor Drive. *IEEE Transactions on Industry Applications*. **25(2)**, 265-273.
129. **Pillay, P. and R. Krishnan** (1989b) Modeling, simulation, and analysis of permanent-magnet motor drives, part II: the brushless DC motor drive. *IEEE Trans. on Industry Applications*, 25(2), 274– 279.
130. **Piltan, F., N. Sulaiman, M. H. Marhaban, Adel Nowzary and M. Tohidian**, (2011) Design of FPGA-based Sliding Mode Controller for Robot Manipulator. *International Journal of Robotics and Automation*, **2(3)**, 173-194.
131. **Piltan, M., A. Kazerouni and A. Rafie** (2015) Design FPGA-Based Chattering-free Sliding Mode Controller for PUMA Robot Manipulator. *International Journal of Hybrid Information Technology*, **8 (12)**, 11-46.

132. **Poorani, S., T.V.S.Urmila Priya, K.Udaya Kumar and S. Renganarayanan** (2005) FPGA Based Fuzzy Logic Controller for Electric Vehicle. *Journal of The Institution of Engineers, Singapore*, **45(5)**, 1-14.
133. **Prasad, K.M.A., Usha Nair, Unnikrishnan A.**, (2015). Fuzzy Sliding Mode Control of a Permanent Magnet Synchronous Motor with two different Membership Functions. *Proceedings of IEEE International Conference on Power, Instrumentation, Control and Computing (PICC)*, 1-6
134. **Pundaleek B. H., Manish G. R. and Vijay K. M. G.** (2010) Speed Control of Induction Motor: Fuzzy Logic Controller v/s PI Controller. *International Journal of Computer Science and Network Security*, **10(10)**
135. **Purnalal, Maloth and Sunil kumar T K**, (2015) Development of Mathematical Model and Speed Control of BLDC Motor. *International Journal of Electrical and Electronics Engineers*, **7(1)**.
136. **Rahman, K. M., N. R. Patel, T. G. Ward, J. M. Nagashima, F. Caricchi, and F. Crescimbin** (2006) Application of direct-drive wheel motor for fuel cell electric and hybrid electric vehicle propulsion system. *IEEE Transactions on. Industrial Applications*, **42 (5)**, 1185–1192.
137. **Ramadan, E. A., M. El-bardini and M.A. Fkirin** (2014) Design and FPGA-implementation of an improved adaptive fuzzy logic controller for DC motor speed control. *Ain Shams Engineering Journal*, **5**, 803–816.
138. **Rind, S. J., Y. Ren, Y. Hu, J. Wang, and L. Jiang** (2017) Configurations and Control of Traction Motors for Electric Vehicles: A Review. *Chinese Journal of Electrical Engineering*, **3(3)**, 1-15.
139. **Roopaei, M., V. E. Balas, T-C. Lin and A. Seifi** (2009) Adaptive gain fuzzy sliding mode control in uncertain MIMO nonlinear systems. *Nonlinear Studies*, **16(3)**, 261-273.
140. **Roux, C, and Morcos, M.** (2002) On the use of a simplified model for switched reluctance motors. *IEEE Transactions on Energy Conversion*, **17(3)**, .400–405.
141. **Sain, C., A. Banerjee, and P. K. Biswas** (2016) Comparative Performance Study for Closed Loop Operation of an Adjustable Speed Permanent Magnet Synchronous Motor Drive with Different Controllers. *International Journal of Power Electronics and Drive System (IJPEDS)*, **7(4)**, 1085-1099.
142. **Sarwer, M. G., Md. Abdur Rafiq and B.C. Ghosh**, (2004) Sliding Mode Speed Controller of a D.C Motor Drive. *Journal of Electrical Engineering, The Institution of Engineers, Bangladesh*. **31(1)**.

143. **Santos M., Dormido S., de Madrid A.P., Morilla F., and De la Cruz J.M.** (1996) Tuning fuzzy logic controllers by classical techniques. *Computer Aided Systems Theory — CAST '94. Lecture Notes in Computer Science*, vol 1105. Springer, Berlin, Heidelberg
144. **Shahat, Adel El and Hamed El Shewy** (2010) Permanent magnet synchronous motor dynamic modelling with genetic algorithm performance improvement. *International Journal of Engineering, Science and Technology*, **2(2)**, 93-106.
145. **Shayanfar, H. A., H. Shayeghi and A. Younesi** (2015) Optimal PID Controller Design Using Krill Herd Algorithm for Frequency Stabilizing in an Isolated Wind-Diesel System. *Proceedings of International Conference on Artificial Intelligence ICAI'15*, 516-521.
146. **Shi, Q., Xiang L., Chen T., and Hu W.** (2009) FPGA-based Embedded System Education. *1st International Workshop on Education Technology and Computer Science*, Wuhan, Hubei, China, **1**, 123-127.
147. **Singh, A. P., Udit Narayan and Akash Verma** (2013) Speed Control of DC Motor using PID Controller Based on Matlab. *Innovative Systems Design and Engineering*. **4(6)**, 22-28.
148. **Sinha, Naresh K., Colin D. Dicenzo, and Barna Szabados** (1974) Modeling of DC motor for control applications. *IEEE Transactions on Industrial Electronics and Control Instrumentation*, **21(2)**, 84-88.
149. **Slotine, J. J. and S. S. Sastry** (1983) Tracking control of nonlinear systems using sliding surfaces with application to robot manipulators. *International Journal of Control*, **38**, 465–492.
150. **Slotine, Jean-Jacques E.**, *Applied Nonlinear Control*, Prentice Hall Englewood Cliffs, New Jersey, 1991
151. **Solanakis, Emmanuel I., Theodoros N. Kapetanakis, Ioannis O. Vardiambasis, George S. Liidakis , George A. Adamidis , and Melina P. Ioannidou** (2013) Telecommunication Circuits Design and Development Using FPGA Technology. *Proceedings of 8th International Conference on New Horizons in Industry, Business and Education*, Chania ,Greece, 153-158.
152. **Sousa, G.C.D. and B.K. Bose**, (1994) A fuzzy set theory based control of a phase-controlled converter DC machine drive. *IEEE Transactions on Industry Applications*, **30(1)**, 34-44..
153. **Spurgeon, S and C. Edwards**, *Sliding Mode Control: Theory and Applications*. London: Taylor and Francis, 1998.
154. **Stefani, Savant, Shahian and Hosterrer**, *Design of Feedback Control systems*, Saunders College Publishing, 1998.

155. **Storn, R. and Price K.** (1997) Differential evolution—A simple and efficient heuristic for global optimization over continuous spaces. *Journal of Global Optimization*, **11(4)**, 341–359.
156. **Sudhoff, S. D., K. A. Corzine and H. J. Hegner** (1995) A flux-weakening strategy for current-regulated surface mounted permanent-magnet machine drives. *IEEE Trans. Energy Conversion*, **10(3)**, 431–437.
157. **Tan, S., C.-C. Hang, and J.-S. Chai,** (1997) Gain scheduling: from conventional to Neuro-fuzzy. *Automatica*, **33(3)**, 411-419.
158. **Thevaril J. and Kwan H. K.,** (2005) Speech Enhancement using Adaptive Neuro-Fuzzy Filtering. *Proc. of 2005 International Symposium on Intelligent Signal Processing and Communication Systems, ISPACS*.
159. **Tripathi, N., Rameshwar Singh and Renu Yadav** (2015) Analysis of Speed Control of DC Motor - A review study. *International Research Journal of Engineering and Technology*, **2(8)**, 1616-1621.
160. **Uddin, M.N., S.Radwan and M.Azizur Rahman** (2002) Performances of Fuzzy Logic Based Indirect Vector Control for Induction Motor Drive. *IEEE Trans. on Industry Applications*, **38(5)**, 1219-1225.
161. **Upalanchiwar, T. and A.V.Sakhare** (2014) Design and implementation of the fuzzy PID controller using MATLAB/SIMULINK model. *International Journal of Research in Computer and Communication Technology*, **3(3)**, 369-392.
162. **Usman, Adil and B. S. Rajpurohit** (2016) Speed control of a BLDC Motor using Fuzzy Logic Controller. *Proceedings of IEEE 1st International Conference on Power Electronics, Intelligent Control and Energy Systems (ICPEICES)*.
163. **Utkin, V.I** (1977) Variable Structure systems with sliding modes. *IEEE Transactions on Automatic control*, **22(2)**, 212-222.
164. **Utkin, V.I.** (1993) Sliding mode control design principles and applications to electric drives. *IEEE Transactions on Industrial Electronic*, **40(1)**, 23-26.
165. **Viljamaa, Pauli** (2002) Fuzzy Gain Scheduling and Tuning of Multivariable Fuzzy Control—Methods of Fuzzy Computing in Control Systems. *Ph.D. Thesis Dissertation*, Tampere University of Technology, Tampere, Finland .
166. **Vincent, U.E.** (2008) Chaos synchronization using active control and back stepping control: A comparative analysis. *Nonlinear Analysis: Modelling and Control*, **13(2)**, 253-261.

167. **Wai, R. J., Meng-Wei Chen and Yao-Kai Liu**, (2015) Design of Adaptive Control and Fuzzy Neural Network Control for Single-Stage Boost Inverter. *IEEE Transactions on Industrial Electronics*, **62(9)**, 5434 – 5445.
168. **Wang, M. and Liu J.** (2005) Fuzzy Logic based robot path planning in unknown environment. *Proc. of the Fourth International Conference on Machine Learning and Cybernetics ICMLC*, 18-21.
169. **Wang, G.-G., A.H. Gandomi and A.H. Alavi** (2014) An effective krill herd algorithm with migration operator in biogeography-based optimization. *Applied Mathematical Model*, **38**, 2454–2462.
170. **Wang, Q. G., B. Zou, T. H. Lee, and Q. Bi** (1997) Auto-tuning of multivariable PID controller from decentralized relay feedback. *Automatica*, **33**, 319-330.
171. **Willis, M. J.**, (1999) Proportional-Integral-Derivative Control. *Dept. of Chemical and Process Engineering University of Newcastle*.
172. **Wlas, M., Z. Krzeminski, J. Guzinski, H. Abu-Rub and H.A. Toliyat** (2005) Artificial-neural-network-based sensor less nonlinear control of induction motors. *IEEE Transactions on Energy Conversion*, **20(3)**.
173. **Yang, X. S.**, *Engineering Optimization: An Introduction with Meta-heuristic Application*, Wiley & Sons, New Jersey, 2010.
174. **Young, K. D, V. I. Utkin, and U. Ozguner** (1999) A control engineer's guide to sliding mode control. *IEEE Trans. Control Sys. Tech.*, **7**, 328-342.
175. **Yu, G. and R. Hwang** (2004) Optimal PID speed control of brush less DC motors using LQR approach. *Proc. IEEE Int. Conf. Systems, Man and Cybernetics*, 473-478.
176. **Zadeh, L. A.** (1965) Fuzzy Sets. *Information and control*, **8**, 338-353.
177. **Zhang, Guoguang, Yongchao Zhang and Fan Yu** (2012) μ -Synthesis controller design for a DC-motor-based active suspension with parametric uncertainties. *Journal of Vibration and Control*, **19(4)**, 585–604.
178. **Zhang, X., Lizhi Sun, Ke Zhao, and Li Sun**, (2013) Nonlinear Speed Control for PMSM System Using Sliding-Mode Control and Disturbance Compensation Techniques. *IEEE Transactions on Power Electronics* **28(2)**, 1358-1365.
179. **Zhao, Z.-Y., M.Tomizuka, and S.Isaka** (1993) Fuzzy gain scheduling of PID Controllers. *IEEE Transactions on Systems, Man, and Cybernetics*, **1(23)**, 1392-1398.

180. **Zhong, L.** (1997) Analysis of direct torque control in permanent magnet synchronous motor drives. *IEEE Transactions on Power Electronics*, **12**, 528-536.
181. **Zhou, J., C. Wen, and Y. Zhang** (2004) Adaptive back-stepping control of a class of uncertain nonlinear systems with unknown backlash-like hysteresis. *IEEE Transactions on Automatic Control*, 49(10), 1751-1759.
182. **Zhou, Y. and S. Hu**, (2015) H infinity control for DC servo motor in the network environment. *IEEE Advanced Information Technology, Electronic and Automation Control Conference (IAEAC)*

LIST OF PAPERS

SUBMITTED ON THE BASIS OF THIS THESIS

I. REFEREED JOURNALS

- [1] **Arun Prasad K.M.** and **Usha Nair** (2014) Sensor less Fuzzy Control of a DC Motor. *Nonlinear Dynamics (Springer)*, **73(3)**, 1933-1941. (SCI, Scopus)
- [2] **Arun Prasad K.M., Usha Nair** and **Unnikrishnan A.** (2016) Fuzzy Sliding Mode Control of a Switched Reluctance Motor. *ELSEVIER Procedia Technology*, **25**, 735 – 742.
- [3] **Arun Prasad K.M., Bindu M. Krishna,** and **Usha Nair,** FPGA Based Intelligent Fuzzy Sliding Mode Controller for BLDC Motor. *International Journal of Power Electronics and Drive Systems* – Accepted.

II. PRESENTATION IN CONFERENCES

- [1] **Arun Prasad K.M., Usha Nair, Unnikrishnan A.,** “Fuzzy Sliding Mode Control of a Permanent Magnet Synchronous Motor with two different Membership Functions”, *Proceedings of IEEE International Conference on Power, Instrumentation, Control and Computing (PICC)*, pp.1-6 December 2015
- [2] **Arun Prasad K.M., Usha Nair, Unnikrishnan A.,** “Fuzzy Sliding Mode Control of a Switched Reluctance Motor”, *ELSEVIER 1st Global Colloquium on Recent Advancements and Effectual Researches in Engineering, Science and Technology – RAEREST2016*, April 2016.
- [3] **Arun Prasad K.M., Usha Nair,** "An Intelligent Fuzzy Sliding Mode Controller for a BLDC Motor", *IEEE International Conference on Innovative Mechanisms for Industry Applications (ICIMIA 2017)*, Bangalore, February 21-23, 2017, pp.274-278

CURRICULUM VITAE

1. **NAME** : ARUN PRASAD K.M.
2. **DATE OF BIRTH** : 11 November 1973

3. EDUCATIONAL QUALIFICATIONS

1996 Bachelor of Technology

Institution : NSS College of Engineering, Palakkad

Specialization : Electrical and Electronics Engineering

2007 Master of Technology

Institution : College of Engineering Trivandrum

Specialization : Control Systems

Doctor of Philosophy (Ph.D)

Institution : Cochin University of Science and Technology

Registration date: 24-11-2011

4. EXPERIENCE

Working as Assistant Professor in Electrical Engineering under the service of Institute of Human Resource Development (IHRD) from 15-06-2001 to till date.